

**AD-A254 346**



2

**PL-TR-92-2076**

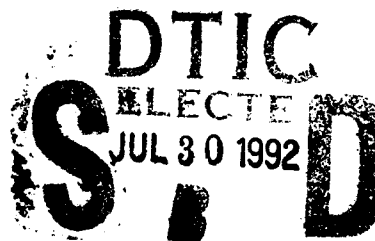
**SSS-TR-92-13129**

**Development of a Comprehensive Seismic  
Yield Estimation System for  
Underground Nuclear Explosions**

**J. R. Murphy  
J. N. Jenab**

**Maxwell Laboratories, Inc.  
S-CUBED Division  
P.O. Box 1620  
La Jolla, CA 92038-1620**

**March 1992**



**Scientific Report No. 3**

**Approved for public release; distribution unlimited**



**Phillips Laboratory  
Air Force Systems Command  
Hanscom Air Force Base, MA 01731-5000**

**2 7 28 046**

**92-20403**

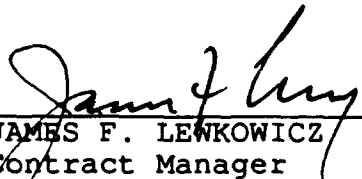


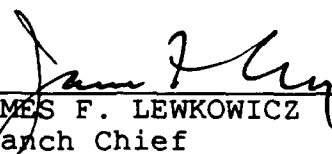
SPONSORED BY  
Defense Advanced Research Projects Agency  
Nuclear Monitoring Research Office  
ARPA ORDER NO. 5307

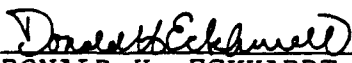
MONITORED BY  
Phillips Laboratory  
Contract F19628-89-C-0026

The views and conclusions contained in this document are those of the authors and should not be interpreted as representing the official policies, either expressed or implied, of the Defense Advanced Research Projects Agency or the U.S. Government.

This technical report has been reviewed and is approved for publication.

  
\_\_\_\_\_  
JAMES F. LEWKOWICZ  
Contract Manager  
Solid Earth Geophysics Branch  
Earth Sciences Division

  
\_\_\_\_\_  
JAMES F. LEWKOWICZ  
Branch Chief  
Solid Earth Geophysics Branch  
Earth Sciences Division

  
\_\_\_\_\_  
DONALD H. ECKHARDT, Director  
Earth Sciences Division

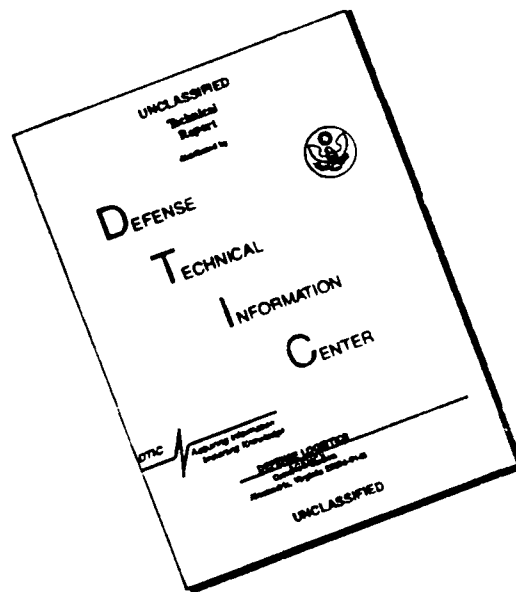
This report has been reviewed by the ESD Public Affairs Office (PA) and is releasable to the National Technical Information Service (NTIS).

Qualified requestors may obtain additional copies from the Defense Technical Information Center. All others should apply to the National Technical Information Service.

If your address has changed, or if you wish to be removed from the mailing list, or if the addressee is no longer employed by your organization, please notify PL/IMA, Hanscom AFB, MA 01731-5000. This will assist us in maintaining a current mailing list.

Do not return copies of this report unless contractual obligations or notices on a specific document requires that it be returned.

# DISCLAIMER NOTICE



THIS DOCUMENT IS BEST QUALITY AVAILABLE. THE COPY FURNISHED TO DTIC CONTAINED A SIGNIFICANT NUMBER OF PAGES WHICH DO NOT REPRODUCE LEGIBLY.

REPORT DOCUMENTATION PAGE			Form Approved OMB No. 0704-0188	
<small>Public reporting burden for this collection of information is estimated to average 1 hour per response, including the time for reviewing instructions, searching existing data sources, gathering and maintaining the data needed, and completing and reviewing the collection of information. Send comments regarding this burden estimate or any other aspect of this collection of information, including suggestions for reducing this burden, to Washington Headquarters Services, Directorate for Information Operations and Reports, 1215 Jefferson Davis Highway, Suite 1204, Arlington, VA 22202-4302, and to the Office of Management and Budget, Paperwork Reduction Project (0704-0188), Washington, DC 20503</small>				
1. AGENCY USE ONLY (Leave blank)		2. REPORT DATE March 1992		3. REPORT TYPE AND DATES COVERED Scientific No.3
4. TITLE AND SUBTITLE  Development of a Comprehensive Seismic Yield Estimation System for Underground Nuclear Explosions			5. FUNDING NUMBERS  PE: 62714E PR 9A10 TA DA WU BF  Contract F19628-89-C-0026	
6. AUTHOR(S)  J. R. Murphy J. N. Jenab				
7. PERFORMING ORGANIZATION NAME(S) AND ADDRESS(ES)  Maxwell Laboratories, Inc. S-CUBED Division P.O. Box 1620 La Jolla, CA 92038-1620			8. PERFORMING ORGANIZATION REPORT NUMBER	
9. SPONSORING/MONITORING AGENCY NAME(S) AND ADDRESS(ES)  Phillips Laboratory Hanscom AFB, MA 01731-5000  Contract Manager: James Lewkowicz/GPEH			10. SPONSORING/MONITORING AGENCY REPORT NUMBER  PL-TR-92-2076	
11. SUPPLEMENTARY NOTES				
12a. DISTRIBUTION/AVAILABILITY STATEMENT  Approved for public release; distribution unlimited			12b. DISTRIBUTION CODE	
13. ABSTRACT (Maximum 200 words)  <p>This report summarizes progress which has been achieved during the past year in the development of a comprehensive new seismic yield estimation system (YES) for underground nuclear explosions. Specifically, a prototype version of YES which is applicable to explosions at the Soviet Shagan River and Novaya Zemlya test sites is described in detail. In its current configuration, the YES encompasses a database of more than 10,000 digital seismograms recorded at stations of the USAEDS, GDSN, CDSN and IRIS networks from explosions at these two test sites. For both test areas, information regarding the explosion source environment is presented to the analyst in the context of SPOT<sup>TM</sup> satellite images of the sites, together with associated surface and subsurface geologic information and DMA topographic data. The on-line database for YES also contains a wide variety of tabular information including complete event and station location files containing both classified and unclassified locations, standard travel-time tables for the seismic arrivals used for yield estimation, propagation path and station</p> <p style="text-align: right;">(continued on reverse)</p>				
14. SUBJECT TERMS Nuclear explosions      Software system      X window Yield estimation      Shagan River      YES Seismic      Novaya Zemlya      CSS			15. NUMBER OF PAGES 110	
			16. PRICE CODE	
17. SECURITY CLASSIFICATION OF REPORT Unclassified	18. SECURITY CLASSIFICATION OF THIS PAGE Unclassified	19. SECURITY CLASSIFICATION OF ABSTRACT Unclassified	20. LIMITATION OF ABSTRACT SAR	

SECURITY CLASSIFICATION OF THIS PAGE

CLASSIFIED BY:

DECLASSIFY ON:

## 13. ABSTRACT (Continued)

corrections for use in magnitude determinations and a comprehensive instrument response database.

The capabilities and functionality of the current version of the YES system are graphically illustrated in Section II using displays of the screens encountered by an analyst in a typical processing session. The selected capabilities displayed in this sample session are related to a more complete definition of the system functionality through references to a series of appendices containing a detailed script of the operator actions required to reproduce the sample session (Appendix B), a complete description of all currently available system options (Appendix C), as well as information regarding software and hardware implementation requirements (Appendix A) and a top level schematic diagram of the main modules of the system and their interdependencies (Appendix D). Taken together, Section II and its associated appendices provide a concise description of the current status of the YES system development effort.

Motif is a trademark of the Open Software Foundation, Inc.

X Window System is a trademark of the Massachusetts Institute of Technology.

Sun SPARCStation is a trademark of Sun Microsystems, Inc.

SPOT data are copyrighted by CNES (1986,1987).

UNIX is a registered trademark of AT&T Bell Laboratories.

<b>Accession For</b>	
NTIS GRA&I	<input checked="checked" type="checkbox"/>
DTIC TAB	<input type="checkbox"/>
Unannounced	<input type="checkbox"/>
Justification	
By	
Distribution/	
Availability Codes	
Dist	Avail and/or Special
A-1	

# ***Table of Contents***

---

List of Illustrations.....	v
Introduction .....	1
Overview of Selected YES Capabilities .....	4
Summary .....	31
References .....	33
Appendix A: Requirements and Startup Instructions .....	35
Hardware Requirements .....	35
Software Requirements .....	35
Startup Instructions .....	35
Shutdown Instructions .....	36
Appendix B: Script For Sample Session .....	37
Appendix C: Reference .....	47
Introduction .....	47
Main Menu .....	49
Satellite Image .....	53
World Map .....	61
Analyst Station .....	63
Magnitude Measurement .....	69
Yield Estimation .....	85
Statistical Summary .....	88
Spreadsheet .....	92
Event Summary .....	94
Appendix D: Dependencies between YES modules .....	95

# **List of Illustrations**

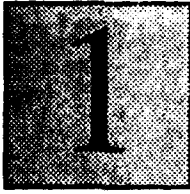
---

Figure 1:	Main menu structure for YES .....	4
Figure 2:	Illustration of pulldown access to individual menus .....	5
Figure 3:	SPOT satellite image of the Shagan River test site with superimposed locations of the historical explosions (squares) and current event (diamond) .....	6
Figure 4:	Full resolution SPOT satellite image of the region surrounding the Shagan River cratering explosion of 15 January 1965 .....	7
Figure 5:	Illustration of interactive modification of brightness and contrast in SPOT satellite image display .....	8
Figure 6:	SPOT satellite image of the Shagan River test site with superimposed surface geologic map and current event location .....	8
Figure 7:	Color-coded representation of DMA topographic data for the Shagan River test site with super imposed topographic contours and current event location .....	9
Figure 8:	Vertical subsurface section through the current event shotpoint along the interactively selected line shown on the SPOT image insert .....	10
Figure 9:	Color-coded representation of depth to the top of the granite surface beneath the Shagan River test site with superimposed depth contours and current event location .....	10
Figure 10:	World Map projections ( $D < 100^\circ$ ) showing locations of stations for which digital teleseismic P (left) and Lg (right) data are available for the current event .....	11
Figure 11:	Analyst station display of vertical-component Lg signals for the current event .....	12
Figure 12:	Magnitude Measurement menu .....	13



Figure 13:	Analyst station display of selected vertical-component teleseismic P wave signals for the current event .....	14
Figure 14:	Example of the specification and subsequent application of a bandpass filter to the data of Figure 13 .....	15
Figure 15:	SPOT locations of Shagan River explosions recorded at station KONO in Norway. The diamond symbols denote those events selected for comparative analysis.....	16
Figure 16:	Comparison of the P wave signal recorded at the station KONO from the current event (top and red) with the signals recorded at that station from the selected events of Figure 15.....	16
Figure 17:	Illustration of the interactive determination of the amplitude and period values used to define single station mb values .....	17
Figure 18:	Comparison of individual station and network-averaged mb magnitudes determined for the current event.....	18
Figure 19:	Comparison of individual station and network-averaged MLg magnitudes determined for the current event .....	18
Figure 20:	Comparison of the observed value of mb-MLg (NORSAR) for the current event with the contours representing observed variation of that parameter for previous events .....	19
Figure 21:	Analyst station display of selected long-period Rayleigh wave signals for the current event.....	20
Figure 22:	Example of the specification and subsequent application of the instrument response normalization feature to the data of Figure 21 .....	20
Figure 23:	Menu options for the estimation of network-averaged P wave spectra .....	21
Figure 24:	Comparison of normalized observed and best-fitting theoretical network-averaged P wave spectra for the current event .....	22

Figure 25:	Comparison of the inferred surface wave moment tensor solution for current event with the corresponding path normalized, observed Rayleigh (left) and Love (right) wave amplitude data .....	22
Figure 26:	Comparison of the surface wave moment tensor solution for the current event (yellow and light blue concentric circles) with those for nearby Shagan River explosions (red and dark blue concentric circles) and with the surface geologic map of the area .....	23
Figure 27:	Menu and sample output for the unified yield estimation module.....	24
Figure 28:	Comparison of unified yield estimates (W) and associated uncertainties (F) obtained with (top) and without (bottom) the surface wave moment tensor magnitude.....	25
Figure 29:	Statistical assessment menu .....	26
Figure 30:	Comparison of the results of three different tests of seismic compliance of the current event with the 150 kt threshold of the TTBT .....	27
Figure 31:	Compliance test results (Test 1) for the scenario in which the current event data were observed from an explosion below the water table at NTS .....	27
Figure 32:	Spreadsheet summary comparison of seismic yield estimates for the current event (09/14/88) with those obtained for selected previous Shagan River explosions .....	28
Figure 33:	Spreadsheet summary illustrating the results of interactively modifying the designated magnitude/ yield relations.....	29
Figure 34:	Summary of analysis results for the selected event .....	30



# Introduction

---

Over the past several years S-CUBED, under DARPA support, has been developing a comprehensive new seismic yield estimation system for underground nuclear explosions. The principal objective of this program has been to implement a flexible, interactive software system in which yield estimates based on a wide variety of different seismic magnitude measurements can be efficiently determined, merged with all available information regarding the test location under consideration and statistically combined to obtain both a unified seismic estimate of explosion yield and quantitative measures of the uncertainty in that estimate. A preliminary prototype version of a system designed to achieve the above objective, designated the Yield Estimation System (YES), has been implemented in a Sun color workstation (SPARCStation) environment at the DARPA Center for Seismic Studies (CSS). This document provides a user's guide which is applicable to the current version of that system. A comprehensive overview of the system software design and technical specifications is provided in a recent report by Murphy *et al.* (1991).

In its current configuration, the system is applicable to underground nuclear explosions at the Soviet Shagan River and Novaya Zemlya test sites and encompasses a database of more than 10,000 digital seismograms recorded at stations of the USAEDS, GDSN, CDSN and IRIS networks from explosions at these two sites. For both test areas, information regarding the explosion source environment is presented to the analyst in the context of SPOT<sup>TM</sup> satellite images of the sites, together with associated surface and subsurface geologic information and DMA topographic data. The on-line database for YES also contains a wide variety of tabular information, including complete event and station location files containing both classified and unclassified locations, standard travel-time tables for the important phases (Herrin *et al.*, 1968), propagation path and station corrections for use in magnitude determinations and a comprehensive instrument

response database. The instrument database is a compilation of information collected from the USGS, AFTAC, IRIS and others which details the characteristics of the recording instruments as a function of station, channel and date. There are currently 750 different response histories in this section of the database.

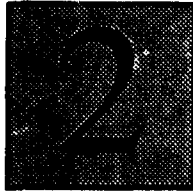
The user interface to the system has been designed to be completely menu-driven and mouse-activated and requires no keyboard entry by the operator once the system has been accessed. This graphical user interface has been built using the X Window system. X was designed specifically to allow hardware independence, to foster ease in porting applications to machines other than those for which they were developed, and to permit running of applications on one computer while displaying their output on another, even if the computers are of different manufacture. YES was designed and implemented on Sun SPARC computers (e.g., SPARCStations), but transfer to any other system that supports X and UNIX could be accomplished easily. The X interface has been written using the X toolkit. The X toolkit enforces an object-oriented approach to programming by combining the windows and the operations on the windows into "widgets." YES uses several widget sets including the Motif widget set from the Open Software Foundation, the X widget set from Hewlett Packard, the Athena widget set from MIT, graphics widgets written by Teledyne-Geotech and SAIC, and special purpose widgets for YES written by S-CUBED.

YES consists of a hierarchy of programs. At the top level is a master program whose primary function is to start the other analysis programs. The top level program allows the user to select the test site, event and seismic phase to be processed, as well as the analysis tools to apply to the seismic data corresponding to that selection. It then starts the appropriate analysis programs with the proper initialization values. All the required software has been written in either the C or FORTRAN programming languages. C was chosen because programmer's calls to the X Window System procedures are in C, and because C is well-suited to the design of complex systems with a variety of data structures. FORTRAN was used because it is optimal for certain types of computational analysis, and because its use permitted the inclusion of many previously existing analy-



sis tools into YES. As a result, the top level programs, interactive modules, database interface, and graphics routines are written in C, and, when appropriate, these routines call FORTRAN subroutines.

This document provides a user's guide and reference manual for the operation of the current version of the YES system. In Section II, the capabilities and functionality of the system are graphically illustrated through displays of the screens encountered by an analyst in a typical processing session for a selected explosion (i.e., the Soviet JVE explosion of 14 September 1988). This is followed in Section III by a brief summary of the current status of the YES system. A detailed script of the operator actions required to reproduce this sample session is provided in Appendix B. This is preceded in Appendix A by an overview of the software and hardware required to implement YES, as well as detailed startup instructions for the system. Appendix C provides a complete description of all the currently available system options, including information regarding their access and application from the menus contained in the individual analysis modules. This is followed in Appendix D by a top level schematic diagram of the main modules of the system and their interdependencies.



## **Overview of Selected YES Capabilities**

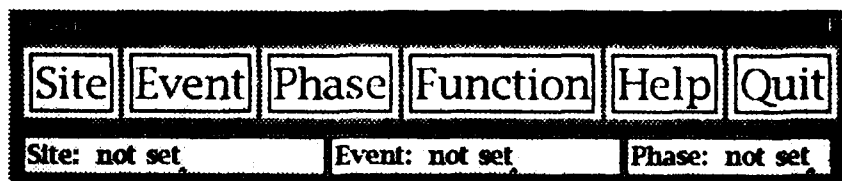
---

In this section, some of the capabilities and functionality of the YES system will be graphically illustrated through displays of the screens encountered by an analyst in a typical processing session for a selected explosion. For this example, the unclassified data from the Soviet JVE explosion of 14 September 1988 will be analyzed and used to illustrate various features of the system. A detailed script of the operator actions required to reproduce this sample session is provided in Appendix B. This is followed in Appendix C by a complete description of all the system options which are available in the current version.

### **Main Menu**

As has been noted previously, a distinguishing characteristic of the YES is that it is completely menu-driven and mouse-activated and requires no keyboard entry by the user. The top level menu providing access to the system is shown in Figure 1. It consists of six buttons which can be used to initiate (SITE, EVENT, PHASE, FUNCTION) or terminate (QUIT) action within the system or to view on-line information regarding the operating characteristics and parameters of the system (HELP). Choosing any of these buttons causes a series of pulldown menus to be activated as illustrated in Figure 2. In this example, the SITE button has been activated to select the Soviet Shagan River (Balapan) test site, and the EVENT button has been activated to select the JVE explosion which was detonated at that test site on 14 September 1988. Once the test site and event have been selected, the remaining analyst interaction with the system is initiated through the PHASE and FUNCTION buttons. The PHASE button provides the analyst with the capability to choose from among the six different seismic phases listed in Figure 2 for which digital waveform data are currently available on the system. The FUNCTION button provides access to the

**Figure 1.**  
*Main menu structure for YES.*

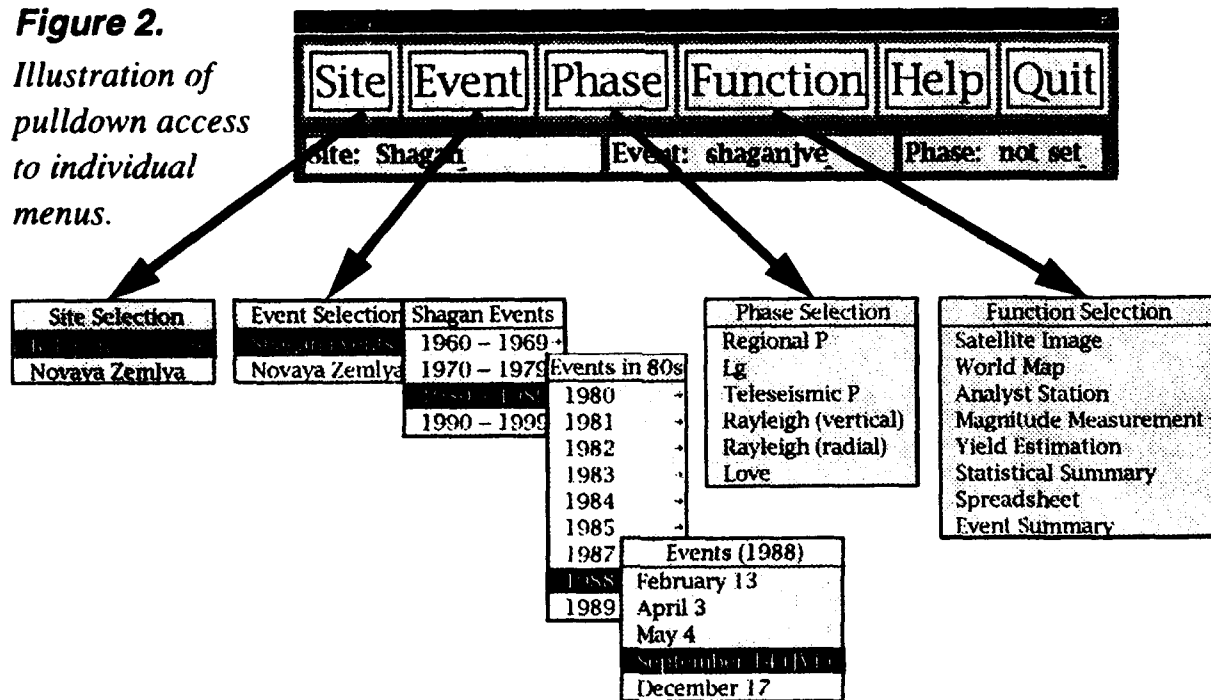


seven principal computational and analysis modules which permit the analyst to

- view the seismic data within the context of the available information regarding the specific test location under investigation (*Satellite Image, World Map*)
- interact with the recorded seismic data to process it and extract the various magnitude measures of interest (*Analyst Station, Magnitude Measurement*)
- formally combine the seismic measures of source size to obtain an optimum measure of explosion yield and quantitative measures of the uncertainty in that estimate (*Yield Estimation*)

**Figure 2.**

*Illustration of pulldown access to individual menus.*



- statistically assess the results with respect to any existing treaty thresholds or other yield levels of particular interest (*Statistical Summary, Spreadsheet*)
- view a one page summary of the results obtained by applying the system to the data recorded from the selected explosions (*Event Summary*).

## Satellite Image

Having specified a test site and a particular explosion (in this case the JVE event), a typical analysis sequence would begin with the selection of the *Satellite Image* option from the **FUNCTION** menu, which brings to the screen the SPOT satellite image display of the Shagan River test site shown in Figure 3. In this initial display of the test site information interface, the locations of previous explosions at this site are shown as color-coded square overlays, with the current event highlighted by a yellow diamond. In this case, the different colors are used to differentiate those explosions about which the Soviets have published data in the open literature (blue) from those for which only seismic information is available (red). It is important to note that this is not merely a static display, but that in fact the image and the overlays to it are formally tied to an extensive on-line database of supplementary information. Thus, for example, in this figure the operator has clicked on one of the blue squares (arrow), which has initiated a process by which available information about that event has been extracted from the database and displayed on the information line below the menu buttons, indicating that this explosion was detonated at Shagan on 10 December 1972 at the specified latitude and longitude and that Bocharov *et al.* (1989) have reported the depth as 478.0 m and the yield as 140 kt.

**Figure 3.**  
*SPOT satellite image of the Shagan River test site with superimposed locations of the historical explosions (squares) and current event (diamond).*





**Full res**

For purposes of display, the satellite image shown in Figure 3 has been compressed to an effective resolution of about 30 m so that the entire test site can be viewed on a single screen. However, the data corresponding to the full 10 m resolution of the SPOT image can also be viewed by activating the appropriate button (*Full res*) on the right hand margin of this display and simply pointing with the mouse to any location on the image. For example, Figure 4 shows the full resolution sub-image corresponding to the location of the cratering explosion of 15 January 1965 which dammed the Shagan River, producing the prominent lake in the southeast quadrant of Figure 3. Another feature provided by this image display module is the capability to interactively adjust the contrast and brightness using the slider bars located at the bottom of the right hand menu margin. Figure 5 illustrates this feature by way of a comparison of the nominal display (right) with that resulting from interactively reversing the contrast and decreasing the brightness (left) by repositioning these sliders with the mouse. It can be seen that different features are emphasized in these two displays, which facilitates analyst identification of both geologic and man made features.

**Surface Geology and Topography**

In addition to the event locations, a number of geologic and topographic databases have been registered to this SPOT image and are available for display from the OVERLAYS and IMAGES menus. For example, Figure 6 shows the overlay of Leith's (1989) color-coded, surface geologic

**Figure 4.**  
Full resolution  
SPOT satellite  
image of the  
region sur-  
rounding the  
Shagan River  
cratering  
explosion of 15  
January 1965.

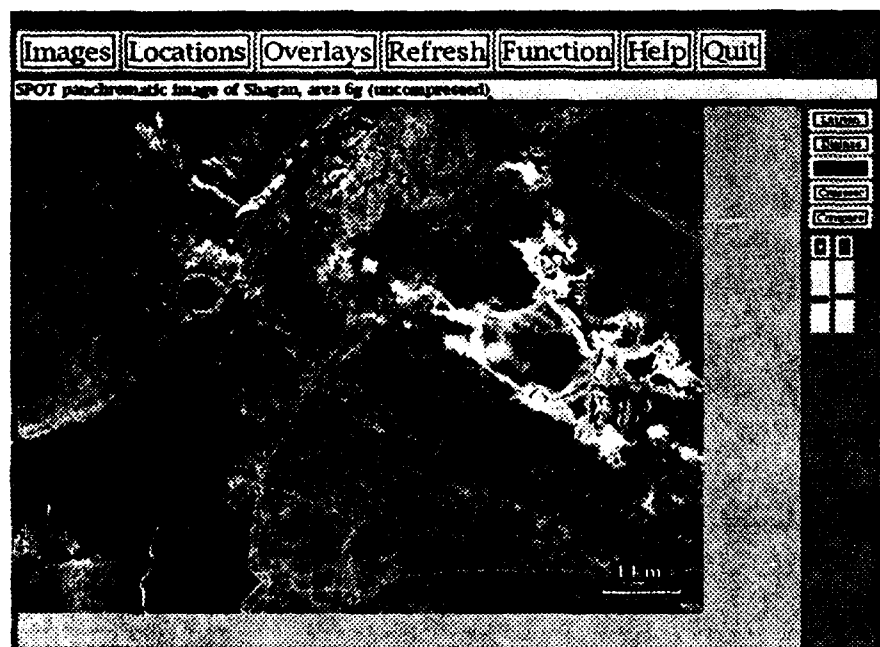


**Figure 5.**  
Illustration of  
interactive  
modification  
of brightness  
and contrast  
in SPOT sat-  
ellite image  
display.

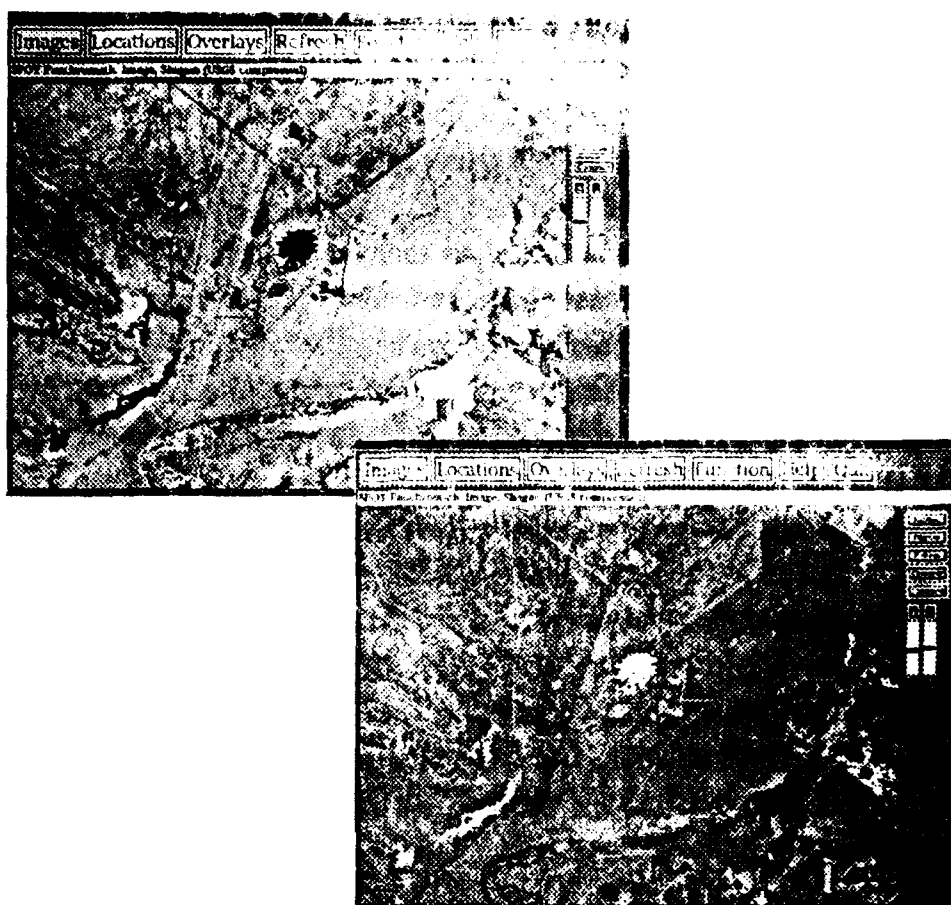
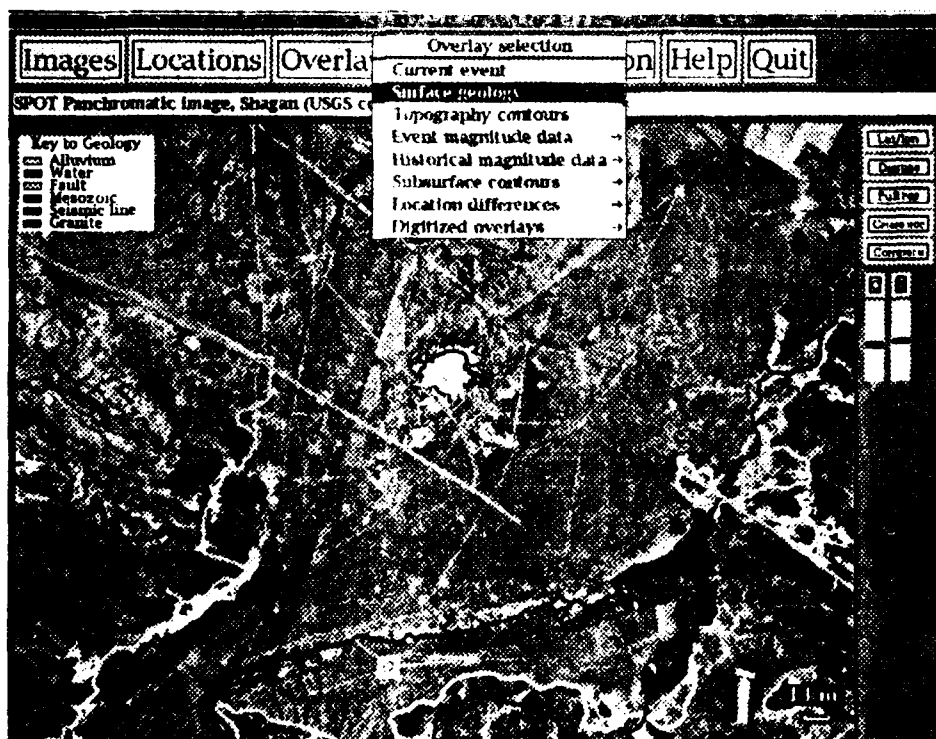


**Figure 6.**  
SPOT satellite  
image of the  
Shagan River  
test site with  
superimposed  
surface geo-  
logic map  
and current  
event loca-  
tion.



map of the area, where the location of the current event (square) is shown in the context of the various exposed geologic units and the trace of the prominent Chinrau fault which intersects this portion of the test site. The Defense Mapping Agency's topographic database for the area is displayed in color-coded image form in Figure 7 together with overlays of the corresponding topography contours and current event location selected from the OVERLAYS menu.

### **Cross Section**

The variation of surface topography, as well as subsurface geology to a depth of about 1 km, along any specified line across the image can be accessed using the cross-section button (*Cross sec*) on the right hand margin of the image display. This feature is illustrated in Figure 8 where the left hand panel shows the line selected by the analyst by pointing with the mouse to two arbitrary points on the SPOT image and the right hand panel shows the resulting vertical section through that line which was automatically produced by the system, together with the locations and approximate depths of penetration of explosion emplacement holes encountered along that line.

**Figure 7.**  
*Color-coded  
representation  
of DMA topo-  
graphic data  
for the Shagan  
River test site  
with superim-  
posed topo-  
graphic  
contours and  
current event  
location.*

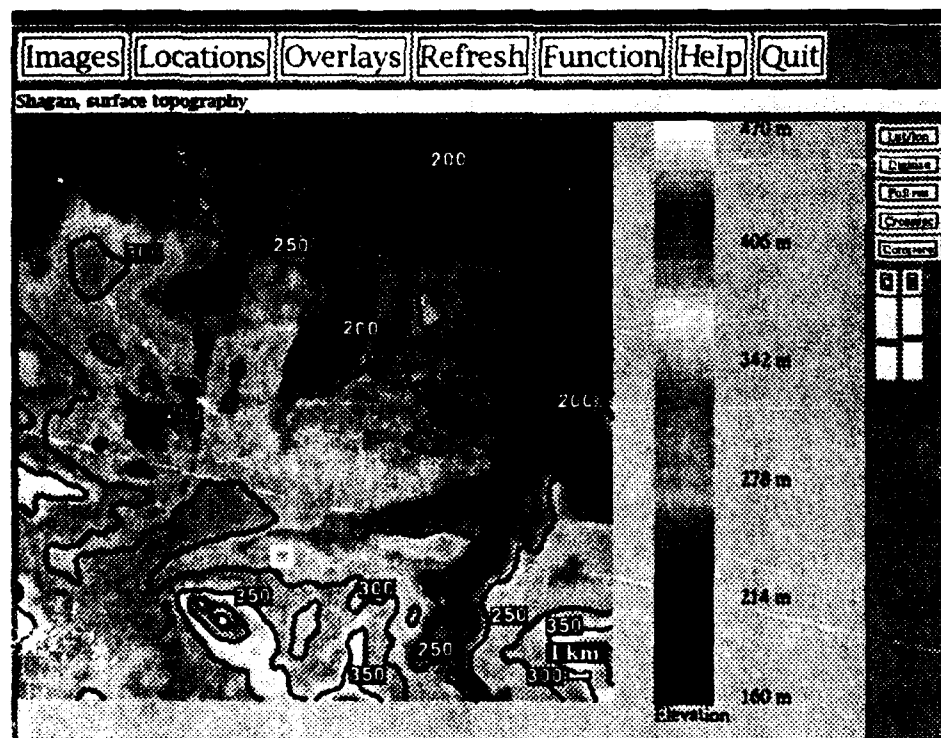
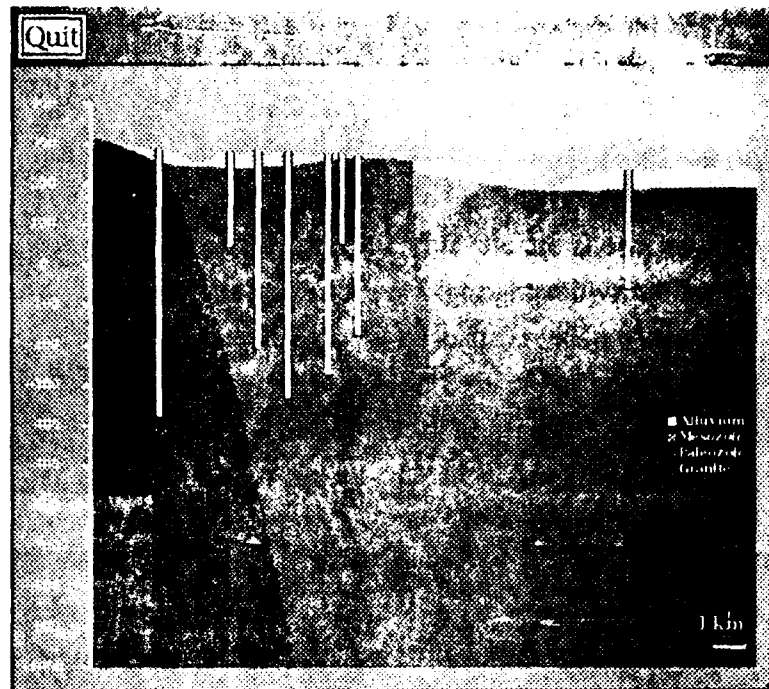


**Figure 8.**

*Vertical subsurface section through the current event shot-point along the interactively selected line shown on the SPOT image insert.*



### **Depth to Granite**

As with the surface topography, the variation in the depth to any selected geologic interface can also be exhibited in image form, as illustrated for the granite surface in Figure 9 where, once again, the corresponding depth contours and location of the current event have been overlaid for reference purposes. It is immediately evident from this presentation that,

**Figure 9.**

*Color-coded representation of depth to the top of the granite surface beneath the Shagan River test site with superimposed depth contours and current event location.*



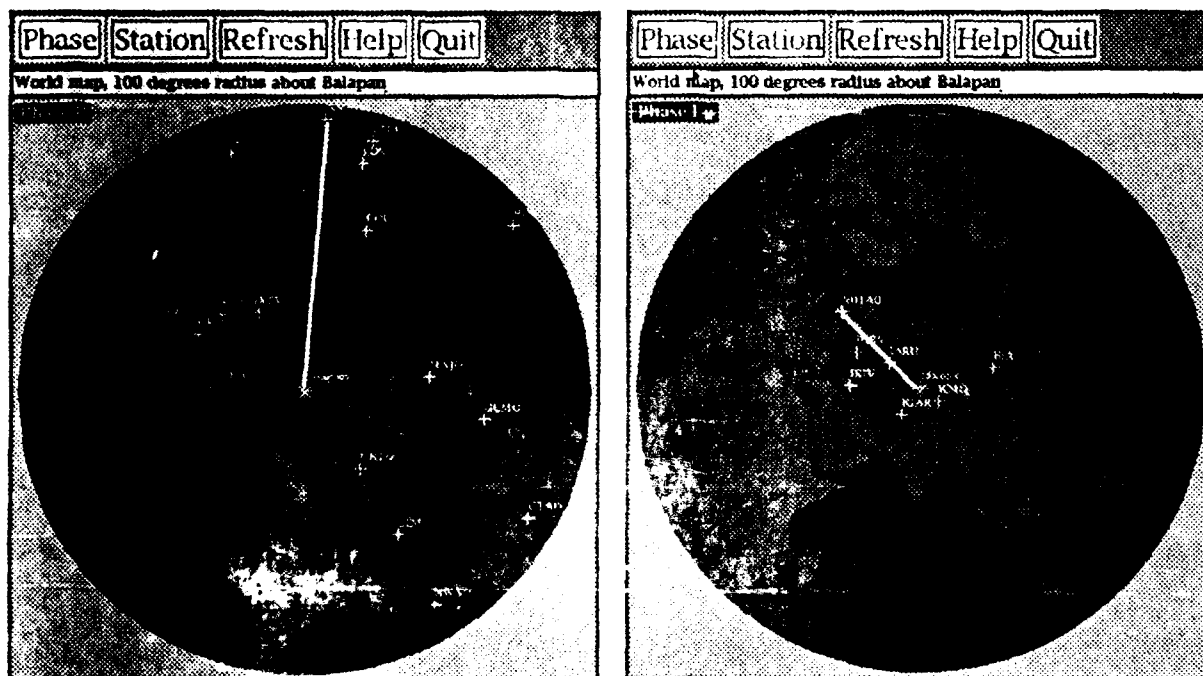
rather than the typical crustal thickness of 30 km. Stations at this test site have been located on a relatively flat topographic surface throughout much of this region lies uniformly below typical explosion emplacement depths.

## World Map

Having completed an initial review of the available information regarding the explosion test environment, the analyst can next proceed to an examination of the corresponding recorded seismic data. As an initial step, an overview of the locations of stations for which data from the selected explosion are available on the system can be obtained by selecting the *World Map* option from the FUNCTIONS menu. The resulting displays for the teleseismic  $P$  and regional  $L_g$  phases are shown in Figure 10, plotted on azimuthal equidistant projections of the globe ( $\Delta < 100^\circ$ ) centered on the Shagan River test site. The STATION menu item within this module provides the user with the capability to select any one of these recording stations from a list and subsequently cause a straight line to be drawn on the screen between the source and the receiver shown in the figure. In this transformation, the straight line corresponds to the great circle path and thus provides the analyst with a view of the surface projection of

**Figure 10.**

*World Map projections ( $\Delta < 100^\circ$ ) showing locations of stations for which digital teleseismic  $P$  (left) and  $L_g$  (right) data are available for the current event.*

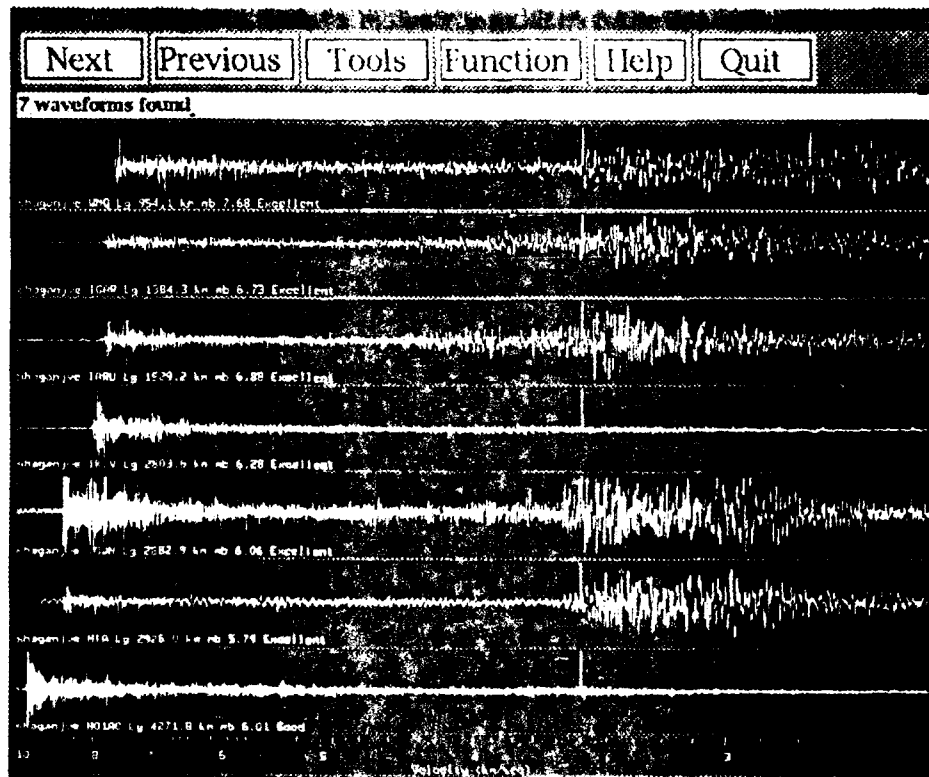


the propagation path (which may be a complex path) between these two points.

## ***Analyst Station and Magnitude Measure- ment***

The seismic data themselves can be accessed by returning to the main menu (Figure 2) and sequentially selecting a seismic phase from the PHASE menu and *Analyst Station* from the FUNCTION menu. Thus, for example, specifying the phase  $L_g$  in this manner automatically initiates a process by which the  $L_g$  recordings from the JVE explosion are extracted from the on-line database of digital waveform data and displayed on the screen in the format shown in Figure 11. In this and subsequent seismogram displays, the stations are ordered by increasing epicentral distance and, for the  $L_g$  and surface waves, the data are plotted as a function of group velocity. It can be seen in this figure that the traces are marked by a vertical line at a group velocity of 3.5 km/sec, indicating the nominal expected onset time of the  $L_g$  phase. This display permits the analyst to quickly assess the quality of the data and identify any prominent characteristics. Thus, for example, it can be seen from Figure 11 that the  $L_g$  signals are relatively weak at the IRIS station KIV (IKIV) and at NORSAR (N01A0), consistent with the expected effects of propagation across the Caspian Sea (KIV) and along the complex, far regional path to Norway.

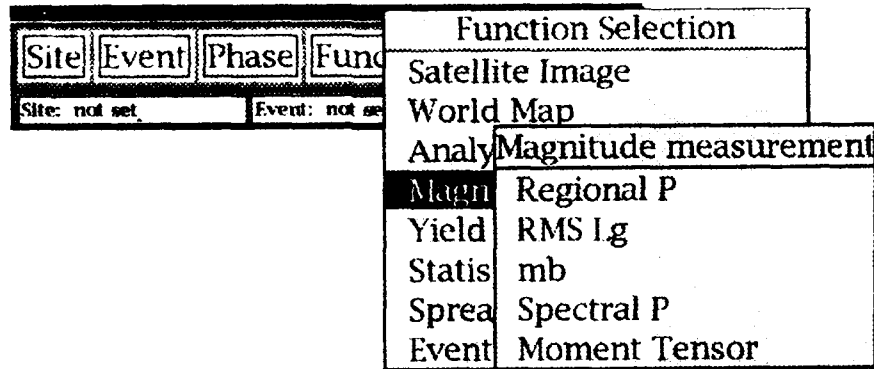
**Figure 11.**  
*Analyst sta-  
tion display  
of vertical-  
component  $L_g$   
signals for  
the current  
event.*



## RMS $L_g$ Startup

Having verified that the available  $L_g$  data are suitable for further processing, the analyst can proceed to magnitude estimation by selecting the *Magnitude Measurement* option from the FUNCTION menu as illustrated in Figure 12. Selecting RMS  $L_g$  from this list of five currently available magnitude measures initiates a series of operations by which the  $L_g$  waveforms recorded from the JVE event are automatically processed using algorithms described by Ringdal (1983) to obtain single-station and network-averaged measures of the  $L_g$  magnitude,  $M_{Lg}$ . Since this processing

**Figure 12.**  
*Magnitude  
Measurement  
menu.*



takes some time to accomplish, it is run in the background, thereby permitting the analyst to move on to other tasks while it is being completed. In the present example, the analyst has selected *Teleseismic P* from the PHASE menu and *Analyst Station* from the FUNCTION menu, resulting in the waveform display shown in Figure 13. The P wave seismograms are plotted here as a function of reduced time, extending from 10 seconds before to 15 seconds after the signal onset time which is denoted by the vertical line segments. Generally, there are more recordings than can be displayed on a single screen in this format and, in such cases, the analyst can readily page forward and backward through these multiple screens using the NEXT and PREVIOUS menu buttons at the top of the analyst station display.

## Tools

An extensive set of signal processing and analysis capabilities has been assembled within the analyst station module, as indicated by the TOOLS menu display in Figure 13. These tools permit the analyst to:

- redefine arrival times (*Pick Arrival*),
- assign waveform quality (*Set Quality*),
- measure amplitudes and periods (*Expand,  $m_b$* ),

- filter the data (*Demean/detrend, Filter*),
- normalize to a common instrument response (*New instrument*),
- compare a selected waveform with waveforms recorded in earlier station from previous explosions (*Compare, Clone*).

### Filter

Thus, for example, it can be seen from Figure 13 that the P wave signal recorded at station MAJO in Japan (bottom trace) is obscured by microseismic noise lying outside the signal passband. Selecting *Filter* from the TOOLS menu causes the interactive filter interface to be displayed as shown in Figure 14, where the analyst has used the mouse to adjust the slider bars to define low and high frequency cutoffs of 0.5 and 5.0 Hz, respectively, and to specify a second order roll-off outside that band by setting the corresponding pole numbers to 2. Subsequent selection of any trace with the mouse causes this filter to be automatically applied and the result displayed, as shown here for station MAJO.

### Compare

Application of the *Compare* function from the TOOLS menu provides another illustration of the powerful capability for interactive analysis which is available in the analyst station. For example, by sequentially

**Figure 13.**  
Analyst station display of selected vertical-component teleseismic P wave signals for the current event.

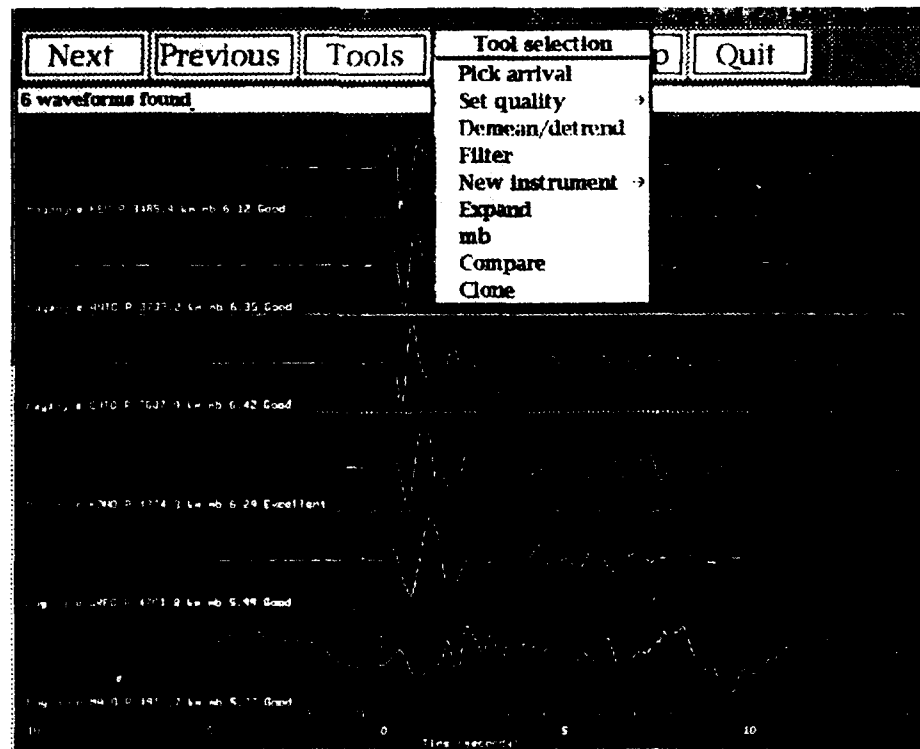
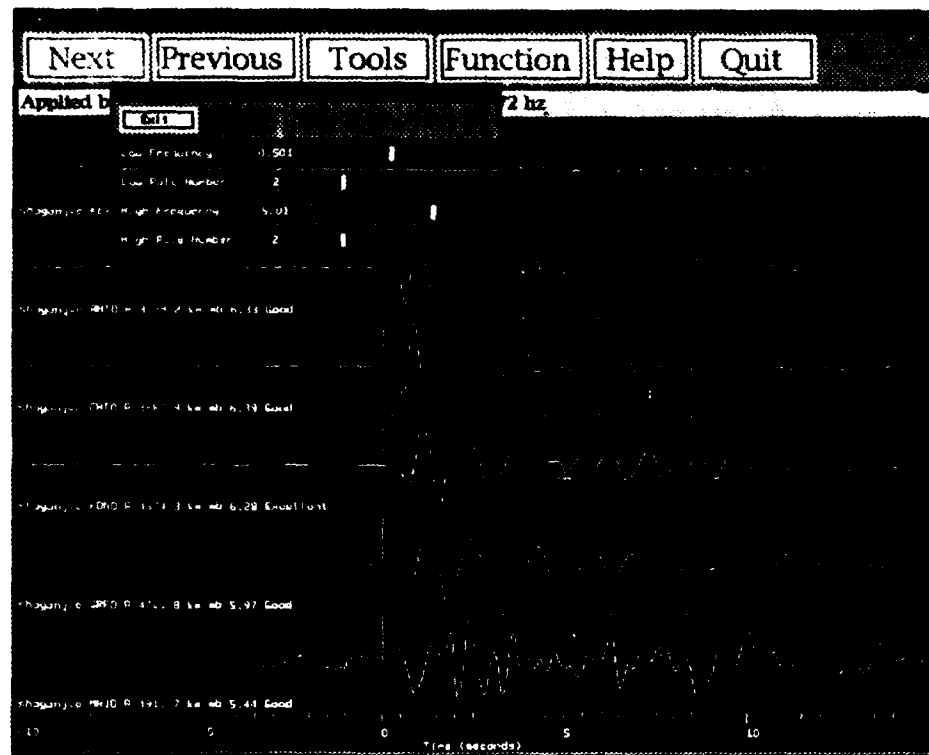




**Figure 14.**  
Example of  
the speci-  
fication and  
subsequent  
application  
of a band-  
pass filter to  
the data of  
Figure 13.



selecting this function and the station KONO waveform from Figure 14, a search through the database is automatically initiated to identify all other available P waveforms recorded at that station from previous Shagan River explosions. Generally, not all of the explosions identified by this search are of equal importance for comparative purposes and selection of a meaningful subset is facilitated by examining their locations in the context of the SPOT image test site information interface, as indicated in Figure 15. Using this interface, the analyst can interactively select specific events with the mouse, as indicated here by the diamond overlays, on the basis of proximity to the current event or some other criterion, and display the corresponding P waveforms in a time expanded analyst station mode such as that of Figure 16. Here the current JVE event recording is shown at the top of the figure and the waveforms from the selected comparison events are displayed beneath it in the order in which they were selected.

### **Clone**

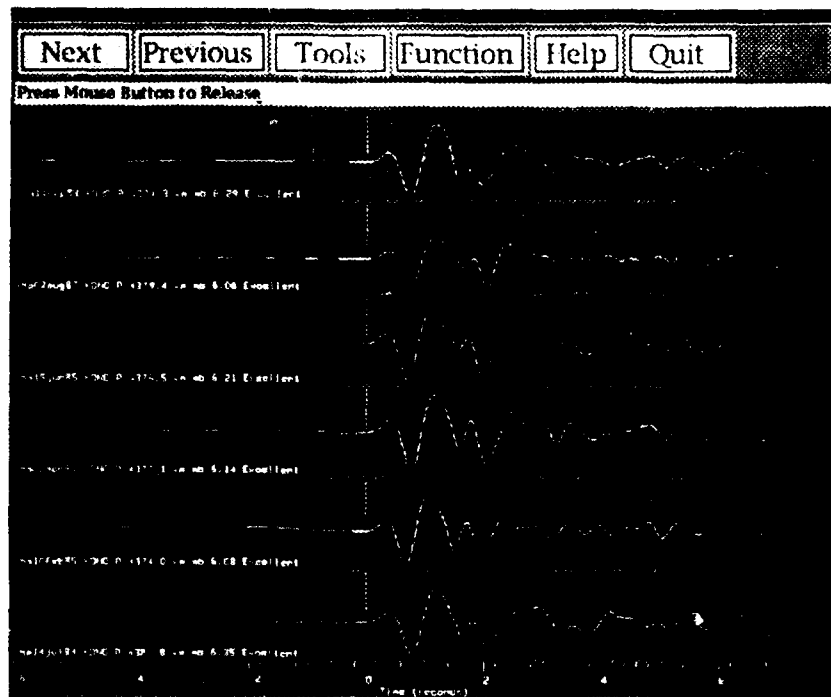
Also illustrated in Figure 16 is the use of the *Clone* feature from the TOOLS menu which permits the operator to select any trace on the screen with the mouse (in this case the JVE recording), create a color-coded (red)

**Figure 15.**  
SPOT locations  
of Shagan River  
explosions  
recorded at sta-  
tion KONO in  
Norway. The dia-  
mond symbols  
denote those  
events selected  
for comparative  
analysis.



copy and drag it to any other location on the screen to conduct detailed waveform comparisons. This capability permits the analyst to quickly assess the consistency of the current observation with past experience and, in this case, to conclude that the JVE recording at KONO is quite consistent with previous observations at that station from other explosions located in that area of the test site.

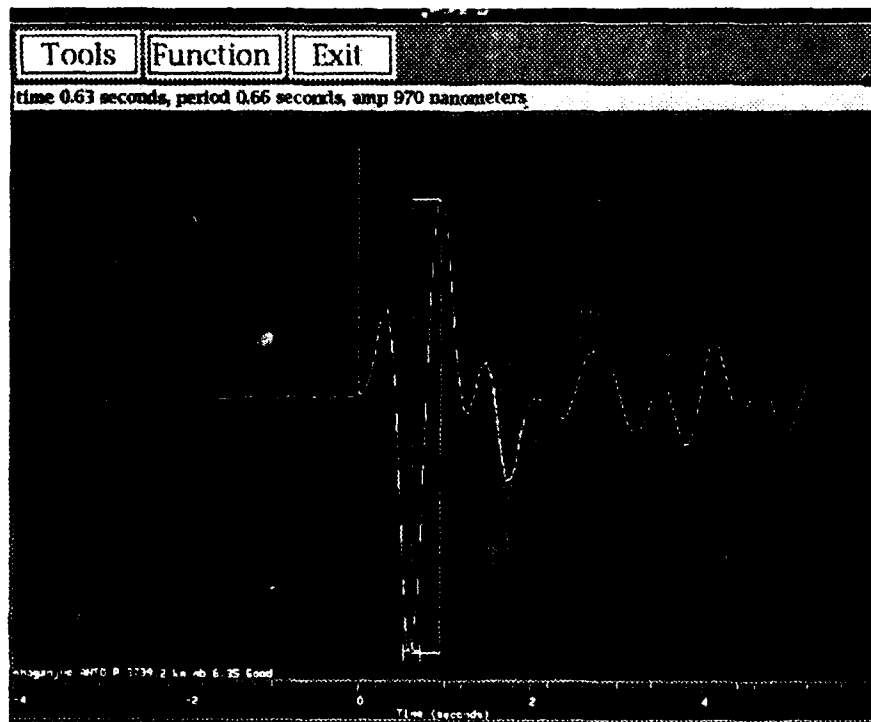
**Figure 16.**  
Comparison of  
the P wave sig-  
nal recorded at  
the station  
KONO from the  
current event  
(top and red)  
with the signals  
recorded at that  
station from the  
selected events  
of Figure 15.



### **Expand and $m_b$**

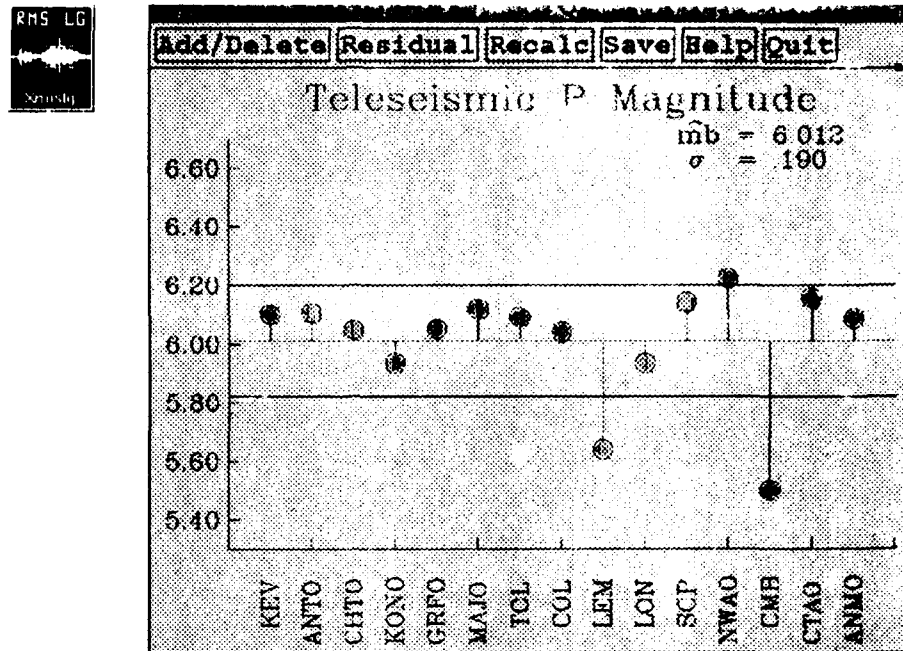
Once the initial waveform review has been completed, the analyst can proceed to magnitude estimation using the *Expand* and  $m_b$  functions from the TOOLS menu. By sequentially selecting *Expand* and any waveform from the analyst station display, a magnified reproduction of that waveform is produced as shown in Figure 17. Then, by employing the  $m_b$  function, the mouse can be used to position a rectangle so as to define the peak-to-peak amplitude and half period of the selected cycle of motion as shown in this figure. After this process has been repeated for each usable trace, the resulting amplitudes are input to the  $m_b$  estimation module using the *Magnitude Measurement* menu of Figure 12 where they are converted to ground motion, corrected for epicentral distance and station effects and logarithmically averaged to obtain a network-averaged  $m_b$  value and associated uncertainty. The resulting individual station  $m_b$  values for the current JVE explosion are displayed in Figure 18, together with the estimated network-averaged value of 6.012. This display module also provides the capability for the analyst to interactively eliminate questionable data points and then to recalculate the network average using the ADD/DELETE and RECALC menu buttons shown at the top of the figure. This process can be continued until a final stable  $m_b$  estimate is obtained, at which time it is written to the database using the designated SAVE menu button.

**Figure 17.**  
*Illustration of  
the interactive  
determination  
of the ampli-  
tude and  
period values  
used to define  
single station  
 $m_b$  values.*



**Figure 18.**

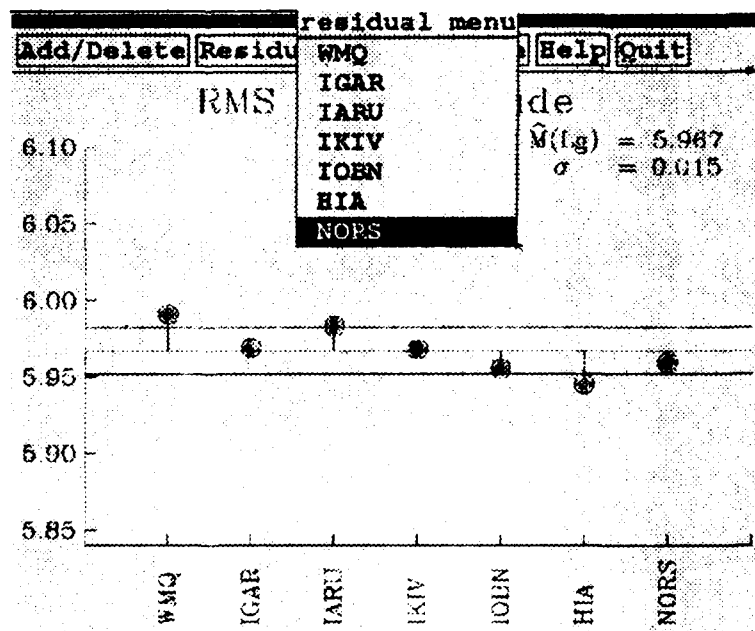
Comparison of individual station and network-averaged  $m_b$  magnitudes determined for the current event.

**RMS  $L_g$** 

Note from Figure 18 that at this point the system has notified the analyst that the RMS  $L_g$  magnitude estimation has been completed, as indicated by the icon in the upper left hand corner of this display. Selecting this icon with the mouse produces the display of individual station and network-averaged  $M_{Lg}$  values shown in Figure 19. It can be seen from this figure that the estimated network-averaged  $M_{Lg}$  value of 5.967 is somewhat lower than the corresponding  $m_b$  value of 6.012 of Figure 18, and it would be natural for the analyst to question whether there is any significance to

**Figure 19.**

Comparison of individual station and network-averaged  $M_{Lg}$  magnitudes determined for the current event.



this difference. This issue can be addressed by selecting a representative station (e.g., NORS) from the RESIDUAL menu on this display and returning to the SPOT image test site information interface to overlay the quantity  $m_b - M_{Lg}(NORS)$  at the current event location as in Figure 20, where contours of this quantity derived from results of previous explosions have also been overlaid for reference purposes. It can be seen from this display that while this magnitude difference is typically negative in the northeast quadrant of the test site (by as much as 0.15 magnitude units), it is generally positive in the vicinity of the current JVE event location, with an average value close to the observed value of 0.043. Thus, this capability permits the analyst to quickly conclude that the current result is entirely consistent with previous experience in this area of the test site.

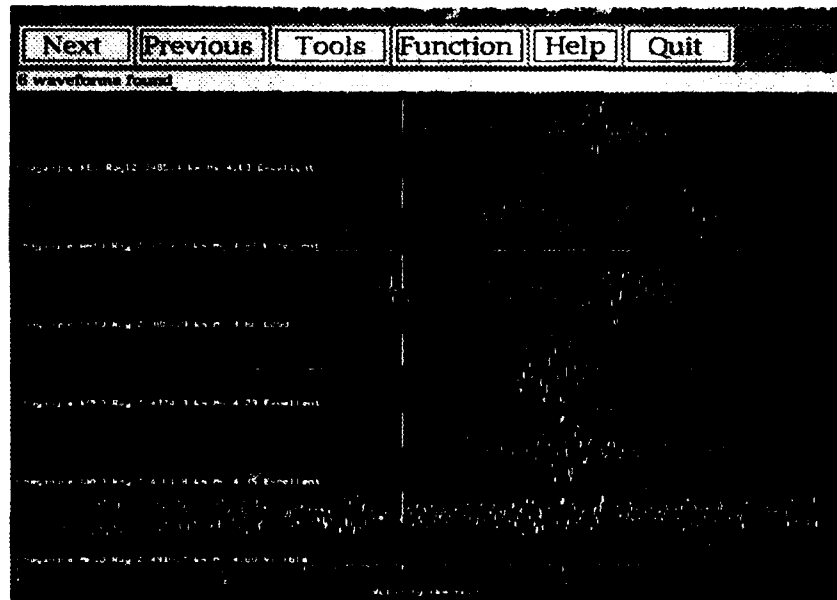
**Figure 20.**  
*Comparison of the observed value of  $m_b - M_{Lg}$  (NOR-SAR) for the current event with the contours representing observed variation of that parameter for previous events.*



### **New Instrument**

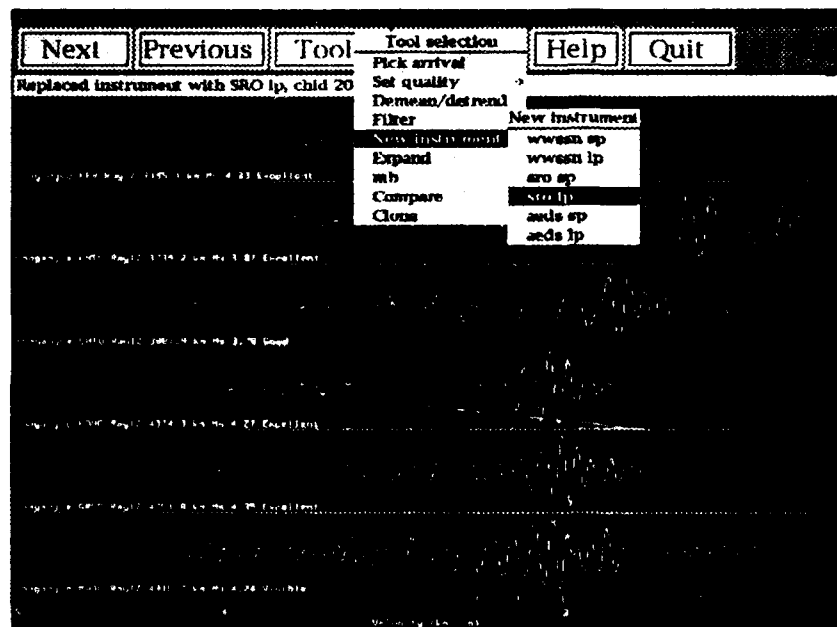
The long-period surface wave data can be accessed in the same manner as the  $L_g$  and P phase data described above, resulting in analyst station displays such as that shown in Figure 21 for the vertical component Rayleigh wave phase. It can be seen from this example that, although these traces are aligned according to a common group velocity scale, the surface wave signals are quite variable and difficult to correlate from trace to trace. This is at least partially due to the fact that the response characteristics of the long-period instruments used to record these data vary significantly between stations. Thus, for example, the station MAJO trace shown at the bottom of this figure was recorded through a relatively broadband system,

**Figure 21.**  
Analyst station display of selected long-period Rayleigh wave signals for the current event.



with the result that the long-period signals of principal interest are obscured by higher frequency arrivals. In order to provide a common basis for comparison, the TOOLS menu includes a function (*New instrument*) which permits the analyst to transform the data to that which would have been observed if the same instrumentation had been employed at each station. This feature is graphically illustrated in Figure 22 where the analyst has selected the nominal SRO long-period response and converted all of the traces in this display to that response by simply designating them with the mouse. It is evident from this example that such a capability greatly facilitates quantitative comparisons and evaluation of data.

**Figure 22.**  
Example of the specification and subsequent application of the instrument response normalization feature to the data of Figure 21.



### Spectral P

Once the available long-period Rayleigh and Love wave data have been reviewed, the analyst can return to the *Magnitude Measurement* menu of Figure 12 and select *Moment Tensor*, thereby initiating a process by which the observed long-period data are phase matched filtered and formally inverted to obtain a surface wave measure of seismic magnitude. While this computationally intensive process is running in the background, the analyst next selects *Spectral P* from this same menu and proceeds with an interactive determination of the network-averaged P wave spectrum corresponding to the current event. The spectrum estimated in this process can be inverted to obtain either an equivalent spectral magnitude or a direct, model-based yield estimate (Murphy, 1989), and Figure 23 shows the menu structure for the latter option, where it is indicated that the Mueller/Murphy granite (M/M Granite) source model has been selected for the current JVE event. The resulting automatic fit to the attenuation-corrected, observed spectrum is shown in Figure 24 where it is indicated that a theoretical spectrum corresponding to a yield (W) of 119 kt, a pP - P delay time ( $T_0$ ) of 0.82 seconds and a pP/P amplitude ratio (A) of 0.17 provides the best overall fit to the data. Alternately, the analyst can elect to interactively change these automatically determined model parameters using the plus and minus buttons located in the box in the upper right corner of this display, to explore solutions corresponding to goodness of fit criteria not incorporated in the automatic algorithm.

**Figure 23.**  
Menu options  
for the estimation  
of network-  
averaged P  
wave spectra.

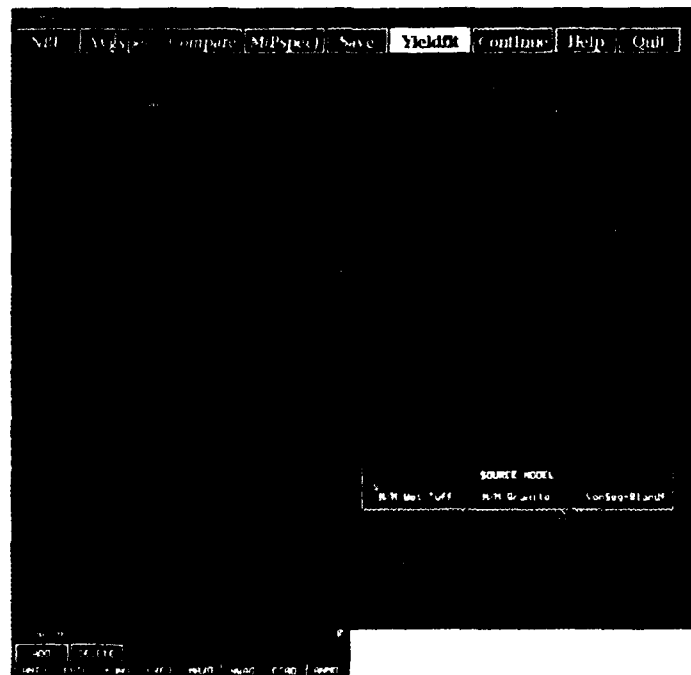
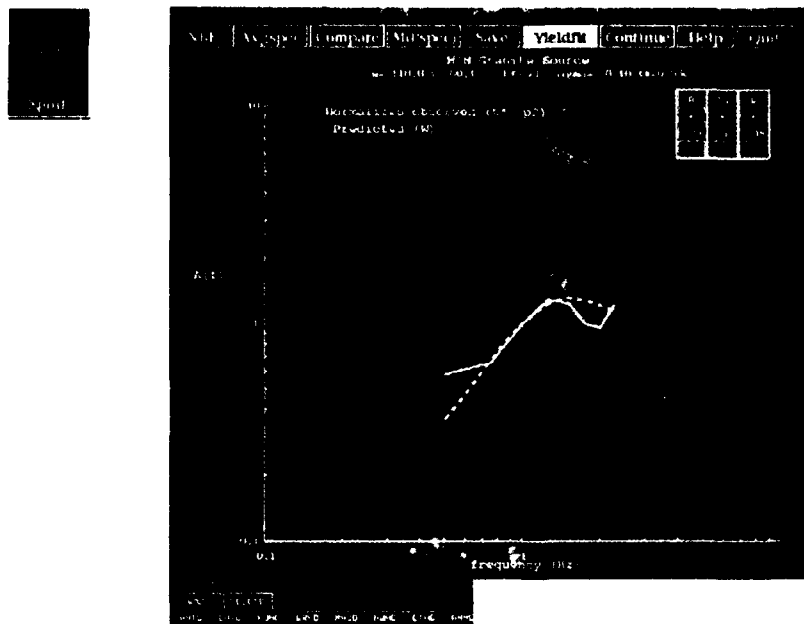


**Figure 24.**  
*Comparison of  
normalized  
observed and  
best-fitting theo-  
retical network-  
averaged P  
wave spectra  
for the current  
event.*



### **Moment Tensor**

The icon appearing in the upper left corner of Figure 24 indicates that the surface wave phase matched filtering processing has now been completed, and selecting it with the mouse provides access to graphical displays of these processing results. Following review of these results, the operator can select the associated MTIS menu option to view a graphical representation of the resulting moment tensor solution shown in Figure 25 where the model fits to the Rayleigh (left) and Love (right) wave data corresponding to a tectonic release F factor of 0.13 are displayed. It is informative to examine this solution in the context of other available information regarding the test environment. This can be accomplished by

**Figure 25.**  
*Comparison of the  
inferred surface  
wave moment ten-  
sor solution for  
current event with  
the corresponding  
path normalized,  
observed Rayleigh  
(left) and Love  
(right) wave  
amplitude data.*

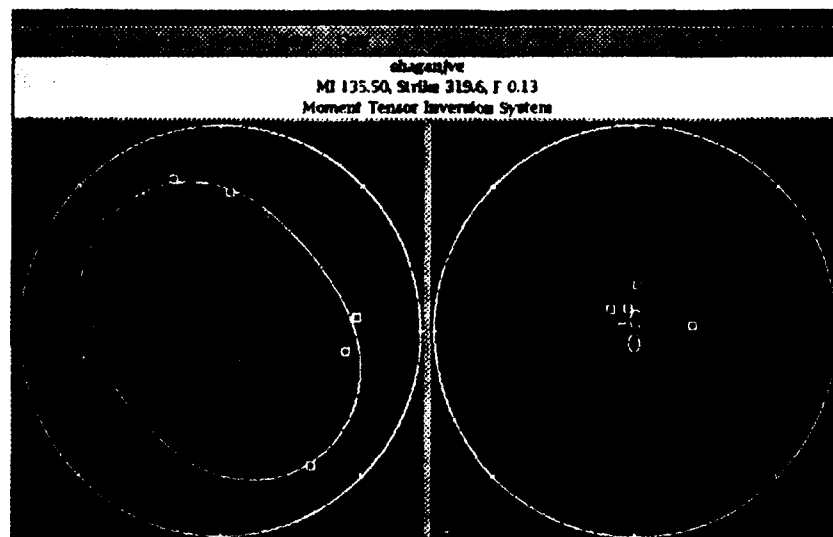
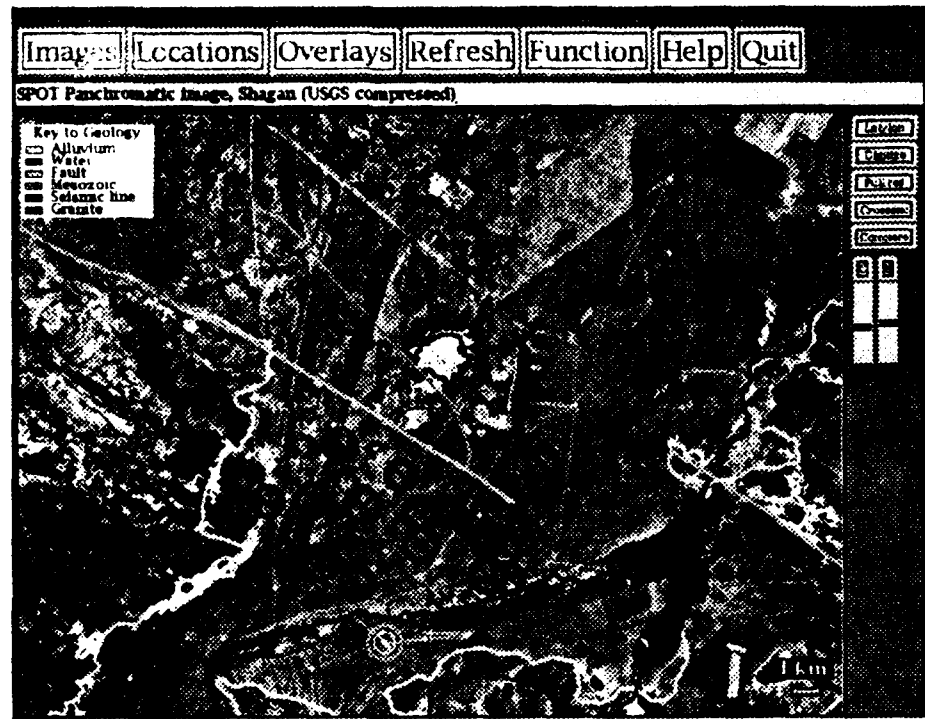




**Figure 26.**

*Comparison of the surface wave moment tensor solution for the current event (yellow and light blue concentric circles) with those for nearby Shagan River explosions (red and dark blue concentric circles) and with the surface geologic map of the area.*



returning once again to the SPOT image test site information interface and successively overlaying the current and historical moment tensor solutions, as well as the map of surface geologic features, as shown in Figure 26. In this display, the concentric circles represent the moment tensor solutions where, for the historical events, the ratio of the diameters of the red-to-blue circles is equal to the inferred tectonic release  $F$  factors and the line segments interior to the circles are parallel to the associated strike of the tectonic component. The solution for the current (JVE) event is differentiated here by an alternate color scheme in which yellow and light blue circles replace red and blue, respectively. It can be seen from this display that the solution for the current event is quite consistent with those previously determined for nearby historical events. Moreover, it is evident that the inferred strikes of the tectonic releases triggered by these explosions are parallel or subparallel to that of the mapped Chinrau fault. Thus, by using the test site information interface, the analyst is able to quickly verify that the surface wave moment tensor solution which was obtained for the current event is consistent with both the solutions from previous nearby explosions and with the regional tectonic environment in which the test was conducted.

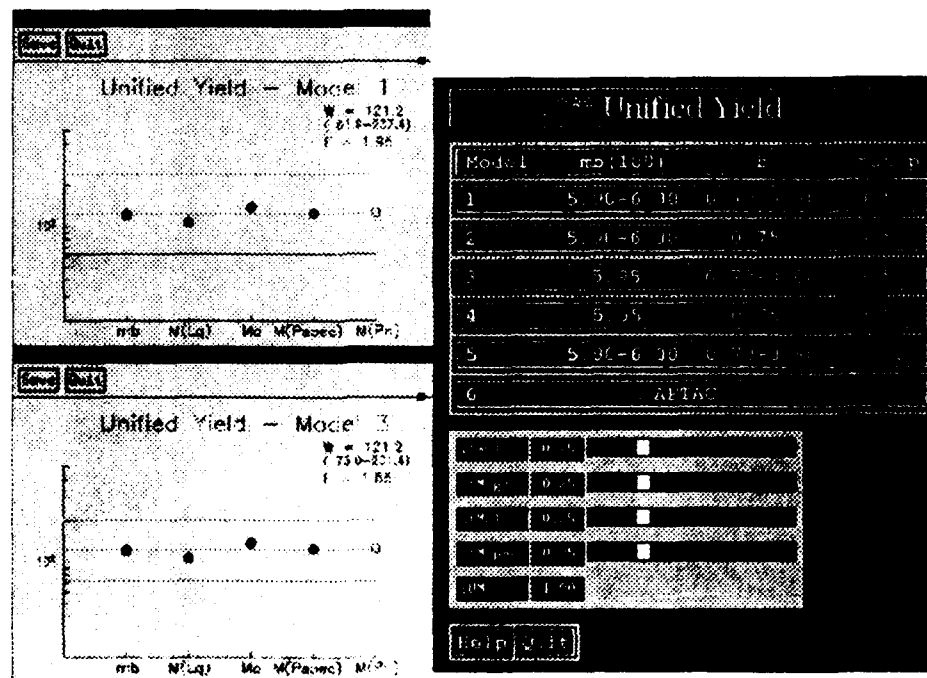
## Yield Estimation

Having determined the various seismic measures of source size (including a regional  $P_n$  magnitude not discussed above), the analyst can proceed to estimate the corresponding explosion yield and the associated uncertainty in that estimate by selecting the *Yield Estimation* feature from the FUNCTION menu of Figure 2. This yield estimation module provides an estimate of unified yield based on multiple magnitude measures and associated extremal confidence limits corresponding to different sets of constraints specified by the analyst. The confidence limits are obtained as the solution of a nonlinear programming problem in which estimates of yield for a training set of explosions are minimized and maximized over the space of admissible parameters (Rodi, 1989; Rodi and Murphy, 1990). Input to this model consists of multiple network-averaged magnitudes for the current event and a nominal  $m_b$ /yield relation based on some combination of data analysis and expert opinion, which for explosions at the Shagan River test site is taken to be (Murphy, 1990):

$$m_b = 4.45 + 0.75 \log W$$

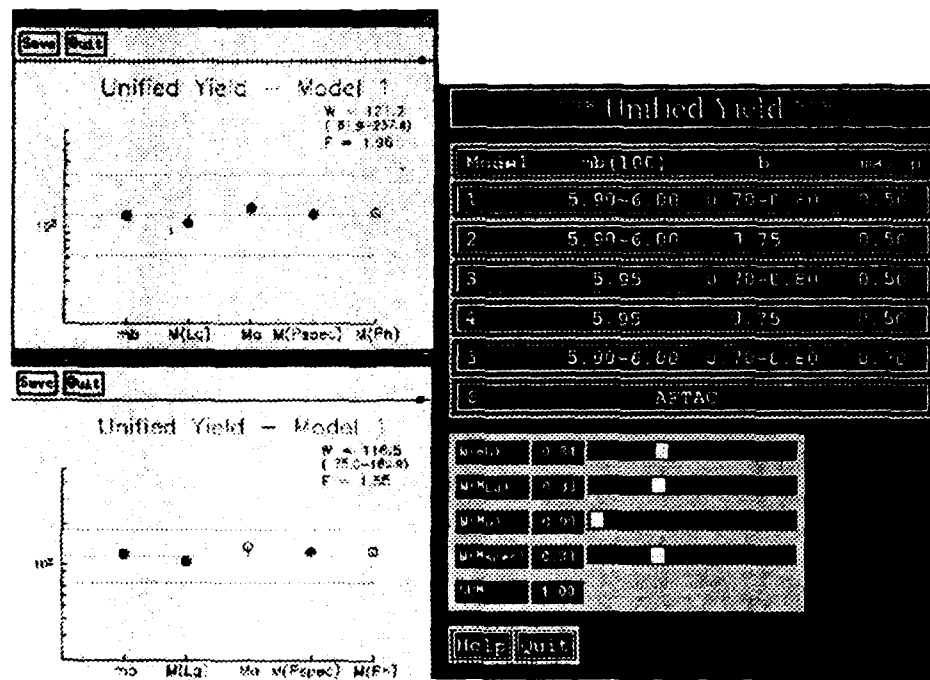
The current module can provide estimates corresponding to five different sets of constraints, parameterized by the uncertainty in the average value of  $m_b$  at 100 kt ( $m_b(100)$ ), the uncertainty in the slope (b) of the  $m_b$ /yield relation and the upper bound on the absolute value of the correla-

**Figure 27.**  
Menu and sample output for the unified yield estimation module.



tion coefficients amongst the yield estimation errors for the individual magnitudes ( $\max P$ ). The menu for the yield estimation module is shown in Figure 27 together with sample output corresponding to the application of Models 1 and 3 to the magnitude data for the current JVE event. In these displays, the resulting unified yield estimates ( $W$ ) and associated upper bound uncertainty factors ( $F$ ) are shown, together with the yield estimates obtained from the individual magnitude values. Note that the  $P_n$  yield value is shown here as an open circle to denote the fact that it was not used in the formal computation of  $W$  and  $F$  due to the fact that an adequate training set of previous values does not currently exist for that magnitude measure. It can be seen that for these two cases, the unified yield estimate is about 121 kt and the uncertainty bounds range from a factor of 1.96 for the case (Model 1) in which  $m_b(100)$  is specified as  $5.95 \pm 0.05$ , to a factor of 1.66 for the case (Model 3) in which  $m_b(100)$  is given as exactly 5.95. In Figure 28, the Model 1 solution from Figure 27 (top) is compared with the result of rerunning Model 1 without the surface wave moment tensor magnitude (i.e., by using the slider bars at the bottom of the menu box to assign a weight of zero to  $W(M_0)$ ). It can be seen that this modification results in a significant reduction of the  $F$  factor from 1.96 to 1.55, reflecting the relatively uncertain yield estimation capability of the surface wave moment as determined from the analysis of the training set of multiple magnitude data.

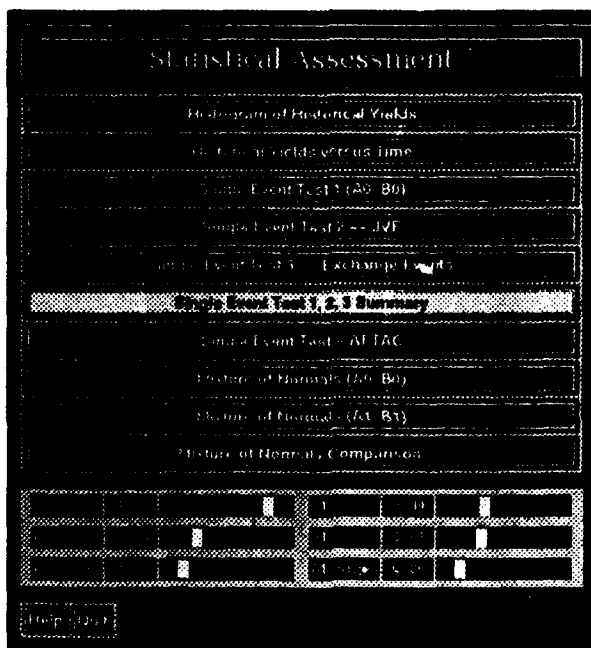
**Figure 28.**  
Comparison of unified yield estimates ( $W$ ) and associated uncertainties ( $F$ ) obtained with (top) and without (bottom) the surface wave moment tensor magnitude.



## Statistical Summary

Given an optimum seismic estimate of unified yield and the associated uncertainty, the analyst can next proceed to assess whether this estimate is consistent with the 150 kt threshold of the Threshold Test Ban Treaty (TTBT) by selecting the *Statistical Summary* option from the FUNCTION menu. This module provides access to a variety of statistical compliance assessment tests developed by Mission Research Corporation (Gray *et al.*, 1990), as indicated by the menu displayed in Figure 29. In this example, the analyst has requested a summary of the results of three single

**Figure 29.**  
*Statistical assessment menu.*

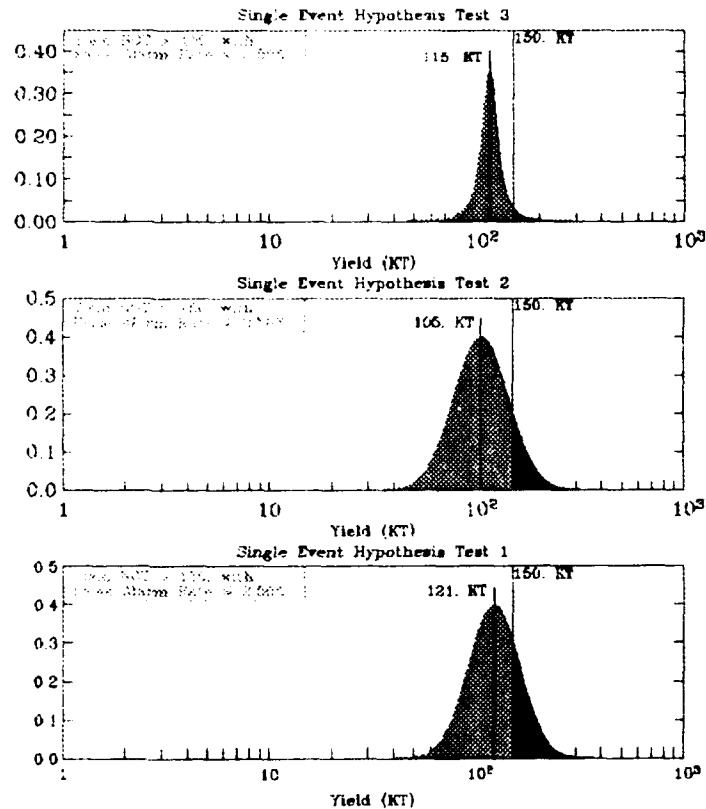


event compliance tests, producing the graphical summary shown in Figure 30, where the red areas under the distribution curves provide a measure of the probability of a violation of the 150 kt threshold. The formal statistical results are summarized in the boxes in the upper left hand corners of these figures, and it can be seen that the results of each of these three tests indicate that the seismic data are consistent with a yield of less than 150 kt at a specified false alarm rate of less than 2.5 percent. The resolving power of such tests can be illustrated by considering the outcome which would have resulted if these same seismic data had been observed from a test below the water table at NTS. In this case, the Shagan  $m_p$ /yield relation would be replaced by (Murphy, 1981):

$$m_p = 3.94 + 0.81 \log W$$

**Figure 30.**

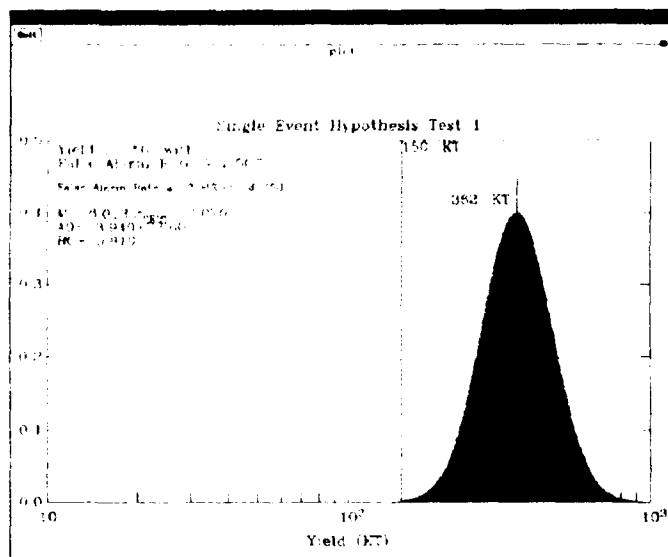
Comparison of the results of three different tests of seismic compliance of the current event with the 150 kt threshold of the TTBT.



resulting in the revised Test 1 outcome shown in Figure 31. It can be seen that under this hypothesis, the yield estimate would be 362 kt and it would be concluded that this explosion violated the 150 kt limit of the TTBT. Thus, this simple example graphically illustrates the importance of the test site magnitude bias effect which has received such intense study since the initial negotiation of the TTBT.

**Figure 31.**

Compliance test results (Test 1) for the scenario in which the current event data were observed from an explosion below the water table at NTS.



## Spreadsheet

Having completed the formal analysis, the *Spreadsheet* option from the FUNCTION menu can be used to provide a less formal environment for evaluating the seismic yield estimate for the current event in the context of the results obtained from analyses of previous explosions at that test site, as well as any available independent yield calibration data, as illustrated in Figure 32. In this display, the four individual seismic yield estimates and corresponding unified yields are listed for forty of the largest Shagan River explosions, together with selected calibration yields (W(Bocharov)), taken here for the purposes of illustration to be the three high yield values published by Bocharov *et al.* (1988). The ratios of the unified seismic to calibration yields are listed in the last column, together with the average offset (Avg Bias) and uncertainty (F) inferred from these limited calibration data. For the nominal magnitude/yield relations listed at the top of this display, the average offset is a factor of 1.07 with an associated F factor of 1.25. Figure 33 shows the result of interactively adjusting each magnitude/yield relation in such a manner that the individual average offsets are minimized. It can be seen that these modifications eliminate the average bias in the unified seismic yield estimate (i.e., Avg Bias = 1.00) and reduces the F factor to 1.20. This example illustrates how the spreadsheet module provides a capability for the analyst to rapidly explore the effects of alternate hypotheses on the seismic yield estimation process.

**Figure 32.**  
Spreadsheet  
summary  
comparison  
of seismic  
yield esti-  
mates for the  
current event  
(09/14/88)  
with those  
obtained for  
selected pre-  
vious Shagan  
River explo-  
sions.

	No	Big	No	Open			
Intercept	4.48	4.45	5.00	4.48			
Weight	0.25	0.25	0.25	0.25			
Event	W(M)	W(M)g	W(M)	W(M)op	W(M)if	W(Bocharov)	W/Wo
1/15/85	88.44			84.81	81.52		
11/24/83	121.88	133.05		118.83	127.45	125.00	1.07
11/26/72	139.55	187.49		255.86	201.37	185.00	1.22
12/16/72	125.84	158.07		125.12	128.46	140.00	0.98
7/23/73	215.44	212.15		246.82	222.39		
12/14/73	85.77	77.27		89.46	77.19		
8/11/78	85.77	54.12	128.82	75.38	81.94		
8/28/78	100.88	119.86	81.28	100.88	88.58		
8/15/78	88.44	87.96	112.20	92.47	95.02		
11/28/78	120.23	106.01	120.23	106.01	112.88		
8/28/78	184.78	138.46	177.89	184.78	178.28		
7/27/78	91.20	105.58	75.86	87.27	81.83		
8/24/79	140.17	158.84	186.21	183.88	186.02		
8/18/79	153.76		104.71	148.58	138.73		
10/26/79	218.59	137.82	184.88	114.81	137.46		
12/26/79	186.88	98.99	138.04	156.91	107.15		
12/22/79	188.53		79.48	183.83	129.95		
8/14/80	251.18		213.80	212.47	225.48		
8/13/81	127.84	165.45	181.97		156.72		
10/18/81	106.33	111.80	144.54		119.49		
12/27/81	173.78	144.89	154.88		157.44		
4/25/82	113.07	148.14	144.54		134.28		
12/05/82	153.70	112.37	154.88		138.82		
8/12/83	113.07	145.88	199.53		148.75		
10/08/83	94.04	77.51	188.21		110.72		
10/28/83	144.54	116.23	213.80		153.15		
7/14/84	121.83	138.44	190.55		191.38		
10/22/84	282.81	149.87	173.78		174.14		
12/18/84	158.48	154.28	229.09		148.58		
12/28/84	94.84	110.82	78.48		98.76		
9/14/88	121.89	106.91	123.88	118.12	119.83		
Avg Bias							1.07
F =							1.25

**Figure 33.**  
Spreadsheet  
summary  
illustrating  
the results of  
interactively  
modifying the  
designated  
magnitude/  
yield rela-  
tions.

Height	M <sub>0</sub>	M <sub>1</sub>	M <sub>2</sub>	M <sub>spec</sub>	M <sub>(Unified)</sub>	M <sub>(Rochford)</sub>	M <sub>0</sub> /M <sub>1</sub>
Slope	0.75	0.75	1.00	0.75			
Height	4.47	4.47	6.00	4.48			
Weight	0.25	0.25	0.25	0.25			
Event	M <sub>(M<sub>0</sub>)</sub>	M <sub>(M<sub>1</sub>)</sub>	M <sub>(M<sub>2</sub>)</sub>	M <sub>(M<sub>spec</sub>)</sub>	M <sub>(Unified)</sub>	M <sub>(Rochford)</sub>	M <sub>0</sub> /M <sub>1</sub>
1/15/85	83.18			83.66	84.95		
11/30/88	123.97	125.12		107.86	118.64	126.00	0.96
11/02/77	178.20	157.52		233.35	187.45	165.00	1.14
12/10/77	127.84	146.78		114.11	128.88	140.00	0.82
7/23/73	202.81	189.53		418.48	207.01		
12/14/73	86.86	72.87		63.28	71.85		
6/11/78	89.68	58.89	128.82	68.76	77.85		
8/23/78	84.84	112.72	81.28	82.84	94.37		
8/15/78	83.18	82.67	112.29	85.24	86.05		
11/28/78	113.07	99.89	128.73	86.88	106.88		
6/28/78	179.78	139.22	177.83	168.53	181.37		
7/07/78	85.77	99.39	76.88	88.72	87.02		
8/04/78	131.83	149.51	186.21	188.98	157.34		
8/18/78	144.54		104.71	136.82	127.66		
10/28/78	189.85	129.42	144.98	114.87	139.27		
12/02/78	84.84	84.72	138.04	86.88	101.55		
12/22/78	158.48		78.43	149.51	123.47		
9/14/80	286.23		213.36	194.69	214.23		
3/13/81	170.23	155.88	181.37		150.43		
10/18/81	100.00	104.39	144.54		114.70		
12/27/81	162.41	196.36	154.28		151.12		
4/25/82	186.33	139.32	144.54		128.88		
12/05/82	144.54	105.68	154.80		132.25		
6/12/83	166.33	137.19	188.53		142.78		
10/06/83	88.44	72.89	186.21		106.28		
10/28/83	135.94	109.31	213.80		147.01		
7/14/84	123.97	129.82	188.55		145.29		
10/27/84	189.85	141.04	173.78		187.15		
12/16/84	149.05	126.28	229.09		182.76		
12/28/84	88.44	102.75	78.43		86.88		
3/14/88	123.97	89.68	128.82	108.64	113.57		
Avg. Size						1.00	
F =						1.20	

## Event Summary

Once the processing has been completed for the current event, the analyst can produce a one-page summary of the analysis results by selecting the Event Summary option from the FUNCTION menu. As is indicated in Figure 34, listed results include the date, origin time and location of the explosion, the derived unified seismic yield and its associated uncertainty, the results of the statistical test of compliance of the current event with the 150 kt limit of the TTBT, a tectonic release characterization of the event based on the surface wave moment tensor analysis and, if available, the CORTEX yield estimate for the explosion. In addition, each of the estimated seismic magnitudes is listed together with its associated yield estimate and assigned weight in the determination of the unified yield estimate.

The sample analysis session described above has provided an overview of some of the capabilities which are currently available within the Yield Estimation System. As was evident from the menu structures shown in the graphical displays, there are, in addition, many other features which were not exercised here in order to hold the description to a manageable length. A complete description of all currently available system options is provided in Appendix C.

**Figure 34.**  
Summary of  
analysis results  
for the selected  
event.

Quit

### Event Summary

Test Site : Shagan  
 Date : 14 September 1988  
 Origin Time : 4:0: 0.00 UT  
 Location : 49.8788N, 78.8225E

Date of Analysis : Jan 15, 1992

Unified Seismic Yield : 116.5 KT  
 CORTEX Yield : Not available  
 Unified Seismic Uncertainty : F = 1.55 (75.0 kt < W < 180.8 kt)

Compliance Assessment : Accept the null hypothesis that  
 the yield is less than 150kt  
 (2.5% significance level test)

Tectonic Characterization : F = 0.13, Strike = 319 degrees

The conclusions presented above were based on the following measurements:

Individual Magnitudes and Yields			
Measurement	Yield	Magnitude	Rel. Weight
mb	120.504	6.011	0.340
M(Lg)	105.925	5.987	0.330
M(o)	136.773	7.132	0.000
M(PSpec)	123.880	6.026	0.330
M(Pn)	125.603	6.026	0.000



# 3

## *Summary*

---

In this report we have presented an in-depth description of the current status of the on-going research investigations directed toward the development of a comprehensive new seismic yield estimation system for underground nuclear explosions. In its current configuration, the YES system is applicable to underground nuclear explosions at the Soviet Shagan River and Novaya Zemlya test sites and encompasses a database of more than 10,000 digital seismograms recorded at stations of the USAEDS, GDSN, CDSN and IRIS networks from explosions at these two sites. For both test areas, information regarding the explosion source environment is presented to the analyst in the context of SPOT satellite images of the sites, together with associated surface and subsurface geologic information and DMA topographic data. The on-line database for YES also contains a wide variety of tabular information, including complete event and station location files containing both classified and unclassified locations, standard travel-time tables for the seismic arrivals used for yield estimation, propagation path and station corrections for use in magnitude determinations and a comprehensive instrument response database. The instrument database encompasses a compilation of over 750 different response histories collected from the USGS, AFTAC, IRIS and others which detail the characteristics of the various recording instruments as a function of station, channel and date.

The capabilities and functionality of the current version of the YES system were graphically illustrated in Section II using displays of the screens encountered by an analyst in a typical processing session. The selected capabilities displayed in this sample session were related to a more complete definition of the system functionality through references to a series of appendices containing a detailed script of the operator actions required to reproduce the sample session (Appendix B), a complete

description of all currently available system options (Appendix C), as well as information regarding software and hardware implementation requirements (Appendix A) and a top level schematic diagram of the main modules of the system and their interdependencies (Appendix D). Taken together, Section II and its associated appendices provide a concise description of the current status of the YES system development effort.

# 4

## References

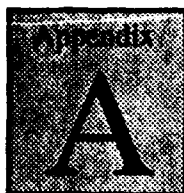
---

- Gray, H. L., W. A. Woodward and G. D. McCartor (1990), "Statistical Issues Concerning Testing for Compliance to the TTBT," paper presented at 12<sup>th</sup> Annual DARPA/GL Seismic Research Symposium, Key West, Florida, GL-TR-90-0212, ADA226635.
- Herrin, E., E. P. Arnold, B. A. Bolt, G. E. Clawson, E. R. Engdahl, H. W. Freedman, D. W. Gordon, A. L. Hales, J. L. Lobdell, O. Nuttli, C. Romney, J. Taggart, and W. Tucker (1968), "1968 Seismological Tables for P Phases," *Bull. Seism. Soc. Am.*, 58, pp. 1193-1241.
- Murphy, J. R. (1981), "P-Wave Coupling of Underground Explosions in Various Geologic Media," in *Identification of Seismic Sources - Earthquake or Underground Explosion*, Proceedings of the NATO Advanced Study Institute, D. Reidel Publishing Company.
- Murphy, J. R. (1989), "Network-Averaged Teleseismic P-Wave Spectra for Underground Explosions, II: Source Characteristics of Pahute Mesa Explosions," *Bull. Seism. Soc. Am.*, 79, pp. 16-31.
- Murphy, J. R. (1990), "A New System for Seismic Yield Estimation of Underground Explosions," paper presented at the 12<sup>th</sup> Annual DARPA/GL Seismic Research Symposium, Key West, Florida, GL-TR-90-0212, ADA226635.
- Murphy, J. R., J. L. Stevens, D. C. O'Neill, B. W. Barker, K. L. McLaughlin, M. E. Marshall (1991), "Development of a Comprehensive Seismic Yield Estimation System for Underground Nuclear Explosions," Annual Technical Report to Phillips Laboratory, PL-TR-91-2161, ADA240814..

Ringdal, F. (1983), "Magnitudes from P Coda and  $L_g$  Using NORSAR Data,"  
in NORSAR Semi-Annual Technical Summary, 1 Oct 82 - 31 Mar 83,  
NORSAR Sci. Rep. No. 2-82/83, NTN/NORSAR, Kjeller, Norway.

Rodi, W. L. (1989), "A Mathematical Program for Unified Yield Estimation,"  
S-CUBED Memorandum to DARPA Yield Technical Review Panel,  
December 22.

Rodi, W. L. and J. R. Murphy (1990), "Numerical Experiments With Unified  
Yield Estimation," S-CUBED Technical Memorandum to DARPA Yield  
Technical Review Panel, April 19.



# ***Requirements and Startup Instructions***

---

## ***Hardware Requirements***

The YES system is designed to run on SUN-4 and SUN SPARCStation computers with a minimum of 32MB of resident memory. It uses the standard SUN 8-bit color monitor with a resolution of 1152x900 pixels, as well as the standard SUN 3-button mouse. YES also requires a minimum of 1 gbyte of disk storage to hold the complete system and its required data.

## ***Software Requirements***

YES is written in C and FORTRAN and uses the X Window System software, version X11 revision 4. It also uses the Hewlett Packard widget set extension to X and the Motif widget set, release 1.1. It has been successfully compiled using the standard SUN bundled C compiler and the SUN 1.3.1 FORTRAN compiler, and is designed to run under the SUN operating system version SUN-OS 4.1.0 or later.

## ***Startup Instructions***

The following instructions assume that the X Window System and YES have been installed according to S-CUBED specifications. Also refer to the information on mouse and window techniques in Appendix C before proceeding.

To bring up the X environment and run YES you must do the following:

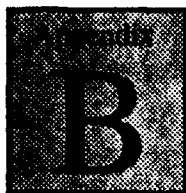
1. Login to UNIX at the console.

2. Add `/usr/bin/X11` to your search path, if it is not already there, and issue the command:  
**prompt> rehash**  
(where `prompt>` denotes the UNIX operating system prompt).
3. Ensure that the files `xinitrc` and `twmrc` as provided on the distribution tape have been copied to `.xinitrc` and `.twmrc` in your home directory.
4. Issue the command:  
**prompt> startx**  
and wait until an X terminal window appears on your screen.
5. Move the cursor into the X terminal window and change to the main directory where YES has been installed.
6. Issue the command:  
**prompt> source Init**
7. Issue the command:  
**prompt> yieldsys&**

## ***Shutdown Instructions***

To shutdown the system:

1. Choose *Quit* from the YES main menu.
2. Exit X by pointing outside any window. Click and hold the right button. Move the pointer down to menu item *Exit X Windows*, stop, then move to the right and release on *Select if you're sure*.
3. Logout of UNIX at the console.



## ***Script For Sample Session***

---

In this section, all of the operator actions required to duplicate the sample session shown in Section II are specified. Note that when run in a classified environment, the values of some of the parameters and processing results will be somewhat different from those shown here. A full description of all system options is provided in Appendix C, including details regarding menu structures and the mouse actions required to initiate specific actions. All figures mentioned in this section are found in Chapter 2 of this manual.

### ***Starting the pro- gram***

The procedures required to initiate and start the program are specified in Appendix A. To recap:

1. ***Change to the YES directory.***
2. ***Type `source Init.`***
3. ***Type `yieldsys&`.***

Once the program has been started, the first screen display is the title page. Clicking anywhere within the display brings up the main menu. A site and an event are normally selected as the first step in the analysis.

### ***Main Menu***

1. ***Choose `Balapan (Shagan)` from the SITE menu.***
2. ***Choose `Shagan Events->1980-1989->1988->September 14 (JVE)` from the EVENT menu.***

This event will be referred to as the current event.

After a site and event have been chosen, one can proceed to analyze the near-source environment of the current event.

## **Satellite Image**

1. Choose *Satellite image* from the **FUNCTION** menu.

This brings up the satellite image of the test site. It will come up with symbols showing the locations of all the events that occurred at the test site and the current event location highlighted (see Figure 3).

2. Click on the current event diamond.

A description of the event is displayed in the information bar below the menu. Experiment likewise with other events (i.e. click on them).

## **Full res**

1. Click on *Full res* in the side menu and then in the center of the crater located at the northern end of the lake.

Once the 10 m resolution image of the crater has come up (see Figure 4), full resolution images of adjacent areas can be viewed by clicking near the edges of the image.

2. Choose *Satellite image* from the **IMAGES** menu.

The original satellite image is now displayed.

3. Click again on the *Full res* button to turn it off.

## **Contrast and Brightness**

1. Adjust the C and B sliders in the side menu.

This reverses contrast and alters the brightness of the image. (see Figure 5)

2. Click on the C and B buttons to restore the original settings.



Use the black bars to adjust the sliders

## **Surface Geology**

1. Choose *Surface geology* from the **OVERLAYS** menu.
2. Choose *Current event* from the **OVERLAYS** menu.

The display will look like Figure 6.





### **Topographic Map**

1. Choose *Surface topography* from the IMAGES menu.
2. Choose *Topography contours* from the OVERLAYS menu.
3. Choose *Current event* from the OVERLAYS menu.

The display should now look like Figure 7.

4. Choose *Satellite image* from the IMAGES menu.

### **Cross Section**

1. Choose *Event locations(SPOT)* from the LOCATIONS menu.
2. Click on *Cross sec* in the side menu.
3. Click below the current event location and again near the northern extremity of the display (see insert in Figure 8).

The cross section of the site along the line is then displayed (see Figure 8).

4. Click on the *Quit* button to return to the satellite image.
5. Click again on *Cross sec* in the side menu to turn it off.

### **Granite Surface**

1. Choose *Depth to granite* from the IMAGES menu.
2. Choose *Subsurface contours->Depth to top of granite* from the OVERLAYS menu.
3. Choose *Current event* from the OVERLAYS menu.

Figure 9 shows what the screen should look like at this point.

4. Choose *Satellite image* from the IMAGES menu.
5. Iconify the Satellite Image module.

### **World Map**

1. Choose *World map* from the main FUNCTION menu.
2. Choose *Teleseismic P* from the PHASE menu.
3. Choose *Teleseismic P->ANMO* from the STATION menu.

This draws the great circle path shown in Figure 10.

4. Click on the REFRESH button.

This removes the stations. Repeat steps 2-4 to draw the great circle path for phase  $L_g$  and the NORSAR(N01A0) station shown in Figure 10.

5. Click on QUIT to return to the main menu.

## Analyst Station

1. Choose  $L_g$  from the PHASE menu.
2. Choose *Analyst Station* from the main FUNCTION menu.  
This displays the  $L_g$  waveforms as shown in Figure 11.
3. Click on the QUIT button and return to the main menu.

## RMS $L_g$ Startup

1. Choose *Magnitude Measurement->RMS  $L_g$*  from the FUNCTION menu.

This spawns off a process, and when done, the following icon pops up. While this process runs in the background, continue with the rest of the analysis.



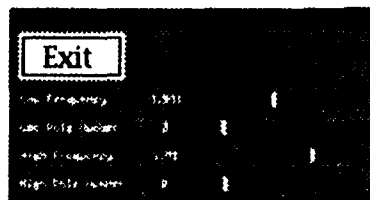
*The RMS  $L_g$  icon*

## Filter

1. Choose *Teleseismic P* from the PHASE menu.
2. Choose *Analyst station* from the FUNCTION menu.

This displays the first six teleseismic P waveforms as shown in Figure 13.

3. Click on the NEXT and PREVIOUS buttons to page through the waveforms.
4. Choose *Filter* from the TOOLS menu.
5. Set: Low Frequency = 0.5  
Low Pole Number = 2  
High Pole Number = 2



*Move the slider bars or click anywhere in the slider box to change the settings*

High Frequency = 5.0

6. Click on the station MAJO waveform.

This applies the selected bandpass filter (second-order, 0.5 to 5 Hz) to the MAJO waveform as shown in Figure 14. To apply this same filter to other waveforms, just click on them.

7. Click on the EXIT button once done with the filter.

**Compare**

1. Choose *Compare* from the **TOOLS** menu.
2. Click on the station **KONO** waveform.
3. De-iconify the **Satellite Image** icon.
4. Choose *Remove locations* from the **REFRESH** menu to remove any event locations on the image.
5. Choose *Compare events* from the **LOCATIONS** menu.
6. Click on *Compare* in the side menu.
7. Double-click on five events surrounding the current event.  
The display should look like Figure 15.
8. Choose *Analyst station* from the **Satellite Image FUNCTION** menu.

This displays the KONO Teleseismic P waves for the selected events beneath that for the JVE event.

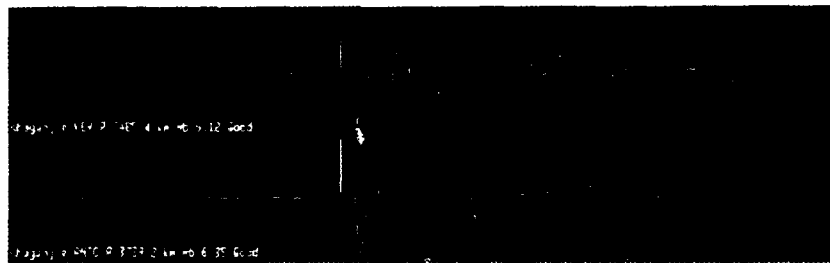
**Clone**

1. Choose *Clone* from the **TOOLS** menu.
2. Click on the **JVE** trace.

A red copy of the JVE trace appears and the cursor changes to a pointing hand.

3. Compare the trace with the others.

Reposition the red trace adjacent to any other desired trace as illustrated in the figure above. Also see Figure 16. When finished with the comparison, click again anywhere in the display to get rid of the clone.



*Move the hand with the mouse and the red trace follows it.*

4. Click on the **QUIT** button to return to the satellite image.
5. Choose *Remove locations* from the **REFRESH** menu.
6. Iconify the **Satellite Image**.

The Analyst Station display should now be on the screen.

**Expand  
and  $m_b$** 

1. Choose *Expand* from the TOOLS menu.
2. Click on station ANTO's waveform.

This brings up the waveform in expanded form as shown in Figure 17. All the tools are still available for use in this mode.

3. Choose  $m_b$  from the TOOLS menu.
4. Measure amplitude and period.

Draw a rectangle over the selected half cycle of motion by clicking the cursor at the peak, dragging the cursor to the trough while holding down the mouse button and then releasing the mouse button (see Figure 17).

5. Click on the QUIT button.

The original full page screen is displayed. Do the measurements for all other waveforms using steps 2-6. Note that the  $m_b$  tool can also be used in the full page display. Therefore, the measurements need not all be done in expanded mode although it is easier on the eye.

6. Choose *Interface file* from the FUNCTION menu.

This saves the amplitude and period measurements along with other information for use by other modules.

7. Click on the QUIT button to get back to the main menu.

**Magnitude  
Measure-  
ment**

1. Choose *Magnitude Measurement->mb* from the FUNCTION menu.

A display similar to that of Figure 18 will result. Not all the station magnitudes shown in Figure 18 will be displayed if not all of them were measured in step 5 under *Expand and  $m_b$* .

2. Click on the QUIT button.

**RMS  $L_g$** 

1. De-iconify the RMS  $L_g$  icon.
2. Choose *NORS* from the RESIDUAL menu.

The display should now look like Figure 19.

3. Click on the QUIT button.

 **$M_{Lg}$  and  $m_b$   
comparison**

1. De-iconify the Satellite Image.
2. Choose *Historical magnitude data->Mb-MLg(NORSAR)* from the OVERLAYS menu.

3. Choose *Event magnitude data->Mb-MLg* from the **OVERLAYS** menu.

The display should look like Figure 20.

4. Choose *Quit* from the **QUIT** menu.

### ***Instrument Response***

1. Choose *Rayleigh(vertical)* from the **PHASE** menu.
2. Choose *Analyst Station* from the **FUNCTION** menu.

The display should look like Figure 21.

3. Choose *New instrument->sro lp* from the **TOOLS** menu as shown in Figure 22.
4. Click on each of the waveforms.

This transforms all the waveforms to the same instrument response.

5. Click on the **QUIT** button.

### ***Moment Tensor Startup***

1. Choose *Magnitude Measurement->Moment tensor* from the **FUNCTION** menu.

This spawns a background process and the following icon pops up when done. Continue the analysis while this is being processed.



*The Xpmf icon*

### ***Spectral P***

1. Choose *Magnitude Measurement->Spectral P* from the main **FUNCTION** menu.
2. Click on *NBF*.

This brings up a display of the P wave signal and noise spectra for the first station.

3. Click on *Continue* until all stations have been processed.
4. Click on *Avgspec*.

The resulting display shows a comparison of the estimated network-averaged P wave spectrum (yellow line) with that expected on average for an explosion having the current event  $m_b$  value (dashed red lines).

5. Click on *Yieldfit*.
6. Click on *M/M Granite* (see Figure 23)

This initiates a process by which the theoretical solution corresponding to the Mueller/Murphy granite source model which provides the best fit to the attenuation-corrected observed spectrum is automatically determined and displayed. The yield value corresponding to this best-fit solution is listed at the top of the display together with its associated upper bound uncertainty.

7. Click on *Continue* twice.

This skips through the graphs to obtain the final automatic solution with the final yield(W) and  $pP(A, T_0)$  values shown in the box in the upper right-hand corner of the display (see Figure 24).

8. Change the yield W from 119 kt to 150 kt and then back down to 119 kt by using the + and - buttons shown below.

A	To	W
+	+	+
0.17	0.82	119
-	-	-

Click on these + and - buttons to change the yield

9. Click on the *QUIT* button.

This takes you back to the main menu.

### **Moment Tensor**

1. De-iconify the Xpmf icon.

This brings up a display of the phase-matched filter output for the first long-period station. Since the data from the JVE event have already been filtered, continue with the moment tensor inversion analysis.

2. Choose *Run MTIS* from the *MTIS* menu.
3. Click on some of the green and red squares.

Individual station information is displayed in the information bar. Also see Figure 25.

4. Choose *SPOT image* from the *VIEW* menu.

This creates a graphical representation of the moment tensor solution that is used in the Satellite Image module.

5. Choose *Confirm Quit?* from the QUIT menu.

This takes you back to the Xpmf display. Quit from it similarly.

6. De-iconify the Satellite Image.

Remove any overlays on the image using the REFRESH menu.

7. Choose *Event magnitude data->Moment Tensor* from the OVERLAYS menu.

8. Choose *Historical magnitude data->Moment Tensor* from the OVERLAYS menu.

9. Choose *Surface geology* from the OVERLAYS menu.

The display should now look like Figure 26.

10. Choose *Quit* from the QUIT menu.

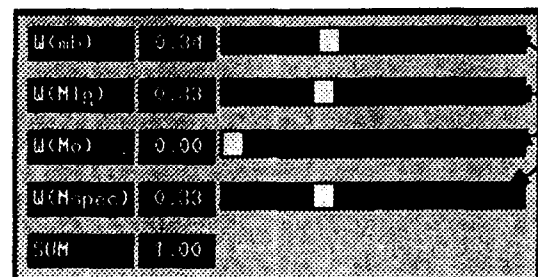
### ***Yield Esti- mation***

1. Choose *Yield Estimation* from the main FUNCTION menu.

2. Click on MODEL 1 and then on MODEL 3.

The display should look like Figure 27.

3. Set the weights to 0.34, 0.33, 0.00 and 0.33, respectively.



*Use these sliders to  
set the weights*

4. Click on MODEL 1 again.

The display should look like Figure 28.

5. Click on the *Save* button in the lower left display.

6. Click on the QUIT button.

### ***Statistical Summary***

1. Choose *Statistical Summary* from the main FUNCTION menu.

2. Click on *Single Event Test 1 (A0,B0)*.

After a few seconds an icon comes up.

3. Click on the icon to see the test results.

4. Click on the QUIT button.

Return to the statistical assessment options menu. Use steps 2-4 to run *Single Event Test 2 -- JVE* and *Single Event Test 3 -- Exchange Events*.

5. Click on *Single Event Test 1,2,3 Summary*.

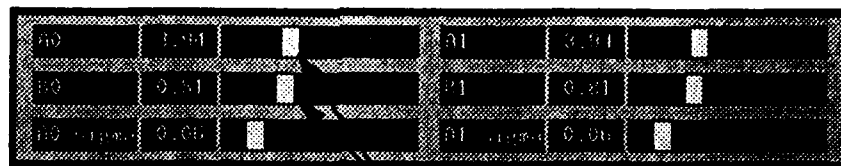
6. Click on the icon to see the test results.

The display should look like Figure 30.

7. Click on the QUIT button.

Return to the statistical assessment options menu.

8. Set  $A0 = 3.94$  and  $B0 = 0.81$ .



Use these sliders to set  $A0$  and  $B0$

9. Click on *Single Event Test 1 ( $A0, B0$ )*.

When the icon comes up, click on it to look at the test results. The display should look like Figure 31.

10. Click on the QUIT button and return to the statistical assessment menu.

11. Click on the QUIT button and return to the main menu.

### Spreadsheet

1. Choose *Spreadsheet* from the FUNCTION menu.

The spreadsheet shown in Figure 32 comes up. Use the arrow keys to move around the spreadsheet.

2. Change the intercepts to 4.47 ( $m_b$ ), 4.47 ( $M_{I,g}$ ), 5.00 ( $M_s$ ) and 4.48 ( $M_{spec}$ ).

Use the arrows to move to the cell and type '=' (an equal sign). Then type the number and hit return.

3. Type Q to quit and N to not save changes.

Return to the main menu.

### Quitting the program

1. Choose *Quit* from the QUIT menu.





## **Reference**

---

### **Introduction**

This section provides a description of the available options in the YES system. It describes the function and usage of every module and its menus and buttons. Following is a review of basic mouse and window techniques required by the user to work with YES.

### **Mouse Techniques**

**Point** To point, position the cursor on something you want to choose.

**Click** To click, point to something and then briefly press and release the left mouse button.

**Double Click** To double-click, point to something and then rapidly press and release the left mouse button twice.

**Drag** To drag, point to something, press and hold down the left mouse button as you move the cursor to another position, and then release the mouse button.

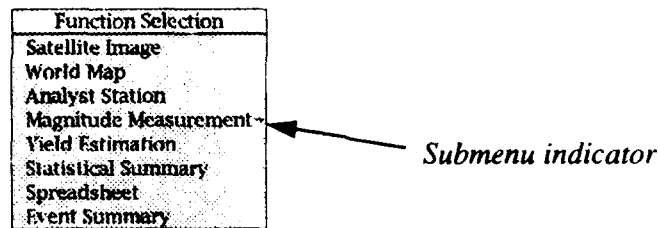
**Highlight a button** To highlight or turn on a button, position the pointer on the button name and click on it.



**Choose from a pull-down menu** To choose an option from a pull-down menu, press and hold down on the menu button name to pull down a menu, drag the highlight to the option you want and then release the mouse button.

**Choose from  
a submenu**

To choose an option from a submenu, first pull down the menu that contains the submenu. While holding down the mouse button, drag diagonally to the submenu indicator (arrow) to pull down the submenu. Drag the highlight to the required option in the submenu before releasing the mouse button.

**Window Techniques****Move a  
window**

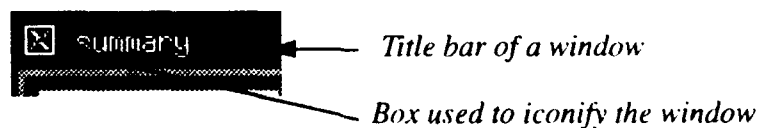
To move a window, point to the title bar of the window to be moved. Click and hold down the middle mouse button. Drag the window to the desired location and release the mouse button.

**Iconify a  
window**

To iconify a window, point to the small box in the far left of the top border and click the left button. The iconified window can be moved by clicking and holding the middle button inside the icon and dragging.

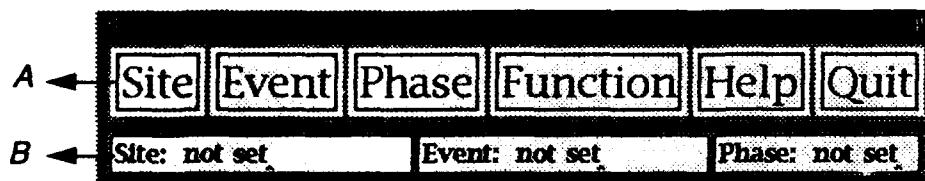
**De-iconify  
a window**

To de-iconify a window, point to the icon and click on the left mouse button.



## Main Menu

The main menu provides top level access to the system. It consists of six menu buttons which can be used to initiate (SITE, EVENT, PHASE, FUNCTION) or terminate (QUIT) action within the system, or to view on-line information regarding the operating characteristics and parameters of the system (HELP). Choosing any of these buttons causes a series of pull-down menus to be activated from which the various system options can be selected.



A - the main menu buttons

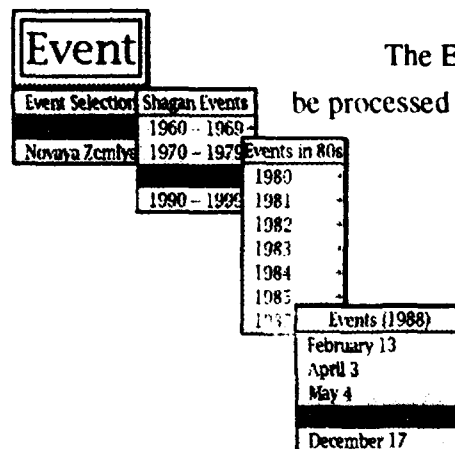
B - the information bar that indicates the selected site, event and phase

## Site



The SITE menu button is used to select the nuclear test site at which the explosion to be analyzed was detonated. Currently, the choices are limited to the *Soviet Shagan River (Balapan)* and *Novaya Zemlya* test sites. Generally, a selection must first be made from this menu before making any other selections.

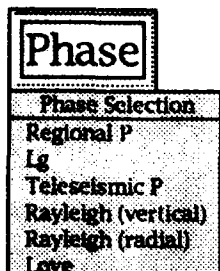
## Event



The EVENT menu button is used to select the specific explosion to be processed from among those for which digital seismic data are currently

available on the system.

## Phase

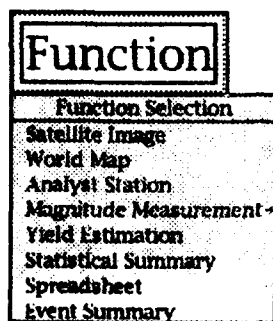


The PHASE menu button is used to select from among the six seismic arrivals for which data are currently available on the system. These consist of:

- the initial P and  $L_g$  arrivals recorded at regional distance stations (*Regional P*,  $L_g$ ),
- the initial short-period teleseismic P arrivals (*Teleseismic P*),
- the three orthogonal components of the long-period surface waves (*Rayleigh (vertical)*, *Rayleigh (radial)*, and *Love*).

A test site and an explosion must be specified from the SITE and EVENT menus before a phase is selected.

## Function



The FUNCTION menu is used to provide access to the eight principal computational and analysis modules of YES. The brief overviews of these modules which are presented below are followed in subsequent sections by complete descriptions of their functionality. Both the test site and explosion of interest should be specified before selecting from this menu.

### Satellite Image

This module provides access to an interactive test site information interface built upon displays of SPOT satellite images of the Shagan River and Novaya Zemlya test sites.

### World Map

This module provides a capability to display the map locations of stations which have recorded digital seismic data from the selected event.

### ***Analyst Station***

This module provides the capability to access and display the digital seismic waveform data available from the explosion under investigation and to interact with them to extract the parametric data required for determination of the various magnitude measures. In addition to the test site and event, the seismic arrival of interest must be selected from the PHASE menu before activating this module.

### ***Magnitude Measurement***

This module provides access to the algorithms which can be used to semi-automatically compute network-averaged magnitudes from the waveforms and parameters corresponding to the individual seismic arrivals previously reviewed by the operator in the Analyst Station module. At the present time, five separate magnitude measures based on teleseismic P waves ( *$m_h$* , *Spectral P*), long-period Rayleigh and Love waves (*Moment Tensor*), and regional P and  $L_g$  waves (*Regional P*, *RMS  $L_g$* ) can be estimated using this module.

### ***Yield Estimation***

This module provides access to a statistical module which permits the operator to obtain unified yield estimates corresponding to the multiple, network-averaged magnitudes determined using the Magnitude Measurement module, as well as quantitative measures of the uncertainty in those estimates.

### ***Statistical Summary***

This module provides access to a variety of statistical tests which can be used to quantitatively assess seismic compliance with the 150 kt threshold level of the TTBT.

## ***Spreadsheet***

This module provides the analyst with the capability to evaluate the seismic yield estimate for the current event in a standard spreadsheet analysis environment, in the context of the results obtained from analyses of previous explosions at that test site, as well as any available independent yield calibration data (e.g., CORTEX).

## ***Event Summary***

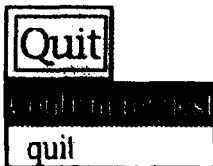


This menu item provides access to a one page summary of the results obtained by applying the YES to the digital seismic data recorded from the selected explosion.

## ***Help***

In this and all subsequent modules to be described, the HELP menu is used to access on-line information regarding the mode of activation and functionality of the various menu options in the current display.

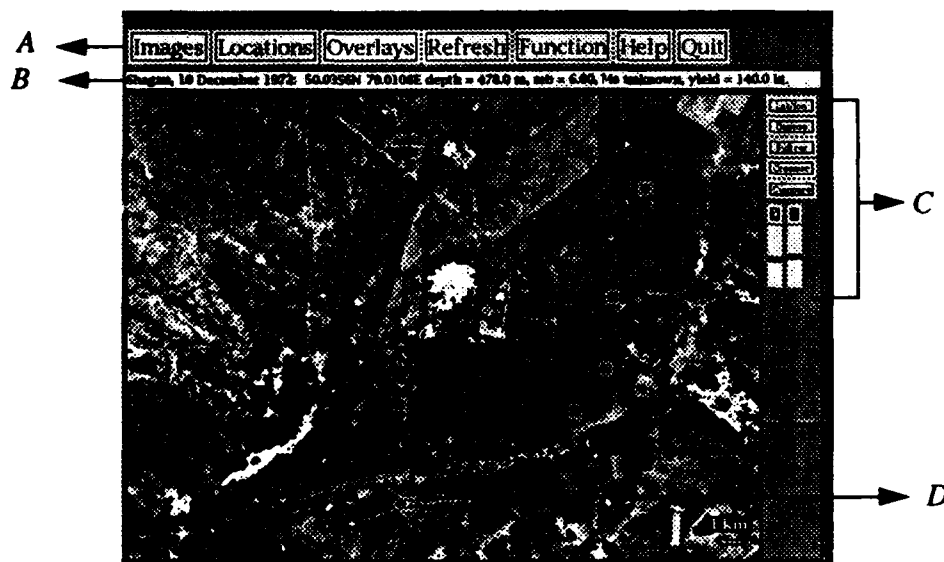
## ***Quit***



In this and all subsequent modules to be described, the QUIT menu is used to terminate the operation of the process which is currently running. Choosing this button activates a pop-up which must also be chosen to verify the request to terminate the program.

## Satellite Image

As was indicated in the summary overview presented in the preceding section, selection of the *Satellite Image* option from the main FUNCTION menu provides access to an interactive test site information interface built upon displays of SPOT satellite images of the Soviet Shagan River and Novaya Zemlya test sites. For the purposes of this application, the image for the Shagan River test site has been compressed to an effective resolution of about 30 m so that the entire test site can be viewed on a single screen. Full 10 m resolution images of operator designated subareas can be accessed using the *Full res* menu option described below. This feature does not apply to Novaya Zemlya, since only 20 m resolution SPOT data are currently available for that test site. In either case, selection of *Satellite Image* from the main FUNCTION menu results in a display of the SPOT image of the designated test site, with the best available locations of previous explosions at that site shown as color-coded square overlays and with the current event highlighted by a yellow diamond.



- A - satellite image menu buttons
- B - information bar
- C - side menu
- D - current event

The different colors are used to differentiate those explosions about which the Soviets have published data in the open literature (blue) from those for which only seismic information is available (red). As can be seen from the display, selections within this module can be made from menu buttons distributed both across the top and down the right side of the display, to initiate various interactions with the image and associated data. These will now be described in order, proceeding from left to right and then top to bottom.

## Images

Image selection
Satellite image
Surface topography
Thickness of alluvium
Depth to mesozoic
Depth to paleozoic
Depth to granite

This menu button is used to access the compressed 30 m resolution SPOT image of the selected test site (*Satellite image*) or color-coded representations of other data which have been registered to the SPOT image. For the Shagan River test site these include the DMA topographic data (*Surface topography*), thickness of the surface alluvium (*Thickness of alluvium*) and the depths beneath the surface to the various subsurface geologic units which have been mapped (*Depth to mesozoic*, *Depth to paleozoic* and *Depth to granite*). For the Novaya Zemlya test site, where the subsurface geology is less well known, only the *Surface topography* (DMA) image is currently available. Where appropriate, color scales are displayed with the images, listing numerical values of the displayed variable in meters.

## Locations

Location selection
Event locations (SPOT)
Event locations (ISC)
Compare events

The LOCATIONS menu is used to overlay different explosion location estimates on the test site image currently being displayed. The choice of *Event locations(SPOT)* or *Event locations(ISC)* from this menu results in the overlay of the corresponding location estimates for all previous explosions at that test site. The choice of *Compare events* results in the overlay of the best available locations for just those events for which data are available for a particular seismic phase and station selected using the *Compare* function from the Analyst Station module.

The location symbols can be used to obtain information about the event or to designate the event for further processing. For example, click-



ing on any location symbol, causes available summary information about the event to be displayed on the information bar.

## Overlays

Overlay selection	
Current event	
Surface geology	
Topography contours	
Event magnitude data	→
Historical magnitude data	→
Subsurface contours	→
Location differences	→
Digitized overlays	→

The OVERLAYS menu is used to access and view a variety of data which have been registered to the SPOT satellite images of the two test sites. These data can be graphically superimposed on any of the available images and automatically adjust to the scale of the selected image.

### Current event

This option overlays the current event location on the displayed image.

### Surface geology

This option overlays a graphical representation of the mapped surface geologic features for the selected test site on the displayed image (see Figure 6 of Chapter 2).

### Topography contours

The *Topography contours* overlay selection can be used to superimpose a contour representation of the DMA topographic data for the selected test site on either the compressed or full resolution SPOT images or on the color-coded surface topography representation from the IMAGES menu. The contours are labeled with the corresponding values of elevation above sea level in meters (see Figure 7 of Chapter 2).

### Event magnitude data

Event magnitude data	
Mb residual	
Mb - MLg	
Moment tensor	
Mb - Mo	

Selection of the *Event magnitude data* option generates a pull down menu listing the various magnitude related overlays available for the current event. Magnitudes must have already been estimated for this event before these overlays are accessed. If the required magnitudes are not

available for a given selection, a message will appear on the screen stating "overlay file not available." The *Mb residual* option produces an overlay to the displayed image listing the difference between the current event network-averaged  $m_b$  value and the  $m_b$  value obtained for that event at an individual station specified in the Magnitude Measurement module, plotted at the current event location. Similarly, selection of the *Mb -  $ML_g$*  or *Mb -  $M_o$*  option produces overlays listing the difference between the current event network-averaged  $m_b$  value and a corresponding single station  $M_{Lg}$  value ( see Figure 20 of Chapter 2) designated in the Magnitude Measurement module, or network-averaged surface wave isotropic moment estimate ( $M_o$ ), respectively. Selection of the *Moment tensor* option from this menu produces an overlay of a graphical representation of the surface wave moment tensor inversion solution at the current event location (see Figure 26 of Chapter 2). This display consists of two concentric circles enclosing a straight line segment, where the ratio of the diameters of the circles is proportional to the ratio of the isotropic (light blue) and tectonic (yellow) moments and the yellow line segment is oriented parallel to the inferred strike of the tectonic release component.

### Historical magnitude data

Historical magnitude data	
Mb residuals	→
Mb - $ML_g$ (NORSAR)	
Moment tensor	
Mb - $M_o$	

Selection of *Historical magnitude data* from the OVERLAYS menu activates a pull down menu which provides access to overlay representations of previous experience with the various magnitude related parameters corresponding to the current *Event magnitude data* selections which were just described. In this case, selection of *Mb residuals* activates a secondary pull down menu listing the various USAEDS stations for which the previously observed differences between network-averaged and single station  $m_b$  values have been contoured as a function of event location within the test site (currently only available for the Shagan River test site). Similarly, selection of *Mb -  $ML_g$  (NORSAR)* produces an image overlay of the differences between the network-averaged  $m_b$  values and corresponding NORSAR  $L_g$  values in either contour (Shagan River) or discrete event (Novaya Zemlya) form. The *Moment tensor* option produces an overlay of graphical representations of all previous surface wave moment tensor solutions for explosions at the selected test site, where the isotropic and

tectonic components are represented by dark blue and red circles, respectively, to differentiate them from the corresponding current event solution (see Figure 26 of Chapter 2). Selection of *Mb* - *Mo* produces an overlay of the differences between the network-averaged  $m_b$  and  $M_0$  values for all previous events for which both these magnitude measures are available.

### Subsurface contours

Subsurface contours
Thickness of alluvium
Depth to top of mesozoic
Depth to top of paleozoic
Depth to top of granite

The *Subsurface contours* option in the OVERLAYS menu provides the capability to overlay contours of the various subsurface geologic layer thicknesses and depths on a displayed image, generally the corresponding image from the IMAGES menu. The contours are labelled with the corresponding numerical values of the displayed variable in meters.

### Location differences

Location differences
Preferred to SPOT
Preferred to ISC
Preferred to Bocharov

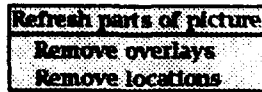
The *Location differences* option provides access to a set of mislocation vector overlays consisting of directed line segments pointing from the preferred to an operator-specified set (e.g., *SPOT*, *ISC*) of explosion location estimates. The preferred locations are those which are thought to be most accurate from among those available, which in the classified environment are generally the NPIC photo locations.

### Digitized overlays

Digitized overlays
Current overlay
Shagan subdivisions

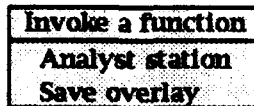
The *Digitized overlays* option provides access to an extensible list of overlay files which have been generated by the operator using the *Digitize* feature to be described below. If a feature has been digitized from the SPOT image in the current session, it can be overlaid on the displayed image by selecting *Current overlay* from this menu. The results of any digitizations which have been saved to a permanent file by the operator in previous sessions (e.g., *Shagan subdivisions*) can also be accessed from this menu and overlaid on any of the available images.

## Refresh



This menu option is used to remove any overlays (*Remove overlays*) or location symbols (*Remove locations*) which are currently superimposed on the displayed image.

## Function



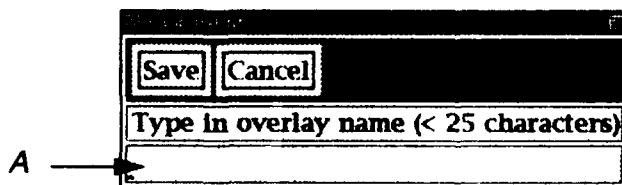
This menu button is used to initiate processes and create permanent overlay files.

### Analyst station

Selection of *Analyst station* initiates a process by which seismic waveforms recorded at a specified station from events selected using the side menu *Compare* function described below are retrieved from the database and displayed on the screen in the standard Analyst station format (cf. Analyst Station description).

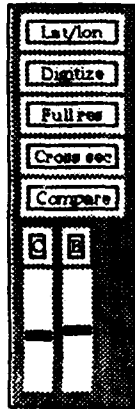
### Save overlay

Selection of *Save overlay* initiates a process by which a digitized overlay can be saved to a permanent file to appear on the *Digitized overlays* menu on all subsequent restarts of the system. This feature is used in conjunction with the *Digitize* button in the side menu. It is implemented through a pop-up menu shown below which allows the operator to type in a name for the file to be saved (e.g., *Shagan subdivisions*) and then save it to a permanent file by clicking on the *Save* button. If at any time during the process the operator decides against saving the file, the sequence can be terminated by clicking on the *Cancel* button.



A - text window used to type in a name.

## Side Menu



The side menu items on the satellite image display provide additional options which permit the operator to interact with the display in a variety of different ways. A notable feature of these buttons is that they initiate processes which remain active while that button is turned on. Consequently, they must be turned off when the associated processing has been completed.

### **Lat/lon**

When this button is highlighted, clicking on any point on the image causes the latitude and longitude of that point to be displayed in the information bar.

### **Digitize**

When the *Digitize* button is highlighted, clicking on any point or a series of points on the image causes the latitude and longitude of the point(s) to be added to a temporary file. When digitization of the selected feature has been completed, the file is closed by clicking on the *Digitize* button again. Any subsequent selection of *Current overlay* from the *Digitized overlays* in the OVERLAYS menu will cause straight line segments to be drawn between these points in the order in which they were selected and overlaid on the image. If desired, this information can also be saved to a permanent named file using the *Save overlay* option from the Satellite Image FUNCTION menu.

### **Full res**

When the *Full res* button is highlighted, in conjunction with the Shagan River test site display, clicking on a point on the image causes the full 10 m resolution SPOT image data to be displayed for the area surrounding that point. Once a full resolution image has been displayed, full resolution images of adjacent regions can be accessed by pointing the cursor near the closest border of the display and clicking on the mouse button. To access the full resolution image for a new area not adjacent to the cur-

rent display, select *Satellite image* from the IMAGES menu and select the new location. Upon completion of the review of the full resolution data, turn off the *Full res* button and proceed.

### ***Cross sec***

When this button is on, a vertical subsurface geologic section along a line between any two points on the image can be created and displayed by sequentially selecting the points with the mouse. The *Quit* button on the cross section display is used to refresh the underlying image display, from which another cross section can be initiated, or, upon completion, the process can be terminated by turning off the *Cross sec* button.

### ***Compare***

When this button is on, events can be selected with the mouse from among those displayed on the image using the *Compare events* option from the LOCATIONS menu. Clicking on any location symbol causes the event location to be highlighted by a diamond and available summary information about the event to be extracted from the database and displayed on the information bar. If, on the basis of this information, the operator decides to select this event, a second click of the mouse button will cause that event identification label to be added to a temporary file and the highlight diamond will turn white. Additional events can be selected in the same fashion and, upon completion, the file is closed by turning off the *Compare* button. Subsequent selection of *Analyst station* from the FUNCTIONS menu causes the designated station waveforms corresponding to the selected events in this file to be retrieved from the database and displayed on the screen, with the current event recording at the top and the selected event waveforms below it in the order in which they were selected.

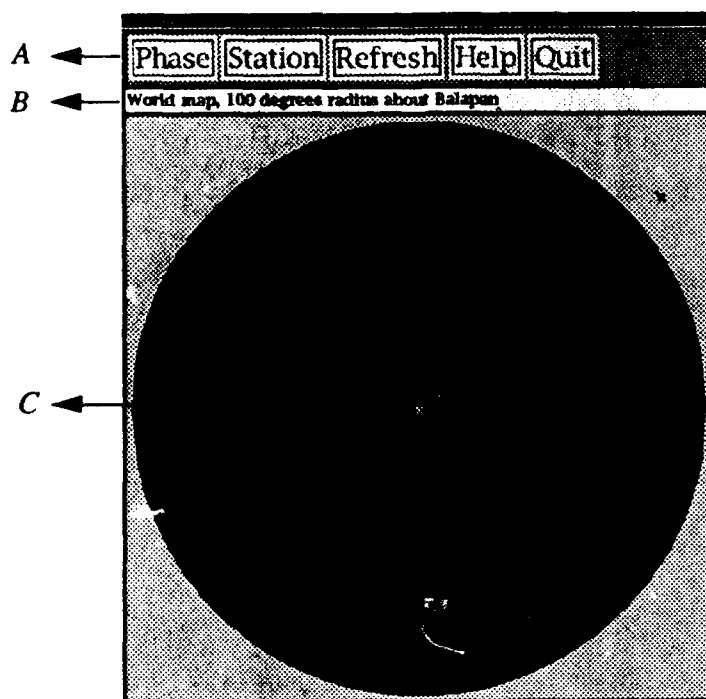
### ***Contrast and Brightness***



The slider bars at the bottom of the side menu can be used to interactively adjust the contrast (C) and brightness (B) of the displayed SPOT image. Clicking on the C or B buttons returns the display to the default setting for that parameter.

## World Map

This module provides a capability to display the map locations of stations which have recorded digital seismic data for the selected event. The maps are plotted as azimuthal equidistant projections of the globe ( $\Delta < 100^\circ$ ) centered on the selected test site.



A - world map menu buttons

B - information bar

C - current test site

## Phase

Phases
Regional P
Lg
Teleseismic P
Rayleigh (vertical)
Rayleigh (radial)
Love

This menu button is used to select the seismic phase for which the database will be searched for stations which recorded data from the current event. The locations of these stations are then automatically plotted on the map display together with the standard three or four letter station abbreviations.

## Station

Stations	
Regional P	Lg
Teleseismic P	HIA
Rayleigh (vertical)	IARU
Rayleigh (radial)	IGAR
Love	IKIV
	IOBN
	NQIAO
	WMO

This menu button is used to select a station from among those which have recorded data for the designated phase and event. Selection of a station causes a straight line to be drawn on the map between the test site and the station which, in this projection, corresponds to the great circle path between these two points.

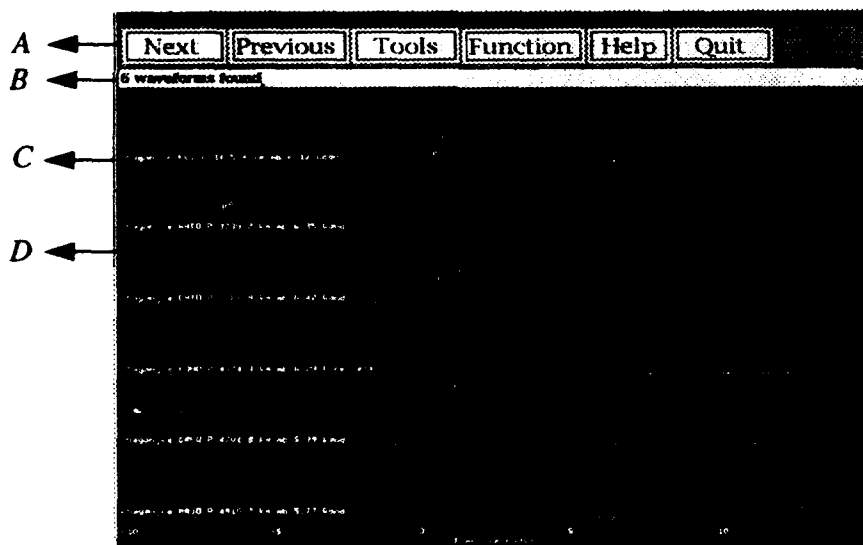
## Refresh

This menu button is used to remove the station location overlays from the map display prior to selection of another phase.



## Analyst Station

Selection of *Analyst Station* from the main FUNCTION menu following the selection of an event and seismic phase produces a display of the corresponding digital seismic waveform data in a format which permits the operator to interact with them to extract the parametric data required for determination of the various magnitude measures for the current event. The default setting provides for the waveforms to be displayed in order of increasing station epicentral distance, with six waveforms per screen or "page." The mode of display varies with the selected phase, with teleseismic and regional P segments denoted (P and  $P_n$ ) displayed as a function of time (from 10 seconds before to 15 seconds after signal onset), while the  $L_g$  and surface wave segments are displayed as a function of group velocity (10 to 2.5 km/sec for  $L_g$ ; 5 to 2.5 km/sec for the Rayleigh and Love phases).



A - analyst station menu buttons

C - waveform information

B - the information bar

D - arrival pick

As is illustrated in the display, each waveform segment is annotated to indicate the event, station, phase, epicentral distance, approximate single station  $m_b$  value and a waveform quality assignment which can be interactively set using the TOOLS menu function *Set quality* to be described

below. The vertical line segments on these displays marks the estimated signal onset time which also can be changed interactively using the TOOLS menu function *Pick arrival* to be described below.

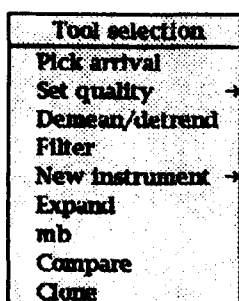
## Next

This menu button is used to page forward through the waveform displays, six waveforms at a time, in order of increasing station epicentral distance.

## Previous

This menu button is used to page backwards from the current display through the available waveforms from stations at smaller epicentral distances.

## Tools



This menu button is used to access the various signal processing and parameter extraction functions which have been provided to facilitate the evaluation of the displayed seismic data and the determination of the various seismic magnitude measures. Once a selection has been made from this menu, the corresponding function remains active until another choice is made or until a new analyst station is initiated.

### *Pick arrival*

This tool permits the operator to change the estimate of signal onset time by pointing at the location of the new estimate on that trace and clicking once. Prior to analyst review, the default onset times are the predicted Herrin 68 travel times for P and  $P_n$  and a group velocity of about 3.5 km/sec for the  $L_g$  and surface wave phases. Upon completion of this review, the revised signal onset estimates can be saved to the database using the *Save* feature from the FUNCTION menu described below. Subsequent analyst station displays of these data will then show the revised arrival estimates.

### Set quality

Data quality
Excellent
Good
Visible
Invisible
Broken
Interfering
Clipped

Selection of this tool activates a pull down menu listing a variety of quality categories which can be assigned to the displayed data. If no prior analyst assignment has been saved to the database, the trace will be displayed initially with a *Not Checked* label. Assignment of a revised quality can be accomplished by selecting a category from this menu and then clicking on any trace to which that category applies. Category assessments are subject to operator judgment, but generally *Excellent* is associated with apparent signal-to-noise ratios of greater than about five, *Good* with signal-to-noise ratios in the range from about two to five and *Visible* to identified signals with signal-to-noise ratios of less than about two. The last four categories (*Invisible*, *Broken*, *Interfering*, *Clipped*) are generally used to designate data which will not be processed to obtain magnitude estimates. *Invisible* signifies that the displayed data contains no evident signal, while *Broken* indicates an instrument malfunction and *Interfering* denotes contamination of the displayed data by arrivals from a different event. The category *Clipped* is assigned only if that portion of the displayed data containing the phase arrivals to be used in the corresponding magnitude determination shows evidence of clipping. New quality assignments can be saved to the database at any time by using the *Save* feature from the **FUNCTION** menu described below.

### Demmean/detrend

This tool permits the operator to remove any DC bias or linear trend from traces which are subsequently selected with the mouse. The resulting displayed time series have mean amplitudes of zero.

### Filter

This tool permits the operator to bandpass filter (Butterworth) any subsequently designated trace between interactively set low frequency and high frequency limits. These frequency bounds are set with slider bars accessed from a pop-up window (see Figure 14 of Chapter 2), as are the slopes (i.e., pole numbers) of the response roll-off outside the specified

band. When the bandpass filter processing has been completed, the interactive slider window can be cancelled by selecting the *Exit* button.

### ***New Instrument***

New Instrument	
wwssn	sp
wwssn	lp
sro	sp
sro	lp
aeds	sp
aeds	lp

This tool permits the operator to analytically transform any subsequently designated trace into the trace which would have been observed at that station if the data had been recorded on any one of three standard instruments (i.e., WWSSN, SRO, USAEDS) whose response characteristics are documented in the EFCRES instrument response file at the DARPA Center for Seismic Studies.

### ***Expand***

This tool permits the operator to produce a full page display of any subsequently designated trace. For P and  $P_n$ , both the amplitude and time scales are expanded, with the displayed time segment extending from four seconds before to six seconds after the estimated signal onset time. For the  $L_g$  and surface wave displays, only the amplitude scale is expanded. This feature is most commonly used in conjunction with the  $m_b$  tool to facilitate the determination of peak-to-peak amplitude and period of the pulse used to define the single station P wave magnitude value. However, any of the other TOOLS menu functions can be accessed from the expanded display and applied to the data. When processing of the expanded data has been completed, the display can be terminated by selecting the *Exit* button.

### ***$m_b$***

This tool allows the operator to use the mouse to draw a rectangle on a selected trace so as to define the peak-to-peak amplitude and half period of the selected cycle of initial P or  $P_n$  motion to be used in the estimation of the corresponding single station magnitude measure. This is accomplished by clicking the cursor at the peak, holding down the mouse and dragging the cursor to the trough of the selected cycle. Upon release of the button the approximate peak-to-peak ground motion amplitude and associated period of the pulse is automatically computed and displayed on

the information line of the analyst station display. After this process has been repeated for each usable trace, the amplitudes and periods can be saved to a file for subsequent input to the corresponding magnitude estimation module using the *Interface file* feature from the FUNCTION menu described below.

### ***Compare***

This tool allows the operator to select a trace and initiate a process in which the on-line seismic database is searched for all other events at the selected test site for which data for the displayed phase were recorded at the designated station. A file identifying the events meeting these criteria is then automatically created and used to update the file used by *Compare events* in the LOCATIONS menu of the Satellite Image module. The map locations of these events can then be overlaid on the SPOT satellite image of the test site and the designated station data corresponding to selected events can be displayed and compared to the data recorded at that station from the current event using the *Compare* and *Analyst station* functions from the Satellite Image menus.

### ***Clone***

This tool allows the operator to select any displayed trace and create a color-coded (red) copy of that trace which can be dragged with the mouse to any position on the screen to permit detailed comparison with other displayed waveforms (see Figure 16 of Chapter 2). This process is applicable to any P or  $P_n$  display or to any analyst station display of compare event data recorded at a fixed station. However, it should be noted that  $L_g$  or surface wave recordings from stations at different distances cannot be directly compared in this fashion because they are displayed as a function of group velocity rather than time.

## Function

Function selection
Interface file
Save
Restore

This menu button is used to save processing results to temporary (*Interface file*) or permanent (*Save*) files, or to undo (*Restore*) the results of any signal processing which has been applied to the displayed waveforms.

### **Interface file**

The *Interface file* option enables the operator to save any interactively determined parametric data to temporary files which will subsequently be used as input to the appropriate magnitude determination modules. More specifically, once the amplitudes and periods for a particular P phase (P or  $P_n$ ) have been determined for each usable recording using the  $m_b$  function from the TOOLS menu, the results can be saved for further processing by invoking the *Interface file* function.

### **Save**

The *Save* option enables the operator to save any revised determinations of data quality (*Set quality*) and signal onset times (*Pick arrival*) to the permanent database. Once this function has been invoked, any subsequent displays of these same data in the analyst station format will incorporate the revised estimates of these parameters.

### **Restore**

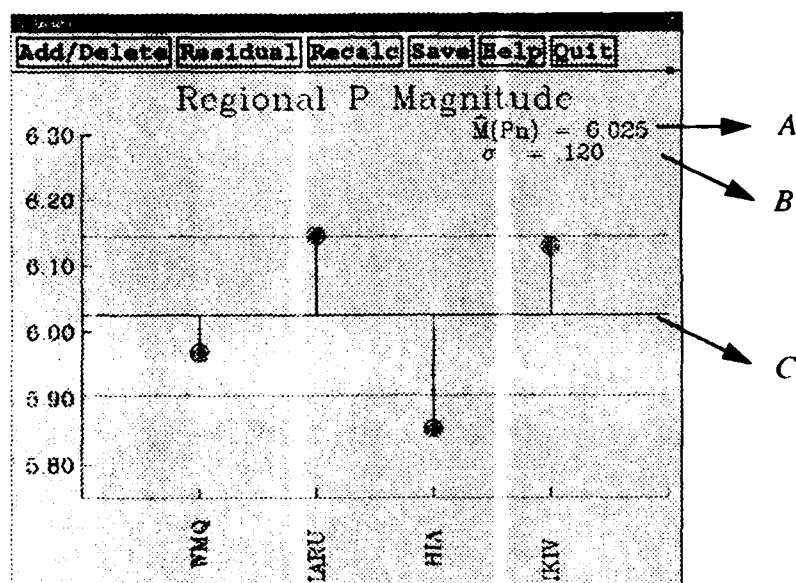
The *Restore* option allows the operator to remove the effects of any filtering or instrument transformations conducted during the current session to return the displayed waveforms to their initial form. However, any revisions to data quality and signal onset estimates made during the current session are retained during this process and, consequently, the *Restore* option can also be used to realign the displayed traces to coincide with any revised signal onset time markers.

## Magnitude Measurement

Magnitude measurement
Regional P
RMS Lg
mb
Spectral P
Moment Tensor

This module provides the capability to estimate network-averaged seismic magnitude measures from the waveform and parameter data corresponding to the individual seismic arrivals previously reviewed by the operator using the analyst station module. At the present time, five separate magnitudes based on regional P and  $L_g$  waves (*Regional P*, *RMS Lg*), teleseismic P waves (*mb*, *Spectral P*) and long-period Rayleigh and Love waves (*Moment Tensor*) can be estimated using this module.

### Regional P



A - network-averaged magnitude

B - standard deviation

C - mean magnitude estimate

Used to estimate single station and network-averaged regional P phase magnitudes ( $\hat{M}(P_n)$ ) from the amplitudes and periods which were saved in the corresponding interface file during the analyst station review of the regional P phase data. The resulting display lists the network-averaged magnitude value ( $\hat{M}(P_n)$ ) and the associated standard deviation of the data ( $\sigma$ ) and shows the corresponding single station magnitude estimates (filled circles) with respect to the mean and plus and minus  $1\sigma$  lev-

els (horizontal lines). At the same time, the ( $\hat{M}(P_n)$ ) value is automatically written to a temporary file and is designated as the regional P wave magnitude for the current event. The menu options on this display can be used to interact with and revise this fully automatic solution.

### **Add/Delete**

Selection of the *Add/Delete* option activates a pulldown menu listing the individual stations contributing to the network-averaged magnitude estimate. If the operator wishes to eliminate a station from the average (e.g., because of large deviation from the mean value), highlighting that station name in the menu causes that station to be eliminated from future estimates of the network-averaged value. This process can be repeated to delete any number of additional stations.

### **Recalc**

Once a desired subset of stations has been defined through this process, the *Recalc* menu option can be selected to automatically generate a revised magnitude estimate and corresponding display. At any point in this review, an eliminated station can be added back into the averaging process by re-selecting it from the *Add/Delete* station list, at which point the highlight on that station name will be eliminated.

### **Save**

If a preferred value of  $\hat{M}(P_n)$  is identified during this review process it can be saved to the current event magnitude file using the *Save* menu option, at which point it replaces the complete network value which was automatically written to this file after the initial calculation.

### **Residual**

Selection of the *Residual* option activates another pull down menu with the same list of stations, any one of which can be selected. This initiates a process by which the difference between the current event network-



averaged  $m_b$  value ( $\hat{m}_b$ ) and the designated station  $M(P_n)$  value is computed and added to the *Event magnitude data* overlay menu in the Satellite Image module, where it can be superimposed on the image at the current event location and compared with values of this difference obtained for previous events at that test site (if available). Note that an  $\hat{m}_b$  value must have already been estimated for the current event before this option can be exercised.

## RMS Lg

This module is used to estimate single station and network-averaged regional  $L_g$  phase magnitudes ( $M(L_g)$ ) from the vertical component  $L_g$  signals recorded at stations for which the data were found to be usable in the analyst station review process. In computing this magnitude measure, the data are first bandpass filtered in a band which typically extends from about 0.6 to 3.0 Hz and then the peak of the RMS amplitude level of the filtered signal is computed over a group velocity interval extending from about 3.6 to 3.0 km/sec. For array stations such as NORSAR, the  $M(L_g)$  value is determined as a logarithmic average of the peak RMS amplitude values at the various array sites. Since this is a computationally intensive process, it is generally run in the background while the operator conducts other tasks. When the process has been completed, an RMS Lg icon will appear on the screen, where it can be activated by the operator at his discretion. The resulting magnitude display and associated functionality are identical to those described above for the Regional P phase module with  $M(L_g)$  replacing  $M(P_n)$ . As with the Regional P phase module, an  $\hat{m}_b$  value must have already been estimated for the current event before the RMS Lg *Residual* menu option is exercised.



RMS Lg icon

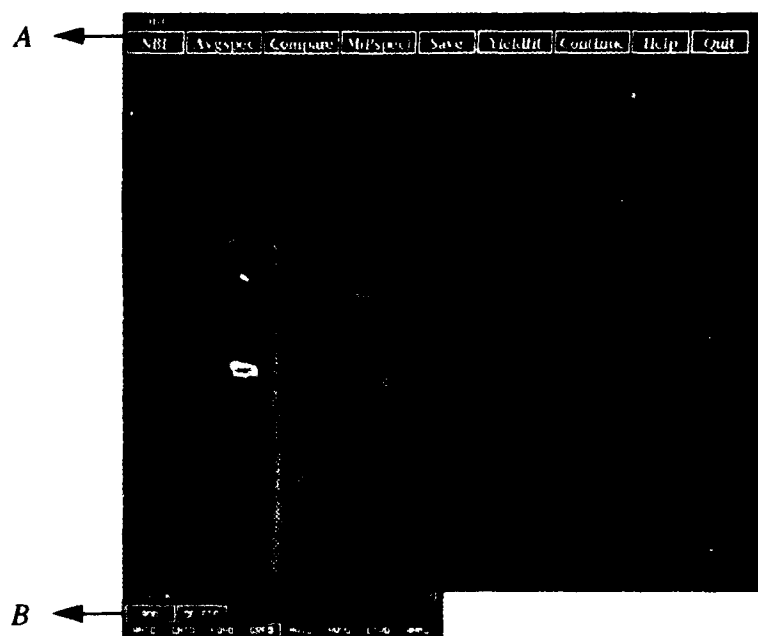
## $m_b$

This module is used to estimate single station and network-averaged teleseismic P wave magnitudes from the amplitudes and periods which were saved in the corresponding interface file during the analyst station review of the teleseismic P phase data. The resulting magnitude dis-

play and associated functionality are identical to those described above for the Regional P phase module with  $m_b$  replacing  $M(P_n)$ . Thus, in the application to  $m_b$ , selection of a station from the *Residual* menu initiates a process by which the difference between the current event network-averaged  $m_b$  value,  $\hat{m}_b$ , and the designated station  $m_b$  value is computed and added to the Event magnitude data overlay menu in the Satellite Image module. At the present time, this value can be compared to previous experience only for USAEDS station recordings of Shagan River explosions for which these single station  $m_b$  residuals have been contoured as a function of event location within the test site.

## Spectral P

This module is used to estimate network-averaged teleseismic P wave spectra and associated spectral P magnitudes ( $M(P_{spec})$ ) and yield estimates through processing of teleseismic P phase data recorded at stations for which frequency dependent station correction factors have previously been estimated through off-line analysis. Once *Spectral P* has been selected from the *Magnitude Measurement* menu, a separate process is ini-

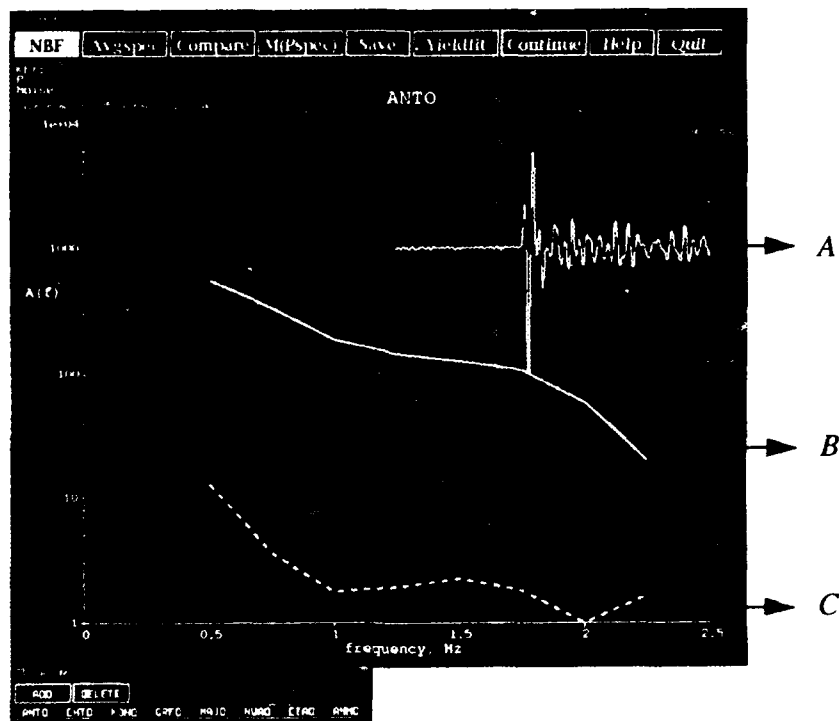


A - Spectral P menu buttons

B - Stations window

tiated with its own display and associated menu. In this initial display, the usable stations for which teleseismic P phase data are available are listed in the Stations window in the lower left hand corner of the display, together with *Add* and *Delete* buttons which can be used by the operator to add or delete stations from the processing stream at any stage. The processing is accomplished by accessing the menu options in the following sequence.

### NBF



A - P wave signal

B - signal spectrum

C - noise spectrum

This module permits the operator to estimate and display single station P wave signal and noise spectra through narrowband filtering of the waveform data over the band from 0.50 to 2.25 Hz. If upon review of these spectra the operator concludes that the data from a particular station are unusable, that station can be deleted from further processing by sequentially selecting the *Delete* and station buttons from the Stations window. Once the review of the spectra for a given station is completed, selection of

*Continue* from the menu automatically refreshes the screen and brings up the spectral display corresponding to the next station. When *Continue* is selected following the last station, the NBF function is automatically terminated, signaling the end of the single station processing.

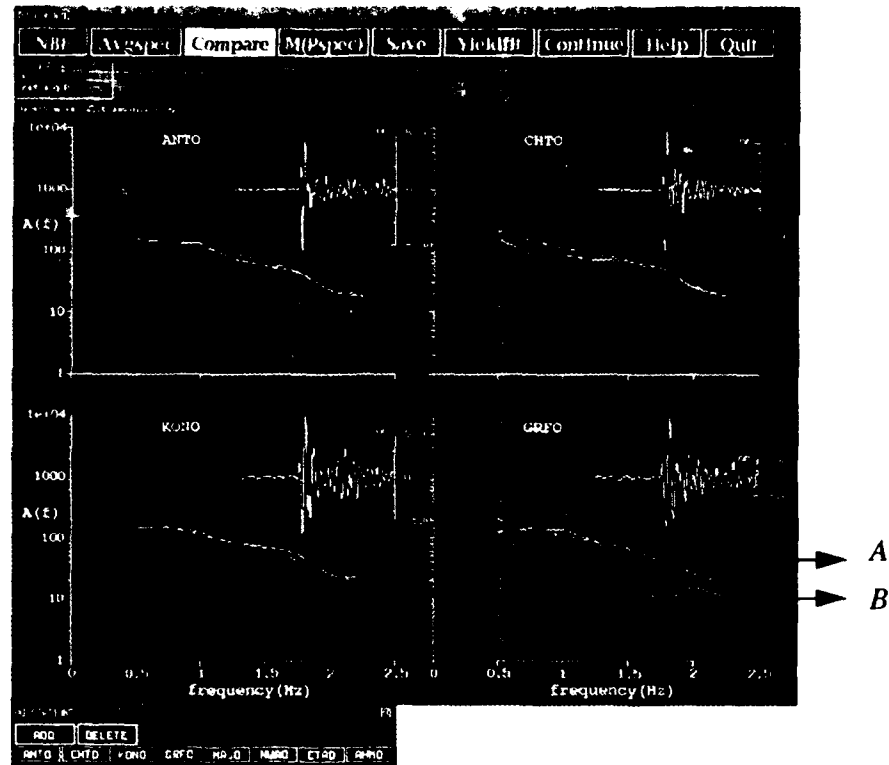
### Avgspec

Selection of this menu option initiates a process by which frequency dependent station correction factors are applied to the single station spectra and the resulting spectra are logarithmically averaged to obtain the initial estimate of the network-averaged P wave spectrum for the current event. The result is displayed (solid line) together with the network-averaged spectrum expected, on average, for an explosion of that  $m_b$  value on the basis of past experience at that test site (dotted line).



### Compare

This module permits the operator to further evaluate the consistency of the spectral data through comparisons of the derived network-averaged spectrum (dotted line) with the individual station-corrected spec-



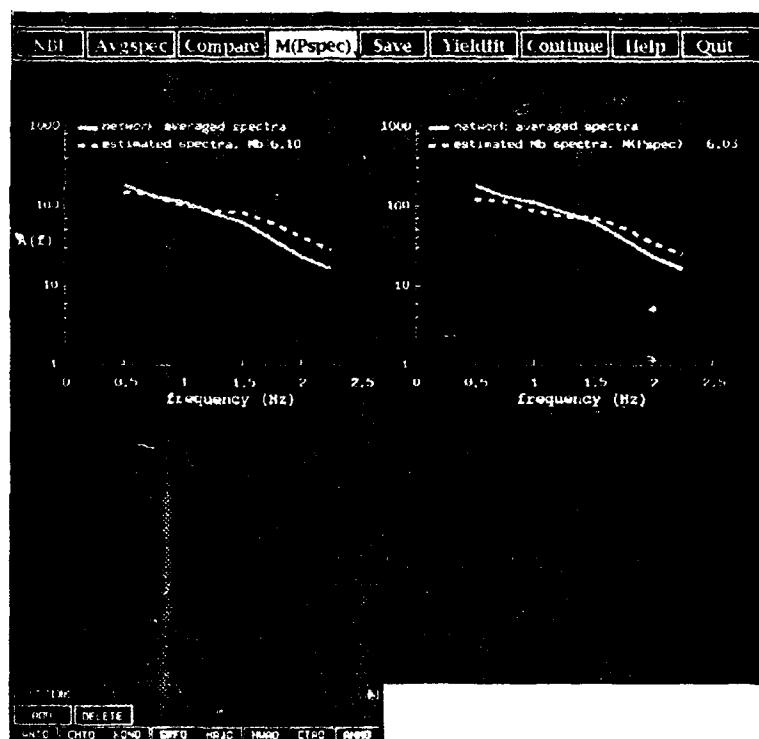
*A - derived network-averaged spectrum*

*B - individual station-corrected spectra*

tra (solid lines) which went into the network average. These comparisons are displayed four stations to a page, with subsequent pages accessed using the *Continue* function. During this review, any stations showing significant spectral discrepancies with respect to the average can be eliminated by sequentially selecting the *Delete* and station buttons from the Stations window. When *Continue* is selected following the last station comparison, the *Compare* function is automatically terminated. At this point the operator has the option of returning to the *AvgSpec* function to recompute the network-averaged spectrum without any stations which may have been deleted in the compare process. In the resulting display, the current network-averaged spectrum is shown as a solid line, the previous estimate as a dashed line and the predicted spectrum based on  $m_b$  again as a dotted line. This process of deleting (or adding) stations and recomputing the network average can be repeated until a satisfactory version of the network-averaged P wave spectrum is obtained for the event under consideration.

*M(Pspec)*

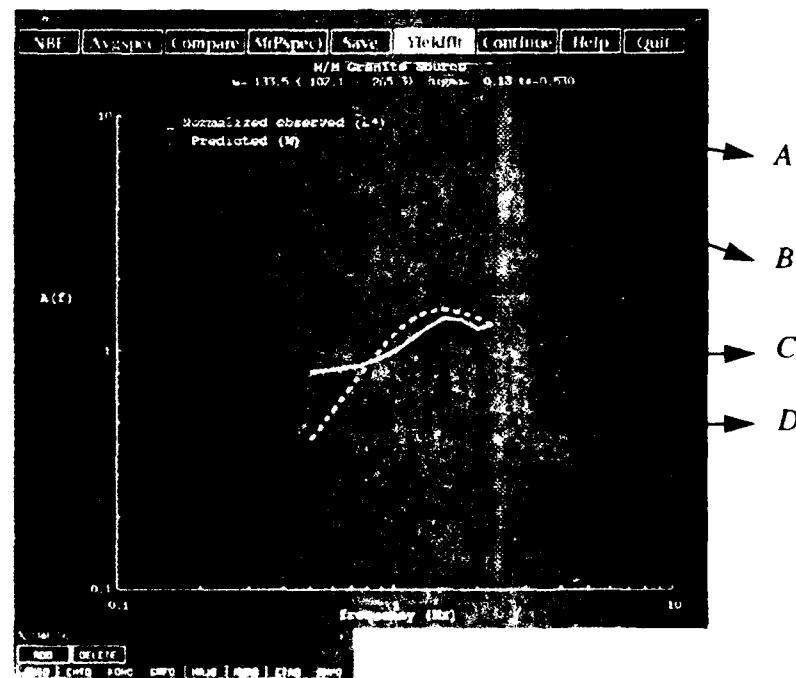
This module permits the operator to estimate a P wave spectral magnitude,  $M(Pspec)$ , from the computed network-averaged spectrum. In the accompanying display, the figure on the left shows the final comparison from the Avgspec module, while the figure on the right shows the comparison between the same observed spectrum (solid line) together with the predicted spectrum (dotted line) corresponding to the  $m_b$  value which provides the best overall fit to the observed spectrum over the frequency band from 0.5 to 2.25 Hz. This value of  $m_b$  is subsequently designated  $M(Pspec)$ .

*Save*

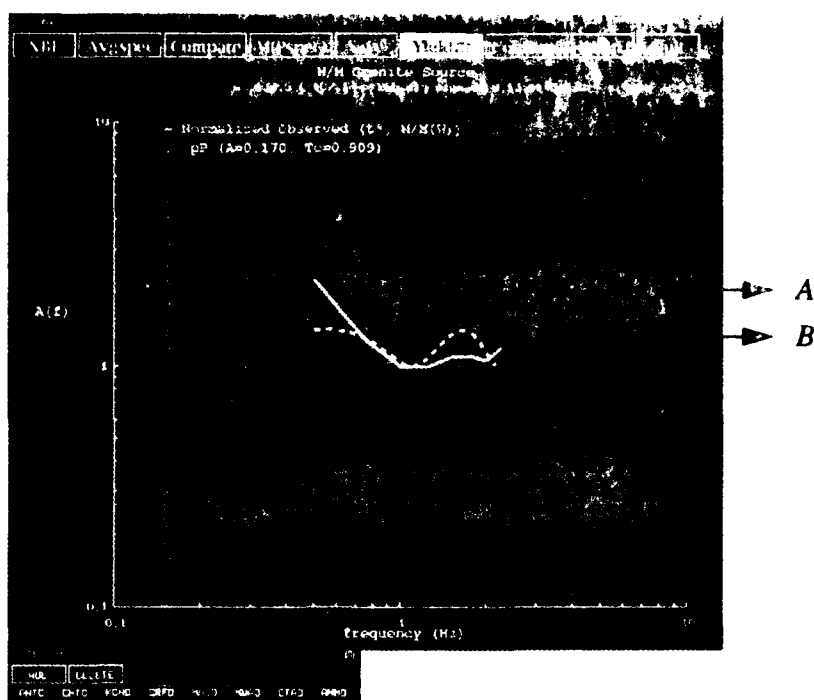
This function can be used by the operator to replace the value of  $M(Pspec)$  which is automatically written to the current event magnitude file following the first execution of the  $M(Pspec)$  function. That is, if the observed network-averaged spectrum is subsequently modified by adding or deleting stations, the corresponding  $M(Pspec)$  value can be substituted into the magnitude file using this menu option.

## Yieldfit

Selection of this module initiates a process by which the operator can obtain model-based estimates of explosion yield and pP effects corresponding to the derived network-averaged P wave spectrum for the current event. The initial display shown in Figure 23 of Chapter 2 provides a menu selection of three alternate source models: Mueller/Murphy saturated tuff/diabase (M/M Wei Tuff), Mueller/Murphy granite (M/M Granite) and von Seggern/Blandford granite (VonSeg-Blandf). Selection of any one of these three source models produces a display showing a comparison between the attenuation-corrected observed spectrum (solid line) and the predicted spectrum corresponding to the yield which provides the best overall fit to the observations over the band 0.50 to 2.25 Hz (dotted line). This best-fit yield value is listed at the top of the display together with its associated upper bound uncertainty range. Selection of *Continue* then results in a display showing a comparison between the attenuation and source normalized



- A - upper bound uncertainty range
- B - best-fit yield value
- C - attenuation-corrected observed spectrum
- D - predicted spectrum corresponding to the best-fit yield value

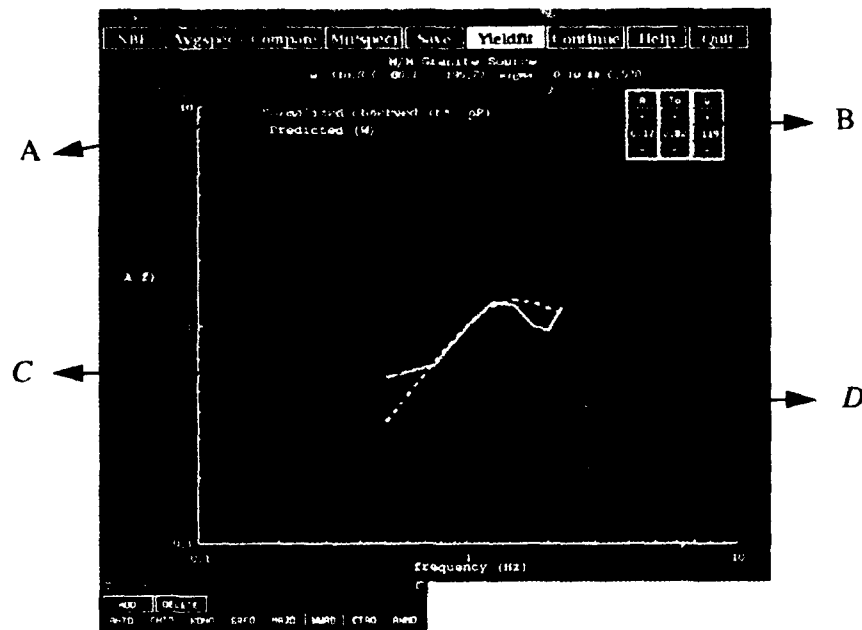


*A - attenuation and source normalized spectrum*

*B - predicted pP spectrum*

spectrum (solid line) and the spectral modulation pattern predicted by the automatically determined best-fit pP model (dotted line). The automatically determined model parameters consisting of the ratio of pP to P amplitude (A) and pP-P delay time ( $T_0$ ), are listed in parenthesis in the legend. By again selecting *Continue*, the operator initiates a process by which this inferred pP modulation spectrum is divided out of the attenuation-corrected spectrum to obtain the final normalized observed spectrum which is then displayed (solid line) together with the predicted spectrum corresponding to the original best-fit yield (dotted line). The modified yield upper bound uncertainty range corresponding to the pP-corrected spectrum is also computed at this time and substituted into the parenthesis at the top of the display. Also appearing on this display is a box in the upper right hand corner with columns labeled A,  $T_0$ , W. This indicates the option for the operator to interactively modify the automatic yield and pP estimates. Thus, selecting the minus (plus) button under W causes the yield to decrease (increase) in increments of five percent from the automatically determined yield and the





*A - modified yield upper bound uncertainty range*

*B - interactive box used to modify the automatic yield and pP estimates*

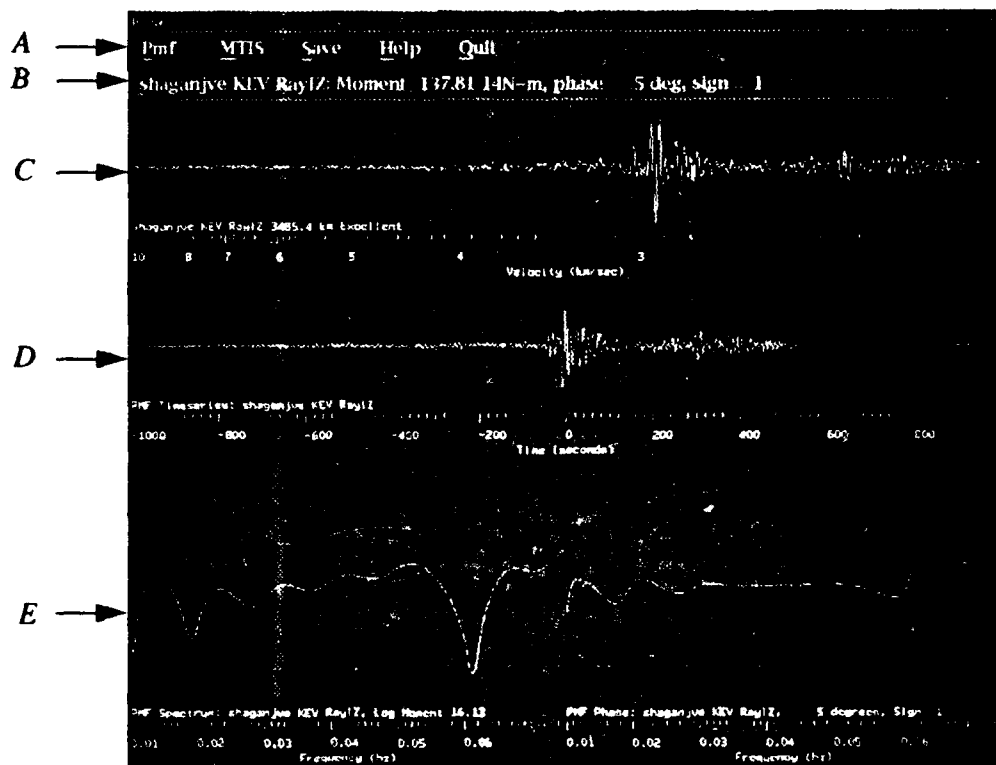
*C - final normalized observed spectrum*

*D - predicted spectrum corresponding to the best-fit yield value*

associated predicted spectrum to be automatically updated in the display to reflect this new yield value. By again selecting *Continue*, the operator causes a new pP fit corresponding to this revised source estimate to be determined and displayed. At this stage, the operator can interactively modify the automatically determined pP parameters by selecting the plus or minus buttons under the columns A and  $T_0$  and the display will continuously update to show the comparisons corresponding to these revised parameters. Once the pP model has been finalized, the operator can select *Continue* once again to obtain the spectral comparison display corresponding to the interactively determined yield and pP parameter values. This interactive modification cycle can be repeated indefinitely, thereby allowing the operator to explore a variety of alternative solutions. Once this process has been completed, the operator can select *Quit* to terminate the *Yieldfit* function. At this point, the operator can either select *Yieldfit* again to explore a different source model, or select *Quit* again to terminate the Spectral P processing.

## Moment Tensor

This module is used to estimate surface wave moment tensor solutions and associated explosion moment magnitudes ( $M_0$ ) through processing of the recorded long-period Rayleigh and Love wave data from the current event. Selection of *Moment Tensor* from the Magnitude Measurement menu initiates a phase matched filtering process with associated display and menu. Since it takes some time to initialize this process, it is done in the background and, when completed, an icon appears on the screen which can be accessed by the operator at his discretion to activate the initial phase matched filter display shown below. Proceeding from top to bottom, this initial display contains the menu, an information bar, a standard analyst station display of one component of the surface wave recording from the nearest station, the time history output resulting from applying a phase matched filter (Pmf) to that surface wave recording and finally, at the bottom of the display, the amplitude (left) and phase (right) spectra corre-



A - moment tensor menu

B - information bar

C - waveform window

D - Pmf time history output

E - amplitude and phase spectra

sponding to that Pmf output. The Pmf output time history is plotted as a function of reduced time, computed with respect to the arrival sequence predicted by the estimated group velocity dispersion curve for the propagation path to that station. If the data are good and the estimated dispersion curve is accurate, this trace should be dominated by a narrow pulse centered on zero lag time. The amplitude and phase spectra are displayed as a function of frequency over the band extending from 0.010 to 0.075 Hz (i.e., over the period range extending from about 13 to 100 seconds). The average value of the amplitude spectrum over this range defines the surface wave moment estimate for that station, which is automatically determined by the system and listed in the information line. Ideally, the associated phase spectrum should oscillate around constant values of either 0 or  $\pi$ , denoting normal (sign + 1) or reversed (sign - 1) phase, respectively. More generally, in the automatic processing mode, the phase is defined to be normal if the absolute value of the average phase over this period range is less than  $\pi/2$  and defined to be reversed if this quantity is greater than  $\pi/2$ , and the corresponding value is then listed in the information line. As will be described below, the operator can interactively reset these automatic phase determinations in cases in which the data are ambiguous.

### ***Pmf***

Pmf  
Pmf  
Next  
Previous  
Auto Pmf  
Delete/Restore  
Change Sign

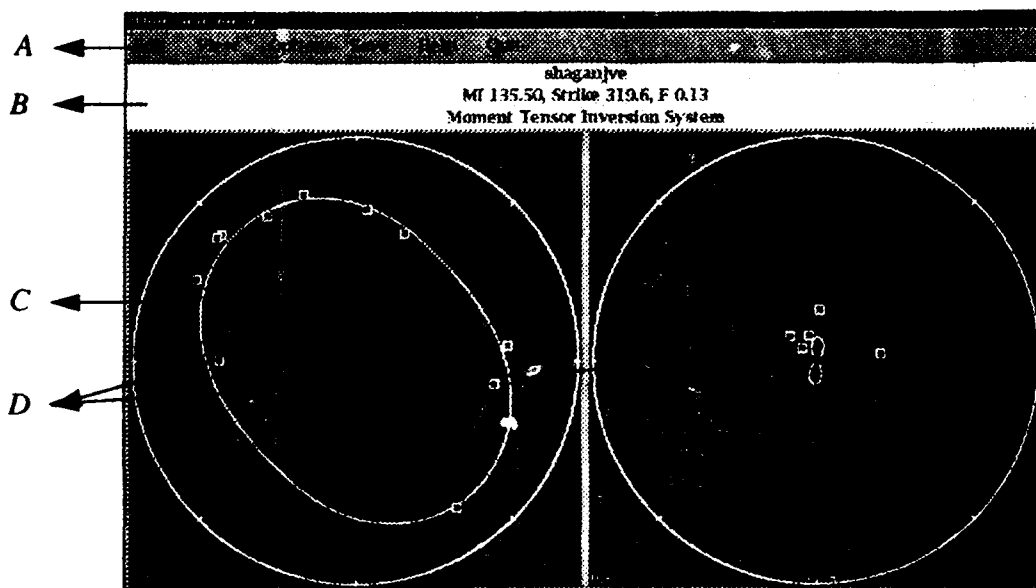
The functions listed under this menu item permit the operator to interact with the displayed surface wave data and associated Pmf results. Selection of the *Pmf* option initiates an automatic process by which the moment and phase corresponding to the displayed waveform are determined and written to both the information line and a temporary file. Selection of *Next* (*Previous*) refreshes the display to show the Pmf results corresponding to the next (preceding) station in the surface wave processing queue. Similarly, selection of *Auto Pmf* initiates a process by which all the usable surface wave data from the current event are automatically processed through the Pmf routine and the results are sequentially displayed on the screen without any operator intervention. Selection of *Delete/Restore* causes the Pmf results for the displayed trace to be either removed or added to the temporary file of processing results (depending on whether it currently is or is not in that file) which is to be used as input to the moment tensor inversion system (MTIS) module. Finally, selection of the

*Change Sign* option causes the phase assignment for the displayed trace to be reversed (i.e., to either  $\pm 1$ , depending on the current setting).

### MTIS

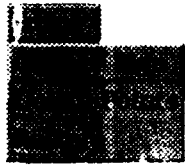
MTIS  
Run MTIS

Selection of this option initiates a secondary process with associated menu which permits the operator to interactively process the individual station moments and phases determined in the Pmf module. The initial display shows the fit to the Rayleigh (left) and Love (right) wave PMF moment estimates corresponding to the automatic moment tensor solution listed in the information line below the menu. The default solution for the tectonic component corresponds to thrust motion on a fault dipping at  $45^\circ$  and the resulting moment tensor solution is characterized by an isotropic moment (MI), together with inferred strike and F factor estimates for the tectonic component. On these displays, open and closed symbols denote normal and reversed phase observations, respectively. The associated menu items on this MTIS display permit the operator to interact with these data to eliminate questionable points and explore alternate solutions.



- A - MTIS menu buttons
- B - information bar
- C - moment tensor solution
- D - single station observations

### Edit



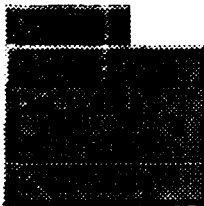
This function permits the operator to select points with the mouse (causing the points to be highlighted) and then to either change their sign or delete them from the inversion input file by selecting the *Change Sign* or *Delete Points* menu options, respectively.

### View



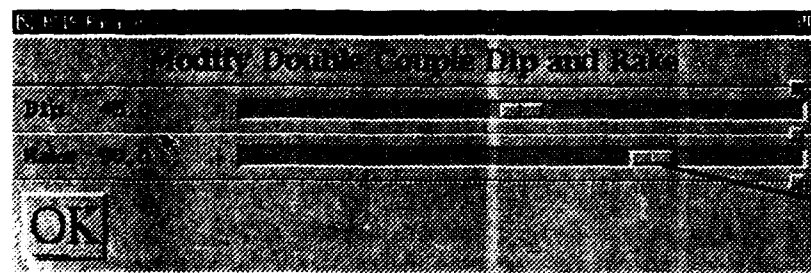
This function permits the operator to either display the seismograms corresponding to stations (points) previously selected with the mouse (*Seismogram*) or to create a graphical representation of the currently displayed moment tensor solution and add it to the *Overlays* menu of the Satellite Image module for display on the SPOT image of the test site (*SPOT image*).

### Options



This function permits the operator to undo any previous selection of points (*Unselect*), to modify the dip and rake of the tectonic solution from the default values for 45° thrust (*Set Dip/Rake*) or to recalculate the moment tensor solution to account for any operator specified changes in sign or deletions of points (*Recalculate*).

Selection of *Set Dip/Rake* activates a display of sliders which permit the operator to interactively set the values of these variables to any physically permissible values. Subsequent selection of *Recalculate* from the *Options* menu initiates a display of the moment tensor solution corre-



A - sliders used to adjust dip and rake values

sponding to these revised estimates of the dip and rake of the inferred tectonic solution. When the operator is satisfied that a stable estimate of the moment tensor solution has been obtained, it can be saved to the current event database together with the associated moment magnitude ( $M_{10}$ ) using the MTIS *Save* function.

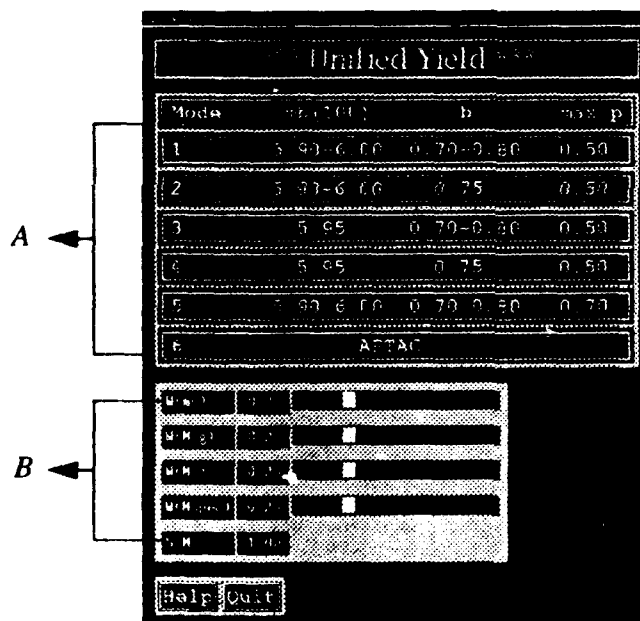
### **Save**

Save  
Save to Database

Selection of this Pmf option initiates a process by which the single station moment and phase estimates obtained during the current processing session are saved to the database for subsequent input to the MTIS moment tensor inversion module.

## Yield Estimation

This module enables the operator to obtain unified seismic yield estimates and associated uncertainty bounds for the current event by applying a variety of statistical models to the corresponding network-averaged magnitudes. At least one network-averaged magnitude must have already been estimated before this module can be activated. Selection of this option from the main FUNCTION menu produces a display listing six different statistical models and providing slider bars to adjust the relative weights of the four magnitude measures which currently can be used in the unified yield analysis (i.e.,  $mb$ ,  $M(Lg)$ ,  $M_o$ ,  $M(Pspec)$ ). These weights must sum to 1.00 and the initial default values provide for equal weighting of all available magnitudes.



A - statistical models

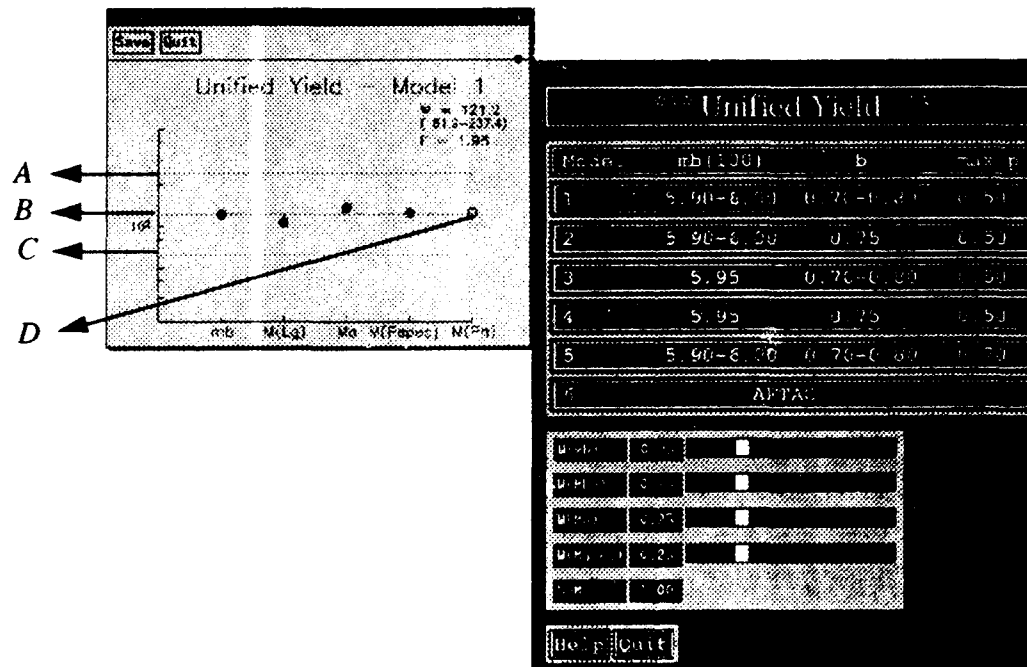
B - sliders used to adjust the weights

The first five of these models provide unified yield estimates and extremal confidence limits on those estimates corresponding to different sets of constraints on a specified  $m_p/yield(W)$  relation which, for explosions at the Shagan River and Novaya Zemlya test sites has been taken to be

$$m_b = 4.45 + 0.75 \log W$$

with associated parameters  $m_b(100)$ ,  $b$  and  $\max p$  where  $m_b(100)$  denotes the estimated uncertainty in the average value of  $m_b$  for explosions with yields of 100 kt,  $b$  denotes the estimated uncertainty in the slope of the linear relation between  $m_b$  and  $\log W$  and  $\max p$  denotes the upper bound on the absolute value of the correlation of the yield estimation errors associated with the different magnitude measures. The five available models of this type provide estimates corresponding to different values of these three parameters which are consistent with the current range of expert opinion. Model number 6, labeled AFTAC, provides a unified yield estimate based on  $m_b$  and  $M(L_g)$  alone, using the current AFTAC standard procedure. When this model is selected, the weights automatically adjust to 0.5 for  $m_b$  and  $M(L_g)$  and to zero for  $M_0$  and  $M(Pspec)$ .

Selection of any one of these models generates a display showing the yield estimates corresponding to the individual magnitudes plotted with respect to the unified yield estimate and its associated uncertainty bounds (horizontal lines). Yield estimates determined from magnitude values not included in the unified yield calculation are shown as open circles for pur-



A,C - uncertainty bounds

B - unified yield

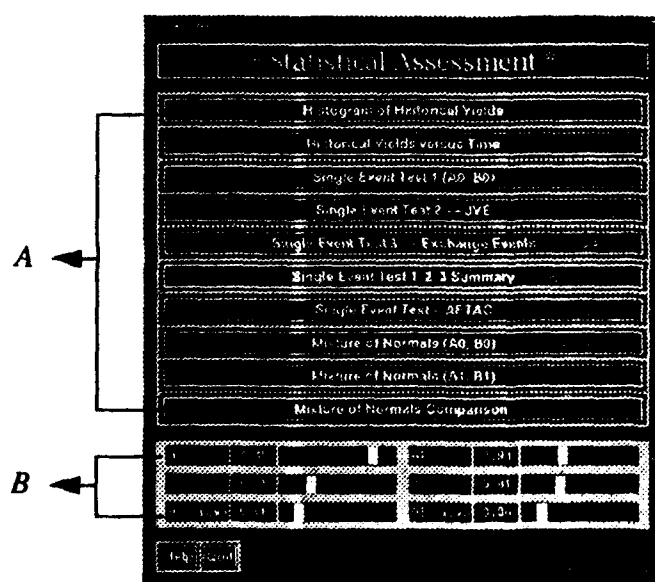
D - value not included in yield calculation



poses of comparison. The unified yield estimate (W) and its associated uncertainty factor (F) are listed in the upper right hand corner of this display together with the yield range corresponding to this F value (in parenthesis). Subsequent selection of models from the menu produce corresponding displays beneath that for the first choice, which remains in place throughout the processing session (See Figure 27 in Chapter 2). When a satisfactory unified yield estimate has been obtained, it can be saved to the current event file using the *Save* option which appears on the menu at the top of each display.

## Statistical Summary

This module provides access to a variety of statistical tests and displays which can be used by the operator to evaluate the yield estimate for the current event in the context of past experience at that test site and to assess whether this estimate is consistent with the 150 kt threshold of the Threshold Test Ban Treaty (TTBT). A unified yield estimate must have already been determined for the current event before this module can be activated. Selection of this option from the main FUNCTION menu produces a menu display listing the available choices of statistical displays and tests, and providing two sets of slider bars which can be used to vary the  $m_p$ /yield relations used in the computations. The slider bars at the lower left of the display determine the  $m_p$ /yield relation to be used in all tests except the second Mixture of Normals test and permit the interactive determination of the intercept (AO), slope (BO) and intercept uncertainty (AO sigma). Initial default values for these parameters are 4.45, 0.75 and 0.06, respectively, consistent with the nominal  $m_p$ /yield relation for explosions at the Shagan River and Novaya Zemlya test sites. The slider bars at the lower right of the display determine the  $m_p$ /yield relation for the second Mixture of Normals calculation and have default values consistent with the nominal  $m_p$ /yield relation for explosions below the water table at the Nevada Test Site (i.e.,  $A1 = 3.94$ ,  $B1 = 0.81$  and  $A1 \text{ sigma} = 0.06$ ).



A - statistical tests

B - slider bars used to set the  $m_p$ /yield relation

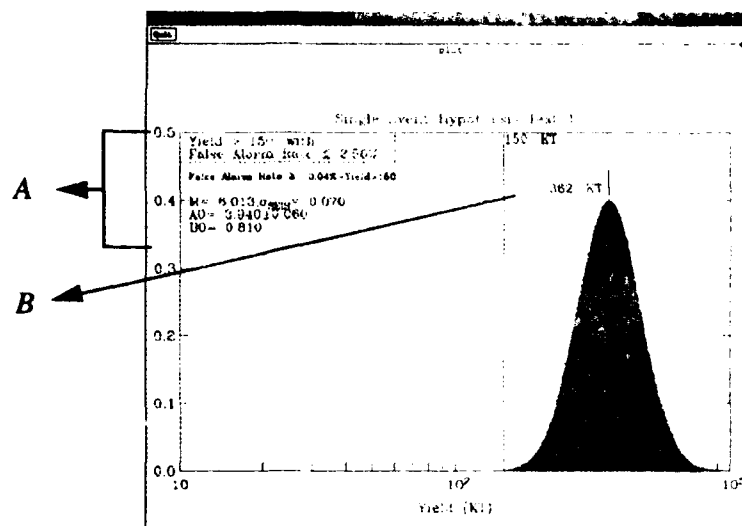
## Histograms

Selection of either of the first two menu items, *Histogram of Historical Yields* and *Historical Yields versus Time*, results in displays showing the unified yield estimate for the current event relative to previous experience at that test site, as a function of yield and date, respectively.

## Single Event Tests

The various single event tests provide access to formal compliance assessment tests which can be used to make quantitative statements about the probability that the current event is or is not seismically compliant with the 150 kt threshold level of the TTBT. *Single Event Test 1(AO,BO)* assumes that only indirect, seismic estimates of the  $m_b$ /yield relation are available and utilizes the specified values of AO and BO in estimating the compliance probability. For Shagan River explosions, *Single Event Test 2--JVE* can be accessed to factor in the calibration results from the JVE CORRT-EX yield determination and utilizes a modified AO value which accounts for this additional information in the test of compliance. Similarly, *Single Event Test 3--Exchange Events* for Shagan River explosions incorporates the announced yields for the JVE exchange events into the estimation of the AO value used in the compliance assessment. The *Single Event Test --AFTAC*, on the other hand, employs the current AFTAC  $m_b$ /yield relation and associated unified yield estimate to assess seismic compliance of the current event with the TTBT threshold based on just the  $m_b$  and  $M(L_g)$  magnitude measures.

Selection of any of these single event tests results in a display showing the distribution function associated with the current event unified yield estimate in relation to the 150 kt threshold. In this representation, the number at the peak of the distribution corresponds to the unified yield estimate and the red shaded area under the curve provides a measure of the probability of a violation of the TTBT limit. The formal compliance assessment results are presented in tabular form in the upper left hand corner of



*A - compliance assessment results*

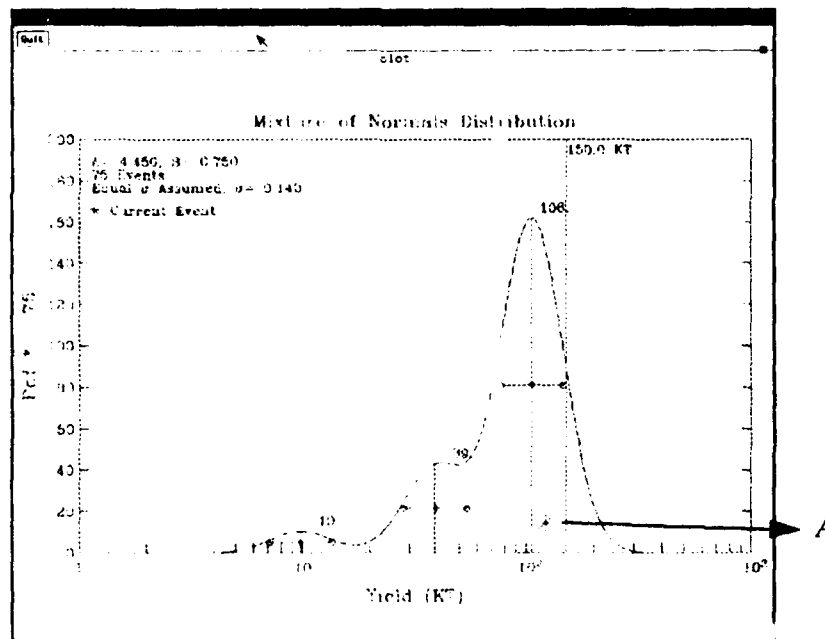
*B - unified yield estimate*

this display. Here, the uppermost box provides a summary of the results of the hypothesis test and indicates whether the current event yield is or is not greater (at the 95% confidence level) than the 150 kt threshold at the nominal false alarm rate of 2.5%. The first line below that box indicates what false alarm rate would have to be accepted to be able to conclude that the true yield of the current event is greater than 150 kt. The lines below that list the unified magnitude ( $M$ ) and associated uncertainty ( $\sigma_{SEIS}$ ), and the intercept ( $AO$ ) and slope ( $BO$ ) of the  $m_b$ /yield curve used in the compliance calculation.

## Mixture of Normals

The Mixture of Normals tests (*Mixture of Normals*( $AO, BO$ ) and *Mixture of Normals*( $AI, BI$ )) provide more formal means of comparing the unified yield estimate of the current event with the distribution of yields of previous explosions at that test site. In this case, it is assumed that the yields of previous explosions are clustered around a few discrete values and their joint distribution is represented as a superposition of normal distributions, the number and means of which are estimated by applying for-

mal statistical criteria. This test can be run using either the (AO,BO) or (A1,B1) definitions of the  $m_p/yield$  relation. In either case, the resulting display shows the unified yield of the current event (\*) with respect to the 150 kt threshold and the best-fitting mixture of normals solution for the historical data, where the yields of the individual distributions in the solution are listed beside their respective peaks. The tabular data in the upper left hand corner of the display lists the  $m_p/yield$  parameters, number of historical events and individual distribution  $\sigma$  values used in the mixture of normals calculation. If both Mixture of Normals tests have been run, selection of the *Mixture of Normals Comparison* option results in a similar display in which color-coded representations of the mixture of normals solutions corresponding to both the (AO,BO) and (A1,B1)  $m_p/yield$  relations are shown in relation to the current event yield estimate and the 150 kt threshold of the TTBT.



A - unified yield of the current event

## Spreadsheet

This module provides a less formal environment for evaluating the seismic yield estimate for the current event in the context of the results obtained from analyses of previous explosions at that test site, as well as any available independent yield calibration data (e.g., CORRTEx). Selection of this option from the main FUNCTION menu produces a standard spreadsheet display listing the four individual seismic yield estimates (based on  $m_b$ ,  $M(L_g)$ ,  $M_o$ ,  $M(P_{spec})$ ) and corresponding unified yields ( $W(Unif)$ ) for selected explosions at the designated test site. For explosions at the Shagan River test site, available calibration yields, including the JVE CORRTEx value, the JVE exchange yields and the yields published in the open literature are listed in the column labeled  $W(Bocharov)$ . The corresponding ratios of unified seismic yield estimates to calibration yield values are listed in the column labeled  $W_u/W_e$  and the logarithmic average value of this ratio is listed at the bottom of the column as Avg Bias, together with the estimate of the 95% bound on the observed ratios (F).

**A**

**B**

### *B - yield estimates*

Operator interaction with this spreadsheet display is restricted to the top three rows of entries specifying the magnitude/yield relations (Slope, Intercept) for each magnitude type and the relative weight (Weight) to be applied to each magnitude in the determination of the unified yield. Default values for the slopes and intercepts are 4.45 and 0.75, respectively, for  $m_b$ ,  $M(L_g)$  and  $M(P_{spec})$  and 5.00 and 1.00 for  $M_0$ . The default values for the weights call for equal weighting of the four magnitudes and, however they are subsequently changed by the operator, it is necessary that they sum to 1.00. Slopes, intercepts and weights can be changed by simply moving the cursor to the appropriate cell using the cursor (arrow) keys and typing an equal sign followed by the new numerical value and then depressing the Return key. This will cause the spreadsheet display to automatically update to show the results corresponding to the revised magnitude/yield relation. When the analysis session is completed, this function may be terminated by sequentially typing the letters q and n.

## Event Summary

This module provides a one page summary of the results obtained by applying the YES to the digital seismic data recorded from the selected explosion. Listed results include the date, origin time and location of the explosion, the derived unified seismic yield and its associated uncertainty, the results of the statistical test of compliance of the current event with the 150 kt limit of the TTBT, a tectonic release characterization of the event based on the surface wave moment tensor analysis and, if available, the CORTEX yield estimate for the explosion. In addition, each of the estimated seismic magnitudes is listed together with its associated yield estimate and assigned weight in the determination of the unified yield estimate.

Quit

### Event Summary

Test Site : Shagan  
 Date : 14 September 1988  
 Origin Time : 4:0: 0.00 UT  
 Location : 49.8788N, 78.8225E

Date of Analysis : Jan 15, 1992

Unified Seismic Yield : 116.5 Kt  
 CORTEX Yield : Not available  
 Unified Seismic Uncertainty :  $F = 1.55$  (75.0 kt <  $W$  < 180.9 kt)

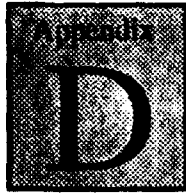
Compliance Assessment : Accept the null hypothesis that the yield is less than 150kt (2.5% significance level test)

Tectonic Characterization :  $F = 0.13$ , Strike = 319 degrees

The conclusions presented above were based on the following measurements:

Individual Magnitudes and Yields			
Measurement	Yield	Magnitude	Rel. Weight
mb	120.504	6.011	0.340
M(Lg)	105.925	5.967	0.330
M(e)	136.773	7.132	0.000
M(PSpec)	123.880	6.026	0.330
M(Ph)	125.603	6.025	0.000

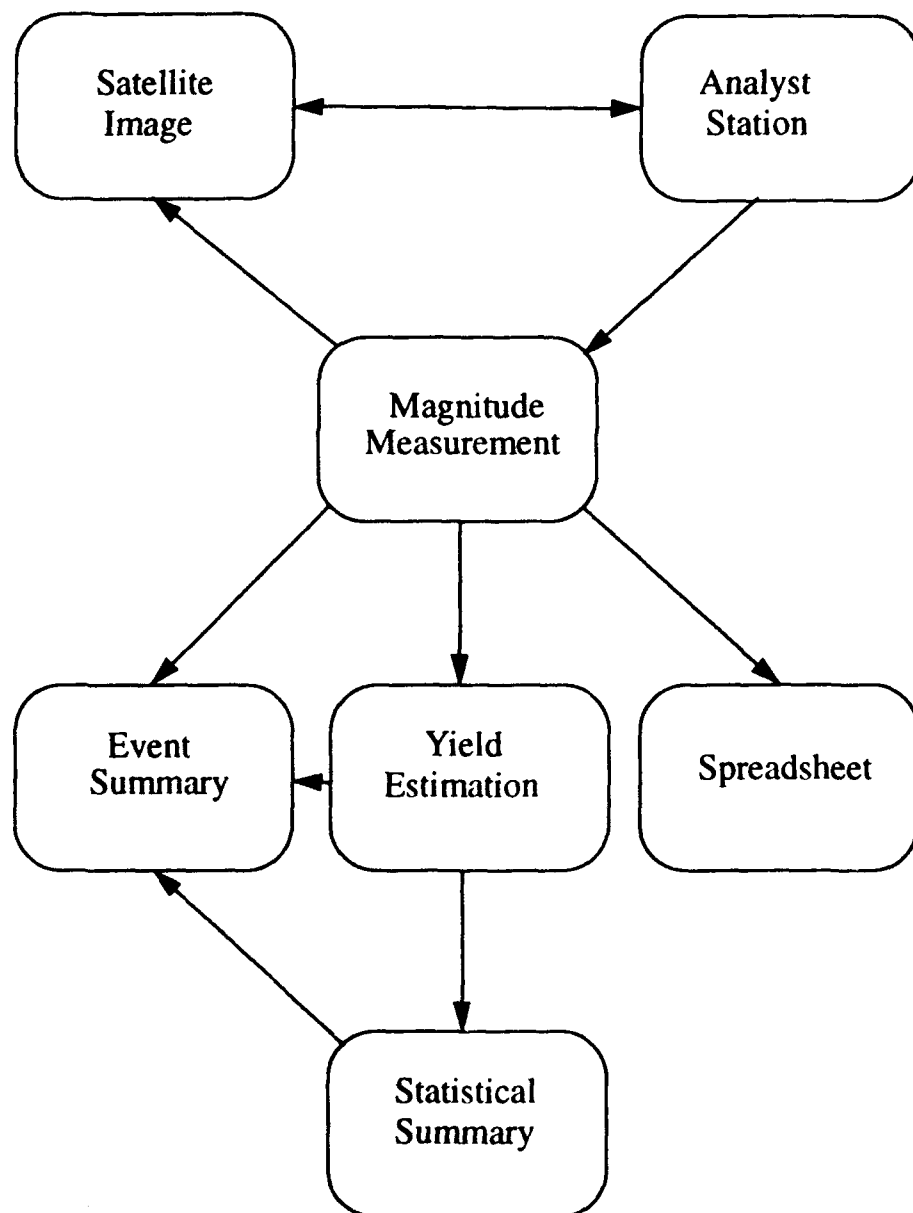




## ***Dependencies between YES modules***

---

The following chart shows the main modules of YES and their interdependencies.



# DISTRIBUTION LIST

Prof. Thomas Ahrens  
Seismological Lab, 252-21  
Division of Geological & Planetary Sciences  
California Institute of Technology  
Pasadena, CA 91125

Prof. Keiiti Aki  
Center for Earth Sciences  
University of Southern California  
University Park  
Los Angeles, CA 90089-0741

Prof. Shelton Alexander  
Geosciences Department  
403 Deike Building  
The Pennsylvania State University  
University Park, PA 16802

Dr. Ralph Alewine, III  
DARPA/NMRO  
3701 North Fairfax Drive  
Arlington, VA 22203-1714

Prof. Charles B. Archambeau  
CIRES  
University of Colorado  
Boulder, CO 80309

Dr. Thomas C. Bache, Jr.  
Science Applications Int'l Corp.  
10260 Campus Point Drive  
San Diego, CA 92121 (2 copies)

Prof. Muawia Barazangi  
Institute for the Study of the Continent  
Cornell University  
Ithaca, NY 14853

Dr. Jeff Barker  
Department of Geological Sciences  
State University of New York  
at Binghamton  
Vestal, NY 13901

Dr. Douglas R. Baumgardt  
ENSCO, Inc  
5400 Port Royal Road  
Springfield, VA 22151-2388

Dr. Susan Beck  
Department of Geosciences  
Building #77  
University of Arizona  
Tucson, AZ 85721

Dr. T.J. Bennett  
SCUBED  
A Division of Maxwell Laboratories  
11800 Sunrise Valley Drive, Suite 1212  
Reston, VA 22091

Dr. Robert Blandford  
AFTAC/TT, Center for Seismic Studies  
1300 North 17th Street  
Suite 1450  
Arlington, VA 22209-2308

Dr. G.A. Bollinger  
Department of Geological Sciences  
Virginia Polytechnical Institute  
21044 Derring Hall  
Blacksburg, VA 24061

Dr. Stephen Bratt  
Center for Seismic Studies  
1300 North 17th Street  
Suite 1450  
Arlington, VA 22209-2308

Dr. Lawrence Burdick  
Woodward-Clyde Consultants  
566 El Dorado Street  
Pasadena, CA 91109-3245

Dr. Robert Burrige  
Schlumberger-Doll Research Center  
Old Quarry Road  
Ridgefield, CT 06877

Dr. Jerry Carter  
Center for Seismic Studies  
1300 North 17th Street  
Suite 1450  
Arlington, VA 22209-2308

Dr. Eric Chael  
Division 9241  
Sandia Laboratory  
Albuquerque, NM 87185

Prof. Vernon F. Cormier  
Department of Geology & Geophysics  
U-45, Room 207  
University of Connecticut  
Storrs, CT 06268

Prof. Steven Day  
Department of Geological Sciences  
San Diego State University  
San Diego, CA 92182

Marvin Denny  
U.S. Department of Energy  
Office of Arms Control  
Washington, DC 20585

Dr. Zoltan Der  
ENSCO, Inc.  
5400 Port Royal Road  
Springfield, VA 22151-2388

Prof. Adam Dziewonski  
Hoffman Laboratory, Harvard University  
Dept. of Earth Atmos. & Planetary Sciences  
20 Oxford Street  
Cambridge, MA 02138

Prof. John Ebel  
Department of Geology & Geophysics  
Boston College  
Chestnut Hill, MA 02167

Eric Fielding  
SNEE Hall  
INSTOC  
Cornell University  
Ithaca, NY 14853

Dr. Mark D. Fisk  
Mission Research Corporation  
735 State Street  
P.O. Drawer 719  
Santa Barbara, CA 93102

Prof Stanley Flatte  
Applied Sciences Building  
University of California, Santa Cruz  
Santa Cruz, CA 95064

Dr. John Foley  
NER-Geo Sciences  
1100 Crown Colony Drive  
Quincy, MA 02169

Prof. Donald Forsyth  
Department of Geological Sciences  
Brown University  
Providence, RI 02912

Dr. Art Frankel  
U.S. Geological Survey  
922 National Center  
Reston, VA 22092

Dr. Cliff Frolich  
Institute of Geophysics  
8701 North Mopac  
Austin, TX 78759

Dr. Holly Given  
IGPP, A-025  
Scripps Institute of Oceanography  
University of California, San Diego  
La Jolla, CA 92093

Dr. Jeffrey W. Given  
SAIC  
10260 Campus Point Drive  
San Diego, CA 92121

Dr. Dale Glover  
Defense Intelligence Agency  
ATTN: ODT-1B  
Washington, DC 20301

Dr. Indra Gupta  
Teledyne Geotech  
314 Montgomery Street  
Alexandria, VA 22314

Dan N. Hagedorn  
Pacific Northwest Laboratories  
Battelle Boulevard  
Richland, WA 99352

Dr. James Hannon  
Lawrence Livermore National Laboratory  
P.O. Box 808  
L-205  
Livermore, CA 94550

Dr. Roger Hansen  
HQ AFTAC/TTR  
Patrick AFB, FL 32925-6001

Prof. David G. Harkrider  
Seismological Laboratory  
Division of Geological & Planetary Sciences  
California Institute of Technology  
Pasadena, CA 91125

Prof. Danny Harvey  
CIRES  
University of Colorado  
Boulder, CO 80309

Prof. Donald V. Helmberger  
Seismological Laboratory  
Division of Geological & Planetary Sciences  
California Institute of Technology  
Pasadena, CA 91125

Prof. Eugene Herrin  
Institute for the Study of Earth and Man  
Geophysical Laboratory  
Southern Methodist University  
Dallas, TX 75275

Prof. Robert B. Herrmann  
Department of Earth & Atmospheric Sciences  
St. Louis University  
St. Louis, MO 63156

Prof. Lane R. Johnson  
Seismographic Station  
University of California  
Berkeley, CA 94720

Prof. Thomas H. Jordan  
Department of Earth, Atmospheric &  
Planetary Sciences  
Massachusetts Institute of Technology  
Cambridge, MA 02139

Prof. Alan Kafka  
Department of Geology & Geophysics  
Boston College  
Chestnut Hill, MA 02167

Robert C. Kemerait  
ENSCO, Inc.  
445 Pineda Court  
Melbourne, FL 32940

Dr. Max Koontz  
U.S. Dept. of Energy/DP 5  
Forrestal Building  
1000 Independence Avenue  
Washington, DC 20585

Dr. Richard LaCoss  
MIT Lincoln Laboratory, M-200B  
P.O. Box 73  
Lexington, MA 02173-0073

Dr. Fred K. Lamb  
University of Illinois at Urbana-Champaign  
Department of Physics  
1110 West Green Street  
Urbana, IL 61801

Prof. Charles A. Langston  
Geosciences Department  
403 Deike Building  
The Pennsylvania State University  
University Park, PA 16802

Jim Lawson, Chief Geophysicist  
Oklahoma Geological Survey  
Oklahoma Geophysical Observatory  
P.O. Box 8  
Leonard, OK 74043-0008

Prof. Thorne Lay  
Institute of Tectonics  
Earth Science Board  
University of California, Santa Cruz  
Santa Cruz, CA 95064

Dr. William Leith  
U.S. Geological Survey  
Mail Stop 928  
Reston, VA 22092

Mr. James F. Lewkowicz  
Phillips Laboratory/GPEH  
Hanscom AFB, MA 01731-5000(2 copies)

Mr. Alfred Lieberman  
ACDA/VI-OA State Department Building  
Room 5726  
320-21st Street, NW  
Washington, DC 20451

Prof. L. Timothy Long  
School of Geophysical Sciences  
Georgia Institute of Technology  
Atlanta, GA 30332

Dr. Randolph Martin, III  
New England Research, Inc.  
76 Olcott Drive  
White River Junction, VT 05001

Dr. Robert Masse  
Denver Federal Building  
Box 25046, Mail Stop 967  
Denver, CO 80225

Dr. Gary McCartor  
Department of Physics  
Southern Methodist University  
Dallas, TX 75275

Prof. Thomas V. McEvilly  
Seismographic Station  
University of California  
Berkeley, CA 94720

Dr. Art McGarr  
U.S. Geological Survey  
Mail Stop 977  
U.S. Geological Survey  
Menlo Park, CA 94025

Dr. Keith L. McLaughlin  
S-CUBED  
A Division of Maxwell Laboratory  
P.O. Box 1620  
La Jolla, CA 92038-1620

Stephen Miller & Dr. Alexander Florence  
SRI International  
333 Ravenswood Avenue  
Box AF 116  
Menlo Park, CA 94025-3493

Prof. Bernard Minster  
IGPP, A-025  
Scripps Institute of Oceanography  
University of California, San Diego  
La Jolla, CA 92093

Prof. Brian J. Mitchell  
Department of Earth & Atmospheric Sciences  
St. Louis University  
St. Louis, MO 63156

Mr. Jack Murphy  
S-CUBED  
A Division of Maxwell Laboratory  
11800 Sunrise Valley Drive, Suite 1212  
Reston, VA 22091 (2 Copies)

Dr. Keith K. Nakanishi  
Lawrence Livermore National Laboratory  
L-025  
P.O. Box 808  
Livermore, CA 94550

Dr. Carl Newton  
Los Alamos National Laboratory  
P.O. Box 1663  
Mail Stop C335, Group ESS-3  
Los Alamos, NM 87545

Dr. Bao Nguyen  
HQ AFTAC/TTR  
Patrick AFB, FL 32925-6001

Prof. John A. Orcutt  
IGPP, A-025  
Scripps Institute of Oceanography  
University of California, San Diego  
La Jolla, CA 92093

Prof. Jeffrey Park  
Kline Geology Laboratory  
P.O. Box 6666  
New Haven, CT 06511-8130

Dr. Howard Patton  
Lawrence Livermore National Laboratory  
L-025  
P.O. Box 808  
Livermore, CA 94550

Dr. Frank Pilotte  
HQ AFTAC/TT  
Patrick AFB, FL 32925-6001

Dr. Jay J. Pulli  
Radix Systems, Inc.  
2 Taft Court, Suite 203  
Rockville, MD 20850

Dr. Robert Reinke  
ATTN: FCTVTD  
Field Command  
Defense Nuclear Agency  
Kirtland AFB, NM 87115

Prof. Paul G. Richards  
Lamont-Doherty Geological Observatory  
of Columbia University  
Palisades, NY 10964

Mr. Wilmer Rivers  
Teledyne Geotech  
314 Montgomery Street  
Alexandria, VA 22314

Dr. George Rothe  
HQ AFTAC/TTR  
Patrick AFB, FL 32925-6001

Dr. Alan S. Ryall, Jr.  
DARPA/NMRO  
3701 North Fairfax Drive  
Arlington, VA 22209-1714

Dr. Richard Sailor  
TASC, Inc.  
55 Walkers Brook Drive  
Reading, MA 01867

Prof. Charles G. Sammis  
Center for Earth Sciences  
University of Southern California  
University Park  
Los Angeles, CA 90089-0741

Prof. Christopher H. Scholz  
Lamont-Doherty Geological Observatory  
of Columbia University  
Palisades, CA 10964

Dr. Susan Schwartz  
Institute of Tectonics  
1156 High Street  
Santa Cruz, CA 95064

Secretary of the Air Force  
(SAFRD)  
Washington, DC 20330

Office of the Secretary of Defense  
DDR&E  
Washington, DC 20330

Thomas J. Sereno, Jr.  
Science Application Int'l Corp.  
10260 Campus Point Drive  
San Diego, CA 92121

Dr. Michael Shore  
Defense Nuclear Agency/SPSS  
6801 Telegraph Road  
Alexandria, VA 22310

Dr. Matthew Sibol  
Virginia Tech  
Seismological Observatory  
4044 Derring Hall  
Blacksburg, VA 24061-0420

Prof. David G. Simpson  
IRIS, Inc.  
1616 North Fort Myer Drive  
Suite 1440  
Arlington, VA 22209

Donald L. Springer  
Lawrence Livermore National Laboratory  
L-025  
P.O. Box 808  
Livermore, CA 94550

Dr. Jeffrey Stevens  
S-CUBED  
A Division of Maxwell Laboratory  
P.O. Box 1620  
La Jolla, CA 92038-1620

Lt. Col. Jim Stobie  
ATTN: AFOSR/NL  
Bolling AFB  
Washington, DC 20332-6448

Prof. Brian Stump  
Institute for the Study of Earth & Man  
Geophysical Laboratory  
Southern Methodist University  
Dallas, TX 75275

Prof. Jeremiah Sullivan  
University of Illinois at Urbana-Champaign  
Department of Physics  
1110 West Green Street  
Urbana, IL 61801

Prof. L. Sykes  
Lamont-Doherty Geological Observatory  
of Columbia University  
Palisades, NY 10964

Dr. David Taylor  
ENSCO, Inc.  
445 Pineda Court  
Melbourne, FL 32940

Dr. Steven R. Taylor  
Los Alamos National Laboratory  
P.O. Box 1663  
Mail Stop C335  
Los Alamos, NM 87545

Prof. Clifford Thurber  
University of Wisconsin-Madison  
Department of Geology & Geophysics  
1215 West Dayton Street  
Madison, WI 53706

Prof. M. Nafi Toksoz  
Earth Resources Lab  
Massachusetts Institute of Technology  
42 Carleton Street  
Cambridge, MA 02142

Dr. Larry Turnbull  
CIA-OSWR/NED  
Washington, DC 20505

DARPA/RMO/SECURITY OFFICE  
3701 North Fairfax Drive  
Arlington, VA 22203-1714

Dr. Gregory van der Vink  
IRIS, Inc.  
1616 North Fort Myer Drive  
Suite 1440  
Arlington, VA 22209

HQ DNA  
ATTN: Technical Library  
Washington, DC 20305

Dr. Karl Veith  
EG&G  
5211 Auth Road  
Suite 240  
Suitland, MD 20746

Defense Intelligence Agency  
Directorate for Scientific & Technical Intelligence  
ATTN: DTIB  
Washington, DC 20340-6158

Prof. Terry C. Wallace  
Department of Geosciences  
Building #77  
University of Arizona  
Tuscon, AZ 85721

Defense Technical Information Center  
Cameron Station  
Alexandria, VA 22314 (2 Copies)

Dr. Thomas Weaver  
Los Alamos National Laboratory  
P.O. Box 1663  
Mail Stop C335  
Los Alamos, NM 87545

TACTEC  
Battelle Memorial Institute  
505 King Avenue  
Columbus, OH 43201 (Final Report)

Dr. William Wortman  
Mission Research Corporation  
8560 Cinderbed Road  
Suite 700  
Newington, VA 22122

Phillips Laboratory  
ATTN: XPG  
Hanscom AFB, MA 01731-5000

Prof. Francis T. Wu  
Department of Geological Sciences  
State University of New York  
at Binghamton  
Vestal, NY 13901

Phillips Laboratory  
ATTN: GPE  
Hanscom AFB, MA 01731-5000

AFTAC/CA  
(STINFO)  
Patrick AFB, FL 32925-6001

Phillips Laboratory  
ATTN: TSML  
Hanscom AFB, MA 01731-5000

DARPA/PM  
3701 North Fairfax Drive  
Arlington, VA 22203-1714

Phillips Laboratory  
ATTN: SUL  
Kirtland, NM 87117 (2 copies)

DARPA/RMO/RETRIEVAL  
3701 North Fairfax Drive  
Arlington, VA 22203-1714

Dr. Michel Bouchon  
I.R.I.G.M.-B.P. 68  
38402 St. Martin D'Herès  
Cedex, FRANCE

Dr. Michel Campillo  
Observatoire de Grenoble  
I.R.I.G.M.-B.P. 53  
38041 Grenoble, FRANCE

Dr. Jorg Schlittenhardt  
Federal Institute for Geosciences & Nat'l Res.  
Postfach 510153  
D-3000 Hannover 51, GERMANY

Dr. Kin Yip Chun  
Geophysics Division  
Physics Department  
University of Toronto  
Ontario, CANADA

Dr. Johannes Schweitzer  
Institute of Geophysics  
Ruhr University/Bochum  
P.O. Box 1102148  
4360 Bochum 1, GERMANY

Prof. Hans-Peter Harjes  
Institute for Geophysic  
Ruhr University/Bochum  
P.O. Box 102148  
4630 Bochum 1, GERMANY

Prof. Eystein Husebye  
NTNF/NORSAR  
P.O. Box 51  
N-2007 Kjeller, NORWAY

David Jepsen  
Acting Head, Nuclear Monitoring Section  
Bureau of Mineral Resources  
Geology and Geophysics  
G.P.O. Box 378, Canberra, AUSTRALIA

Ms. Eva Johannisson  
Senior Research Officer  
National Defense Research Inst.  
P.O. Box 27322  
S-102 54 Stockholm, SWEDEN

Dr. Peter Marshall  
Procurement Executive  
Ministry of Defense  
Blacknest, Brimpton  
Reading FG7-FRS, UNITED KINGDOM

Dr. Bernard Massinon, Dr. Pierre Mechler  
Societe Radiomana  
27 rue Claude Bernard  
75005 Paris, FRANCE (2 Copies)

Dr. Svein Mykkeltveit  
NTNT/NORSAR  
P.O. Box 51  
N-2007 Kjeller, NORWAY (3 Copies)

Prof. Keith Priestley  
University of Cambridge  
Bullard Labs, Dept. of Earth Sciences  
Madingley Rise, Madingley Road  
Cambridge CB3 0EZ, ENGLAND